M.Tech (Structural Engineering)

Niraj Kumar

2025

ANALYSIS OF BEAM-COLUMN JOINTS

A Dissertation Submitted

in Partial Fulfilment of the Requirement for the Award of the

Degree of

MASTER OF TECHNOLOGY

in

Structural Engineering

by

NIRAJ KUMAR

(2K23/STE/12)

Under the supervision of

Mr.GP Awadhiya,

Associate Professor

Department of Civil Engineering, DTU

DEPARTMENT OF CIVIL ENGINEERING
DELHI TECHNOLOGICAL UNIVERSITY
(Formerly Delhi College of Engineering) Bawana Road, Delhi- 110042

May 2025

DELHI TECHNOLOGICAL UNIVERSITY
(Formerly Delhi College of Engineering)
Bawana Road, Delhi-110042

CANDIDATE'S DECLARATION

I, **Niraj Kumar**, hereby declare that the work which is being presented in dissertation entitled "**Analysis of Beam-Column joints**" which is submitted by me to the partial fulfilment of the requirement for the award of the degree of Master of Technology, submitted in the Department of Civil Engineering, Delhi Technological University, Delhi is an authenticate record of my own work carried out during the period from 2024 to 2025 under the supervision of **Mr. GP Awadhiya**

The matter presented in the dissertation has not been submitted by me for the award of any other degree or any other institute.

Candidate's Signature

This is to certify that the student has incorporated all the corrections suggested by the examiners in the thesis and the statement made by the candidate is correct to the best of our knowledge.

Signature of Supervisor (S)

Signature of Examiner

DELHI TECHNOLOGICAL UNIVERSITY
(Formerly Delhi College of Engineering)
Bawana Road, Delhi-110042

CERTIFICATE BY THE SUPERVISOR

Certified that **Niraj Kumar** (2K23/STE/12) has carried out their research work presented in this dissertation entitled "**Analysis of Beam-Column joints**" for the award of Master of Technology from the Department of Civil Engineering, Delhi Technological University, Delhi, under my supervision. The dissertation embodies results of original work, and studies are carried out by the student himself and the contents of the dissertation do not form the basis for the award of any other degree to the candidate or to anybody else from this or any other University.

30.05.2025

Signature

Mr.GP Awadhiya

Associate Professor

Delhi Technological University

Bawana Road, Delhi-110042

Date: 30/05/2025

ABSTRACT

Stiffness and Drift is a primary concern of a structural designer in the design and maintenance of structures, as reduction in stiffness and increment of drift can lead to the failure of whole structure which cause economic and safety consequences. This study investigates the analysis of different types of beam-column joint using ANSYS, widely used for FEA analysis of structures under different loading condition.

The research focuses on comparative study of beam-column joint using different material like M25 concrete with reinforcement , FRC and then by using M40 grade concrete without reinforcement. Obtained analysis disclosed that the variation of shear stress and maximum principal strain is acceptable in all the case while using FRC material. The study foregrounds the role of FRC material in enhancing the overall stability and performance of joints, providing valuable cognizance. Analysis under 300KN vertical loads stipulate that the maximum principal strain and shear stress for the different types of joints is not so much variable in comparison to joint having M25 grade concrete with reinforcement and joints having M40 grade of concrete without reinforcement.

The study seeks to identify the region of maximum shear stress and maximum principal strain so that its helps to identify the types of cracks and the cause of cracks that is obtained at the different region of the different types of joints.

The study highlights the analysis of the beam-column joints using effectiveness of Ansys software .They serve as a fixed supporting system for the structure and increase the overall stiffness and reduce the displacement studied under FEA analysis.

KEYWORDS: FRC, RCC, FEA, Shear Stress, Strain Energy, Maximum Principal Strain etc

ACKNOWLADGEMENT

I **Niraj Kumar** would like to express my deepest gratitude to all those who have contributed to the successful completion of this thesis.

First and foremost, I extend my sincere appreciation to my supervisor, **Mr. GP Awadhiya**, for their invaluable guidance, support, and expertise throughout the entire research journey. The knowledge he has imparted and the unwavering commitment he has shown have been instrumental in enabling me to achieve this remarkable feat. He advisor provided valuable guidance on the theoretical framework and methodology of the research, ensuring its soundness and relevance to the field.

I am grateful to the faculty and staff of Delhi Technological University [DTU], especially the Civil Engineering Department, for providing a conducive academic environment and necessary resources for carrying out this research. The access to the laboratory facilities and library resources has greatly facilitated the experimental work and literature review.

Heartfelt appreciation to my family and friends for their encouragement, motivation, and moral support that kept me inspired and focused on completing this thesis successfully.

This thesis would not have been possible without the support, guidance, and contributions of all those mentioned above. I am truly grateful for their invaluable assistance, and their involvement has played a significant role in the successful completion of this research.

NIRAJ KUMAR

2K23/STE/12

Table of Contents

List of Tables

List of Figures

Chapter 1

Introduction

1.1 Overview of Beam Column Joint

The beam-column junction is a crucial location within a reinforced concrete framed structure where the components intersect in all three dimensions. The integrity and stability of a structure are ensured through the transmission of forces that occur at the ends of structural elements, facilitated by the presence of joints. The beam-column junction is a crucial component of a reinforced concrete structure, as it often encounters beam failure. The critical behavior observed in this case can be attributed to the intricate stress distribution at the joint and a sudden alteration in geometry. Historically, the main objective of joint design in reinforced concrete structures was to meet the anchoring requirements. The influence of various factors on the geometry of the connections was determined through subsequent investigations. These factors include the strength of the concrete, the quantity and configuration of reinforcement, and the loading pattern.

The primary objective of a beam column junction in a reinforced concrete structure is to effectively transfer the load from connected components under both gravitational forces and seismic vibrations. The beam-column junction is a critical component of a reinforced concrete moment-resistant structure. Ensuring precise design and meticulous workmanship is crucial when the structure is vulnerable to seismic stress. The collapse of reinforced concrete beam column junctions during earthquakes is primarily governed by brittle shear and bond failure processes.

1.2 Functional Requirement of Beam Column Joint

The functional requirement of a beam-column joint is a critical aspect in structural engineering. It refers to the specific performance criteria that the joint must meet in order to ensure the overall stability and integrity of the structure. The functional requirement of a beam-column joint is typically determined by considering factors such as load transfer, stiffness, strength, durability,

The junction, also known as the intersection of beams and columns, serves the purpose of facilitating the expansion and upkeep of neighboring members at their highest possible capacity. The connectors must possess adequate rigidity and strength to endure the internal stresses

generated by the framework components. The prerequisites for achieving optimal joint function can be clearly defined as follows:

1. The strength of the joint must meet or surpass the most rigorous criterion related to the formation of the structural plastic hinge mechanism for the frame. The elimination of the need for combined processes to distribute energy and restore power in a region that is challenging to reach would be achieved. It will be subsequently shown that joint mechanisms undergo significant reduction in rigidity and strength when exposed to cyclic operations within the inelastic range.
2. The capacity of the column to bear weight should not be affected by any potential decrease in joint strength. The column is considered incomplete if the joint is not present.
3. The inclusion of unnecessary joint reinforcement, which does not contribute to achieving optimal performance, should not add complexity to the construction process.

1.3 Types of Beam Column Joint

The beam column joints can be classified on the basis of connection geometry, loading geometry and rigidity of the joint as shown in figure 1.1.

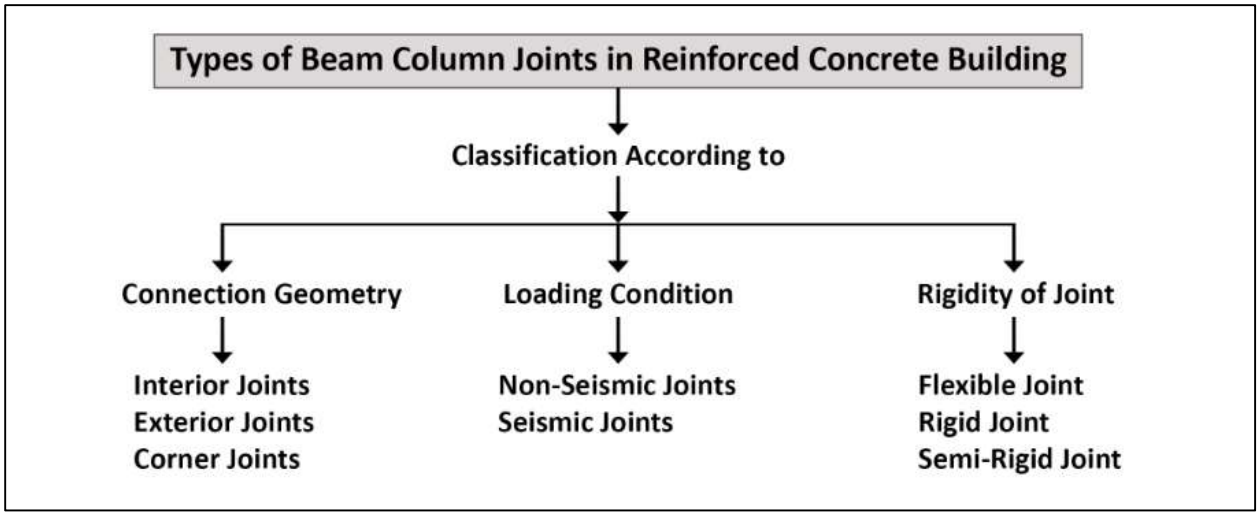

Figure 1.1: Classification of Beam Column Joint

1.3.1 Classification Based on Construction Geometry

a. Interior Joints

An internal joint is formed when four timbers are attached to the vertical sides of a column.

b. Exterior Joints

An external joint is formed when a column intersects with two beams at a 90-degree angle, and one of the beams is connected to the vertical side of the column.

c. Corner Joints

Corner joints are a type of joint used in various applications. They are formed by joining two pieces of material at a right angle, creating a corner. Corner joints are commonly used in woodworking, metalworking,

1.3.2 Classification Based on Loading Condition

ACI-ASCE Committee 352 classifies the beam column joint in the following two categories:

a. Type 1 Joints – Non-Seismic Joints

The design of non-seismic joints does not consider specific ductility requirements. Instead, the focus is on prioritizing strength. The described connection is suitable for use at any intersection within a structural framework designed to withstand both gravitational forces and wind pressures, as well as lateral loads.

b. Type 2 Joints – Seismic Joints

Seismic joints are designed to retain their structural integrity when deformation reversals occur in an inelastic area. The observed joint is commonly found in framed structures designed to resist horizontal forces generated by earthquakes.

1.3.3 Classification Based on Rigidity of Joint

a. Rigid Joint

Following deformation, the inflexible joint retains its original 90-degree angle between intersecting components. Columns are created through the process of converting timbers. Within a rigid-jointed frame structure, the beam column joints are of utmost importance and require careful design and detailing. Rigid beam-column connections are commonly located at the base of various structures in multi-story frame buildings. These structures include portal frames, cantilever retaining walls, and box culverts.

b. Pin Joint

The transmission of moment from beams to columns is hindered by the presence of pegs located in the columns at a junction. The presence of needles located at the ends of the columns indicates

that moments are not transferred from the beams to the columns. The instability of the structure is attributed to the lack of any type of reinforcement.

c. Semi Rigid Joint

A semi-rigid joint in a beam-column connection refers to a junction that demonstrates a defined level of rotational rigidity. This level of rigidity falls between the completely rigid and completely pinned (hinged) states. The equilibrium between moment resistance and rotational flexibility in these joints can provide benefits for various structural applications.

1.4 Beam Column Joint Failure

Following the occurrence of the earthquake, subsequent inspections have indicated that the structures were rendered in a state of destruction due to the inadequate adherence to construction protocols. Some residential and corporate structures were built without adequate measures to ensure their resistance to earthquakes. The structural failures observed in the earthquake-affected region can be attributed to a combination of various factors. The structural issues of the building can be attributed to several factors. These include the use of short columns, the presence of non-symmetric unreinforced masonry infill walls that cause certain slender columns to behave as short columns or weaken the ground floor, an insufficient capacity design that promotes column sway, particularly on lower floors, and a deficiency of shear reinforcement at the joint. The seismic performance of structures built with reinforced concrete (RC) is negatively impacted by the inadequate strength of beam-column connections. The presence of structures that have suffered significant damage or complete destruction within the seismic zone serves as evidence for this phenomenon.

(a) Failure of beam-column joint

(b) Close-up of beam-column joint failure

(c) Damage to beam-column joint of building under construction in Adapazari, Turkey
(Image source: http://nisee.berkeley.edu/elibrary/Image/IZT-749)

Figure 1.2: Damage to reinforced concrete moment framed building after Kocaeli earthquake

Chapter 2

Literature Review

Ghayeb et. al. [1] The structural linkage systems pose a significant challenge for precast building systems. It is essential for designers of a dowel system to have a comprehensive understanding of the fundamental requirements for seismic loading. Consideration of unforeseen impact loads is crucial for preventing building collapse during an earthquake. The existing construction regulations lack comprehensive design and analysis criteria for beam-to-column connection systems. This paper provides a comprehensive analysis of the literature on dowel precast beam-column connections for academicians. This review examines four main areas: (1) the performance of precast dowel beam-column connection systems in seismic-prone regions, (2) the design and development of precast dowel connection components, (3) the evaluation of influential parameters in precast connection systems, and (4) the identification of precast beam-to-column connections suitable for seismic loads. The performance of the dowel connection system was evaluated by considering factors such as strength, ductility, energy dissipation, rotation, and the presence of plastic hinges in critical regions.

Webber et. al. [2] The effective length technique is utilized by industry codes of practice to assess the stability of multi-story systems. The effective length technique is utilized to determine the critical buckling load by focusing on a specific column within a frame and evaluating the stiffness of its end restraints in terms of translation and rotation. The NCCI document SN008a to BS EN 1993-1 (BSI, 2005) has the potential to produce occasional inaccurate results. The lack of consideration for the rotational stiffness of the end restraints from columns above and below, as well as the translational stiffness of the end restraints from other columns on the same storey, is the reason for this. The following paper proposes two enhancements to the existing methodology. The effective length at the outset is determined by considering the axial load in adjacent columns. In addition, it is recommended to adjust the effective length ratio to consider the buckling stresses of adjacent columns. The effectiveness of the adjustments has been demonstrated, consistently yielding findings within a 2% margin of those obtained through structural analysis software. This comparison is made with the results obtained from the NCCI, which may exhibit variances of up to 80%.

Batalha et. al. [3] The objective of this investigation is to analyze the behavior of composite beam-column connections that employ different detailing techniques. The purpose of this investigation is to enhance the comprehension of their performance and facilitate the secure utilization of seismic applications. The connections will be integrated into precast moment-resisting structures and exposed to simulated reversed cyclic loading. A comprehensive numerical and experimental investigation was conducted to accomplish the research objectives. The experimental component involved subjecting precast concrete beam-column specimens, which had six distinct anchoring details in the beam element, along with companion specimens cast monolithically, to reversed cyclic stress. The numerical section of the study utilized a nonlinear finite element analysis (FEA) approach to accurately simulate the experimental behavior of a particular moment-resisting precast

concrete beam-column connection under reversed cyclic load testing. In order to showcase the feasibility of the suggested finite element method, three-dimensional (3D) finite element models were created for a standard monolithic beam-column connection and multiple precast hybrid beam-column connections. These models were generated using ABAQUS, a nonlinear finite element analysis software. The models are designed to provide a comprehensive analysis of the performance of steel and concrete materials until they reach the point of failure. The implementation of a Concrete Damage Plasticity model (CDP) was carried out to simulate the cyclic behavior commonly observed in fractured reinforced concrete materials. The model takes into account both the compression-softening and tension-stiffening effects. The Kinematic Bilinear Elasto-Plastic nonlinear model was utilized to describe all steel components. This model considers the bond-slip effect of all reinforcing bars embedded in concrete. The correlation between the finite element results and the tested components confirms the accuracy of the suggested finite element model, even when considering the complexity of the connections being studied. The failure modes of the precast connection components were accurately depicted and analyzed using a developed finite element model. Following that, a comparison was made between the failure modes of these components and the failure modes of the similar monolithic connection. Recent research has shown that making small modifications to the details of a connection can greatly enhance its ability to dissipate energy and increase its strength. In addition, these modifications have a significant impact on the potential failure modes of the connection. The study demonstrates that precast connectors display advantageous performance characteristics under cyclic stress conditions. Furthermore, the results of this study can be utilized to analyze the influence of different design elements on the performance of these connections.

Kremmyda et. al. [4] An analysis of the behavior of connections between structural components is conducted during the design and construction process to consider service, environmental, and seismic load factors in precast technology. Therefore, it is crucial to consistently design and specify the connections, considering the expected structural response. The objective of this research study is to present an analytical equation that can be used to predict the resistance of precast pinned connections when subjected to shear monotonic and cyclic stresses. The proposed formula has been specifically developed to address scenarios where the connection failure occurs simultaneously with the flexural failure of the dowel and the compression of the surrounding concrete. The occurrence of this event is expected in two specific scenarios: (i) when the dowels have a concrete cover that exceeds six times their diameter ($d > 6\ D$), or (ii) when the dowels have sufficient reinforcement as outlined in the article, in situations where the concrete cover is less than six times their diameter ($d < 6\ D$). The equation is calibrated by employing numerical results obtained from a nonlinear numerical analysis and existing experimental data. The objective of this study is to assess the impact of different factors on the horizontal shear resistance of the connection. The factors that need to be considered include the initial axial stress in the dowels, the strength of the materials such as concrete, grout, and steel, the depth at which the dowels are embedded within the concrete, the thickness of the elastomeric pad, the type of shear loading (whether it is cyclic or monotonic), and the rotation of the joint. In addition, the quantity and dimensions of the dowels are taken into consideration. Guidance is offered for the design of precast anchored beam-to-column connections in the field of earthquake-resistant structures.

Cimmino et. al. [5] Contemporary seismic building regulations require adherence to specific rules and construction criteria for capacity design in order to prevent vulnerable failure modes at the material, element, and structural levels. The seismic building code of Italy, based on Eurocode 8, mandates the design of beam-to-column connections in single-story precast reinforced concrete structures. These connections, where the beams are pinned to the columns, must be designed to prevent connection failure prior to the formation of a plastic hinge at the base of the column. However, there is a lack of specific information regarding the methods employed to attain this level of performance. The seismic performance of beam-to-column dowel connections in Europe has been shown to be significantly inadequate based on recent earthquakes. The purpose of this study is to analyze a range of factors that are linked to dowel beam-to-column connections in Europe. The following tasks are included in this study: (a) evaluating the accuracy of existing formulations in describing failure modes and shear strength; (b) identifying potential failure modes related to connection elements such as steel dowels, transversal steel reinforcement, and dowel concrete cover; (c) assessing the impact of connection failure on the seismic safety of newly designed single-story rod constructions at the point of collapse; and (d) examining various connection configurations based on seismic design. The design of the reference structures and the connections between the beams and columns takes into account various structural configurations and seismic hazard levels. The scope of this study includes two different soil types and four distinct locations. The evaluation of structural capacity considers both local failure modes related to connection shear strength and global column plastic hinge degeneration, which is quantified in terms of top lateral displacements. The process of conducting multi-stripe nonlinear investigations is an integral part of seismic assessment.

Manfredi et. al. [6] The seismic response of reinforced concrete precast structures in Europe has been shown to be significantly affected by the connecting systems, as evidenced by recent earthquakes. Moreover, the inadequate strength of the connections when subjected to seismic stresses has been identified as the root cause of specific instances of beam-to-column failures in past seismic events. The seismic performance of precast structures is greatly impacted by the seismic safety of connections. The purpose of this study is to assess the cyclic shear performance of a new connection system used as a retrofitting solution for a damaged beam-to-column connection. To achieve this, two cycle shear tests are conducted on two different configurations. The performance of the redesigned connections under horizontal cyclic stresses has been demonstrated through experimental tests, indicating their effectiveness. The objective is to compare the behavior of a standard beam-to-column dowel connection with the connection under investigation. This comparison will help analyze the fundamental components of the dowel connection system.

Fawzia et. al. [7] Square hollow sections (SHSs) are commonly used as beam-column connectors in civil applications, despite their vulnerability to cyclic stress. The performance of both onshore and offshore civil infrastructure is affected by cyclic forces such as wind, waves, currents, and earthquakes. Additionally, it is important to note that the beam-column connections have the potential to become structurally insufficient over time due to various factors. These factors include material degradation, design or manufacturing defects, and increasing service pressures. In order to enhance the performance of SHS beam-column connections under continuous monotonic and cyclic loadings, it is crucial to reinforce them. This article primarily focuses on the efficacy of beam-column connections in structural hollow sections (SHS) that have been reinforced with externally bonded glass fiber reinforced polymer (GFRP) and carbon fiber reinforced polymer

(CFRP). An experimental study was conducted on the bare, CFRP, and GFRP-augmented SHS connectors to evaluate their performance under both monotonic and cyclic stresses. The results indicate that CFRP and GFRP reinforced SHS beam-column connections exhibit enhanced ultimate moment capacity, moment degradation behavior, secant stiffness, energy dissipation capacity, and plastic hinge behavior compared to their non-reinforced counterparts. Under monotonic stress, both types of reinforced connections demonstrate enhanced secant rigidity, ductility, and moment capacity. In addition, the utilization of CFRP reinforcement enhances the maximum load-bearing capacity of a structure, whereas the implementation of GFRP reinforcement improves the plastic deformation capacity of a structure.

Thambiratnam et. al. [8] The fracture of welded beam-column connections can be attributed to cyclic tension. The connections may lack the required capacity due to design deficiencies, material degradation resulting from severe environmental conditions, or an increase in service demands. It may be necessary to reinforce the structures in order to withstand both static and cyclic stresses. Several comprehensive investigations have been carried out to examine the behavior of welded beam-column connections, both reinforced and unprotected, under significant cyclic stress and monotonic loads. The current study utilizes epoxy adhesive as the adhesive agent and carbon fiber reinforced polymer (CFRP) as the reinforcement material. The experimental research clearly demonstrated a significant improvement in the performance of welded joints when CFRP composites were used, both under cyclic and monotonic loadings. The ultimate moment capacity, stiffness, energy dissipation, and ductility were all enhanced by reinforcing the welded connections with CFRP under monotonic loading. Moreover, the welded connections that were strengthened with carbon fiber reinforced polymer (CFRP) demonstrated superior moment hysteresis behavior, increased rigidity, and an enhanced capacity to dissipate energy when subjected to cyclic stress, as compared to the unmodified connections. Furthermore, there is a notable level of consensus between the moment capabilities that are predicted based on theory and those that are determined through empirical methods.

Waqas et. al. [9] The beam-column junctions (BCJs) located on the exterior of reinforced concrete (RC) structures are of utmost importance and often prone to vulnerability. These areas have the potential to undergo catastrophic collapse. Accuracy is particularly important in the context of earthquakes. Achieving a robust and ductile joint design is highly significant. Further research is necessary to explore the implementation of a weak beam-strong column mechanism in moment frames, despite the presence of established design principles for developing flexible and durable connections. The objective of this study is to utilize finite element modeling (FEM) to examine different reinforcement configurations in the joint area of BCJs (beam-column joints). These configurations are intended to replace the conventional shear stirrups and enhance the performance of BCJs. The objective is to address the problem of congestion in the joint area reinforcement during the process of concrete installation, which could potentially impact the seismic resistance. Ten Finite Element Method (FEM) models were generated in order to facilitate evaluation. There were nine models designed with different reinforcement configurations, while one model was developed without any additional reinforcement. The primary objective of this study was to assess the effectiveness of various designs in BCJs (Bridge Column Joints) under monotonic loading. This was achieved by comparing the distribution of damage, load-deflection behavior, and damage-rotation curves. As a result, there was a significant decrease of 22-37% in the number of

core injuries when diagonal bars that were aligned with the plane performed better than those that were not. The configuration featuring two X-shaped reinforcements, as opposed to the conventional joint stirrups, was determined to be the most optimal choice among the available options. The load-carrying capacity of this construction was increased by 13.7%. Additionally, core damage in tension and compression was reduced by approximately 83%. Moreover, the construction design promoted the formation of plastic hinges away from the junction, aiming to achieve the desired weak beam-strong column mechanism. The discovery made in this study not only enhances the ability of reinforced concrete (RC) structures to withstand seismic forces, but also has significant implications for their practical design and construction. As a result, it contributes to improving the safety of built environments.

Behnam et. al. [10] The seismic design criteria for reinforced concrete (RC) wide beam-column connections are primarily based on a limited amount of experimental research, as specified in international standards. A study was undertaken to examine the influence of the beam width ratio, defined as the ratio of the beam width to the column breadth, on the seismic performance of exterior beam-column connections. The purpose of this analysis was to enhance the existing data. The specimens were subjected to cyclic loading conditions in the opposite direction. The primary test variables included the beam width ratio and the joint shear stress ratio (γd). The specimens were fabricated following the guidelines outlined in ACI 352R-02 and ACI 318-14. The gamma-d values obtained were 0.74, 1.12, 1.63, and 2.03. The beam width ratios of the objects were measured to be 1, 1.5, 2, and 2.5. According to ACI 352R-02, the γd value must be less than γn = 1.25 when the joints are restricted on three sides. The results indicate that beam plastic hinges can be effectively developed in specimens with a ductility ratio (ηd) ranging from 0.74 to 1.12, as well as beam width ratios of 1 and 1.5, without experiencing any significant cracks in the joint region. However, specimens with beam width ratios of 2 and 2.5, along with γd values of 1.63 and 2.03, displayed observable damage at the joint core. The specimen, which had a beam width ratio of 2.5, experienced torsional failure in the spandrel beam.

Alaee et. al. [11] This study focuses on the experimental investigation and reporting of the seismic performance of outside beam-column joints that have been reinforced with Grade 600 longitudinal reinforcing bars. The construction of these connections utilizes high-strength concrete with a compressive strength of 70 MPa. Six half-scale reinforced concrete (RC) exterior connections were fabricated to meet the requirements specified in the ACI 318-14 Code in order to achieve this outcome. The investigation involved subjecting all specimens to quasi-static reversed cyclic loading, with drift ratios reaching up to 5.3%. The investigation was facilitated by the ability to analyze various variables, including the compressive strength of concrete, the yield strength of longitudinal bars, the flexural reinforcement ratio, the ratio of the column to beam flexural capacity, and the size of the longitudinal bar. The length of the longitudinal reinforcing bars in the beam and column decreased by 27% in specimens with identical flexural strengths due to an increase in their yield strength. The seismic behavior of all specimens reinforced with high-strength steel (HSS) reinforcing bars closely resembled the behavior observed in joints containing Grade 420 MPa bars, up to a drift ratio of 4.5%. This similarity was observed in terms of load-carrying capacity, failure mode, energy dissipation capacity, pinching width ratio, and secant stiffness. During that period, every specimen had reached its peak capacity for bearing loads. The experimental data demonstrated a 30% improvement in the pinching width ratio and a 26% improvement in cumulative energy dissipation when high-strength concrete (HSC) was utilized in Grade 600 specimens. These improvements were observed at a drift ratio of 4.5% and with the

same ratio of reinforcing bars. However, the High Strength Concrete (HSC) did not have a significant impact on the average peak load and secant rigidity. In addition, the study utilized finite-element analysis (FEA) to perform parametric investigation. The objective was to evaluate the impact of different design parameters on the strength, rigidity, energy dissipation capacity, and analogous damping of the specimens. The parameters included the ratio of column depth to bar diameter, the grade and spacing of joint hoops, and the ratio of column-to-beam flexural capacity.

Waqas et. al. [12] The objective of this study is to analyze the behavior of beam-column junctions (BCJs) under seismic forces and highlight their significance in reinforced concrete (RC) structures. The accurate prediction of the load-carrying capacities of exterior beam-column joints (BCJs) under seismic stresses poses a significant challenge. To optimize the efficiency and security of reinforced concrete structure design processes, it is essential to develop a prediction model that is user-friendly and dependable. To fulfill this requirement, we provide an artificial intelligence (AI) model that utilizes gene expression programming (GEP) to accurately predict the capacity of external BCJs to transport masses under monotonic loading conditions. The model is constructed utilizing Gene Expression Programming (GEP) and is based on a database consisting of 128 values representing the load-carrying capacity of external Ball and Cup Joints (BCJs). The values were derived using a validated finite element (FE) model in ABAQUS. The finite element (FE) model takes into account the influence of both geometry and material properties, aspects that have often been overlooked in previous studies. The variables include a range of factors, such as the axial stresses exerted on the columns, the longitudinal reinforcements present in the beams and columns, the properties of the concrete, and the dimensions of the beams and columns. In this study, the proposed GEP model's results were compared to the numerical data obtained from the validated FE model. This comparison confirmed a high level of precision and reliability. The proposed method has the potential to enhance the accuracy and reliability of load-carrying capacity estimation for joints. This improvement would aid in the design of cost-effective and safe reinforced concrete structures.

Tsang et. al. [13] The beam-column junction, located on the exterior of a limited-ductile reinforced concrete frame system, is often the most vulnerable area. The implementation of diagonal haunch sections has been recognized as an effective seismic retrofit technique for reducing the seismic demand at the junction. Prior global research has focused on the utilization of two haunches. However, the effectiveness of using a single haunch component as a retrofit option that offers architectural benefits and is less intrusive has not been studied. This study aims to assess the practicality of implementing a single haunch system for improving the connections between exterior beams and columns made of reinforced concrete (RC). This paper presents the essential equations required to generate a single diagonal haunch. In addition, the equations for the non-retrofitted subassembly, double haunch retrofitting system, and single haunch retrofitting system have been generalized. The formulations have been verified for both the non-retrofitted subassembly and the double haunch retrofit system using the available experimental data. Finally, a parametric analysis is performed to evaluate the effectiveness of the double haunch retrofitting system compared to the single haunch retrofitting method.

Khan et. al. [14] This study assesses the seismic performance of beam column joints (BCJs) reinforced with ultra-high performance fiber reinforced concrete (UHPFRC) that have insufficient

shear strength. In order to conduct testing, standard concrete bridge column joints (BCJs) were enhanced by applying a thin layer of Ultra-High Performance Fiber-Reinforced Concrete (UHPFRC). These fortified BCJs were then exposed to seismic loading and subsequently repaired, as they did not possess the required strength to withstand seismic activity. Two distinct techniques were utilized to enhance the strength of the standard concrete BCJ specimens. The first technique involved connecting structurally weak BCJs with pre-made UHPFRC plates that were 30 mm thick. This connection was achieved using epoxy resins and specialized fillers. The second technique involved sandblasting the surface of the regular concrete substrate of BCJs and then applying a 30 mm thick UHPFRC jacket through in-situ casting. An experimental assessment was conducted to evaluate the effectiveness of UHPFRC jacketing in strengthening seismically vulnerable BCJs during reverse cyclic loading. The assessment employed a displacement control approach. The column's axial tension was consistently maintained at a force of 150 kN. When comparing the first reinforcement method with the second, the test data indicated that the former exhibited significantly higher levels of success in terms of energy dissipation capacity, shear capacity, deformation capacity, and rigidity characteristics.

Sharma et. al. [15] The performance of RC-framed structures during seismic events is significantly affected by the effectiveness of beam column joints (BCJs). The presence of non-linear rotation in pre-seismic designed RC beam column joints leads to a higher level of damage. This is primarily because these joints lack ductile detailing. The retrofitting procedure enhances the damaged beam-column joint, resulting in increased flexibility. The effectiveness of the retrofitting procedure is greatly impacted by the constraints imposed by the retrofitting materials and the extent of initial damage in the reinforced concrete beam-column junction. An experimental study was conducted to assess the effectiveness of ultra-high performance hybrid fiber reinforced concrete (UHP-HFRC) in retrofitting. Moreover, the investigation examines the effect of initial damage on the functionality of the external beam column junction that has undergone retrofitting with Ultra-High Performance High Fiber Reinforced Concrete (UHP-HFRC). The damage indices model, developed by Park and Ang [1], is utilized to classify the initial damage into four categories: complete, severe, moderate, or little. The exterior boundary condition joint (BCJ) is enhanced using Ultra-High Performance Hybrid Fiber Reinforced Concrete (UHP-HFRC) following the initial damage. The retrofitted BCJ exhibits enhanced load bearing capacity, energy dissipation, and ductility when compared to the control specimen. These improvements are attributed to the UHP-HFRC retrofitting, as evidenced by the test results. The performance of BCJ is affected by the initial damage level. As the initial damage level increases from minor to complete damage, there is a decrease in ductility, rigidity, strength retention at increasing drift, and energy dissipation.

Tsonos et. al. [16] This research investigates the feasibility and effectiveness of shotcrete and cast-in-place concrete retrofitting solutions to improve the shear and flexural performance of columns and beam-column connections in reinforced concrete frame structures. An experimental study was conducted to assess the effectiveness of utilizing two- and four-sided reinforced shotcrete or cast-in-place concrete casings for strengthening beam-column connections and columns prior to an earthquake. A study was conducted to compare the effectiveness of reinforced shotcrete jackets with cast-in-place jackets of similar characteristics. Additionally, the performance of two-sided jackets was compared to four-sided jackets of similar characteristics, with a focus on their lateral

performance. The exceptional reinforcing capacity of each type of concrete jacket for existing frame structures was determined.

Wang et. al. [17] This research presents the findings of a scientific study that examined the use of carbon fiber reinforced polymer (CFRP) to enhance the structural integrity of beam-column junctions in reinforced concrete (RC) structures that are prone to seismic activity. A study was conducted to evaluate the seismic performance of six external RC beam-column junctions by testing their lateral strength and ductility. The objective was to identify the most effective method for enhancing their performance. The collection consists of six specimens in total. Among them, four have undergone restoration using various methods. One of the restored specimens was specifically designed to withstand seismic activity, while the other was not originally intended for such conditions. The study examined the application of externally bonded CFRP sheets and near-surface mounted (NSM) CFRP strips as reinforcement techniques for these designs. The test results have shown that the seismic performance of a beam-column junction, which currently lacks seismic resistance, can be significantly improved by incorporating CFRP reinforcement. The effectiveness of this seismic retrofit method is demonstrated by the finding that the plastic hinge is successfully relocated from the joint region through the utilization of NSM CFRP strips in beams and joints. This relocation leads to a ductile failure mode, specifically beam flexural failure. An in-depth understanding of the hinge relocation processes has been attained by implementing comprehensive strain measurements during the testing program.

Ilia et. al. [18] There are many historical buildings constructed of reinforced concrete (RC) that still have beam-column assemblies which were designed and built before the current seismic laws were put into effect. Consequently, these structures have the potential to experience irreversible failure due to non-ductile behaviors when subjected to ground vibrations. Examples of such failure modes include column flexural hinging or joint shear failure. The objective of this experimental investigation was to evaluate the efficacy of newly proposed rehabilitation programs in strengthening faulty RC beam-column connections using fiber-reinforced polymers (FRPs). To accomplish this objective, a series of experiments were conducted on five beam-column junctions that were constructed at a reduced scale of half the original size. The junctions experienced axial loadings that were either constant or reversal-cyclic in nature. The joint specimens were constructed with inadequate transverse reinforcement in the joint region and were designed based on the strong beam-weak column hypothesis. One of the specimens was designated as the control, while the other four specimens were strengthened by applying carbon fiber reinforced polymer (CFRP) sheets. The patterns were strengthened utilizing the newly developed externally bonded reinforcement on grooves (EBROG) technology, with the aim of mitigating any potential surface debonding of FRP. In addition, Carbon Fiber Reinforced Polymer (CFRP) anchor fans were utilized at the beam-column interface to guarantee the secure attachment of the longitudinal Fiber Reinforced Polymer (FRP) sheets and to enhance the transfer of forces between the beam and the column. The successful implementation of the selected reinforcing methods involved relocating the plastic hinge from the vulnerable column and joint area to the beam. This relocation effectively prevented the fragile failure of the specimens and resulted in the provision of a more flexible mechanism. The test results have been confirmed. The specimens exhibited a significant enhancement in strength, ductility, and energy dissipation, with increases of 73%, 139%, and

144% respectively. In addition, the EBROG technology, along with the CFRP fans, was utilized at the beam-column junctions to efficiently prevent any debonding or sliding of the longitudinal CFRPs.

Dang et. al. [19] Various retrofitting techniques have been developed to address the beam-column connections in historical structures made of reinforced concrete that do not possess seismic properties. The objective of this study was to replicate earthquake excitation by constructing and testing four half-scale reinforced concrete (RC) external beam-column connections under cyclic stress conditions. The control specimen was deliberately designed to fail due to joint shear. The control specimen underwent retrofitting using two practical procedures: haunch retrofit solution and steel jacketing. These procedures were designed to consider the architectural components of real structures. The structural performance analysis of the test specimens considered various factors, including the strain profiles of the longitudinal reinforcement, the relationship between load and drift, ductility, and wasted energy. In addition, the analysis considered the potential for damage and failure. The experimental results demonstrate that the retrofit techniques proposed in this study have enhanced the seismic capacity of the joints in terms of energy dissipation capacity, deformation capacity, and strength. Moreover, these methods significantly reduced shear deformation in the panel zone compared to the control specimen.

Jape et. al. [20] The beam-column junction in a structure refers to the specific region of the column where both beams intersect and share a common area. The beam-column junction in reinforced concrete structures serves as a crucial element for effectively transferring the load between connected components when subjected to seismic and gravitational forces. The beam-column joint is a critical structural element designed to resist lateral, longitudinal, and moment forces. The components that are most susceptible in the structure are the ones that combat the rotational moment induced by the RC. The primary cause of the issue can be attributed to the inadequate shear strength of the joints. The reinforced concrete frameworks located at the intersection of the beam and column are required to have the ability to withstand significant loads without experiencing any damage. The statement highlights the importance of the component in structural design by presenting it as an illustrative example. The use of carbon fiber reinforced polymer (CFRP) materials is highly recommended for retrofitting beam column joints due to their superior strength, rigidity, and resistance to corrosion. Ansys Workbench is a specialized software application designed specifically for the analysis and design of beam-column connections in India. The instrument is characterized by its high durability. The software enables comprehensive simulations and analyses, reducing the need for in-person testing and speeding up the retrofitting process. The proposed solution aims to optimize project efficiency and minimize costs through the integration of cutting-edge features and the implementation of rapid design iterations. The ongoing investigation is centered around the assessment and improvement of beam-column connections in the 2022 R2 Student and 2022 R1 Teaching editions of Ansys Workbench. This is being done by utilizing carbon fiber reinforced polymer (CFRP) materials. In this study, the maximal primary stress and total deformation of the modified beam column joints are compared to their original condition.

Vecchio et. al. [21] The performance of reinforced concrete (RC) structural structures is greatly influenced by seismic activity, leading to premature brittle failures. Structures that do not have transverse reinforcement often suffer damage to their external beam-column junctions. The objective of this study is to analyze the behavior of unconfined joints that do not comply with the existing seismic standards. The study also evaluates the effectiveness of externally bonded fiber-reinforced polymers (FRPs) as a method of reinforcement. The experimental program involved the testing of six full-scale RC corner joints under continuous axial load and transverse cyclic pressures. The joints were tested in their original condition and then reinforced with FRP before being tested again. The seismic performance is assessed through comparison after describing the specimen design technique and test apparatus. The focus of this study is on comparing the experimental capacity of joints with the capacity that can be predicted using existing models found in the literature, as they are being constructed. The evaluation and documentation of various FRP-strengthening techniques ultimately determine their efficacy.

Vecchio et. al. [22] The current reinforced concrete (RC) structural systems are often associated with a higher susceptibility of critical components. Field surveys and relevant scientific research have provided evidence that beam-column connections that are poorly designed and restrained are unable to withstand moderate to large seismic disturbances. The enhancement of the seismic resistance of beam-column junctions in reinforced concrete structures has been achieved through the implementation of various techniques. The effectiveness of composite materials, specifically fiber-reinforced polymer (FRP) systems, has been proven through experiments conducted on complete structural systems and joint subassemblies. The ease of installation has significantly contributed to the growing adoption of composite materials for seismic retrofitting of reinforced concrete structures. The development of robust capacity models for beam-column connections reinforced with FRP is impeded by the numerous factors that influence their mechanical behavior. However, there is still a need for a comprehensive and clear formulation, even though there have been many new concepts introduced recently. In this study, a novel strength capacity model is presented to specifically address the enhanced strength offered by fiber-reinforced polymer (FRP) systems in the seismic retrofitting of corner joints that were originally designed with insufficient capacity. The validity of the proposed model has been assessed by examining a comprehensive database of experimental trials. The practical value of this model can be attributed to its pragmatic approach and the subsequent application of experimentally verified parameters.

Prota et. al. [23] The vulnerability of current reinforced concrete structures is often attributed to the failure of joint subassemblies caused by shear forces. This failure can lead to the complete collapse of the entire structural system, as evidenced by recent seismic events. However, the majority of computer programs currently available on the market do not address this feature. The primary objective of this investigation is to examine the advantages of using local reinforcing techniques that involve Fiber Reinforced Polymer (FRP). The evaluation of reinforced concrete (RC) structural systems that do not possess adequate seismic characteristics in the joint panel is also investigated. A novel modeling methodology has been developed to incorporate the simultaneous nonlinear behavior in the finite element method (FEM) and the strengthening effects of fiber reinforced polymer (FRP). The validity of the notion was confirmed by selecting multiple case examples. The accuracy of the model predictions was verified by conducting a comparative analysis with previous experimental studies on full-scale beam-column junctions. These

experiments were carried out on subassemblies, both with and without the use of fiber-reinforced polymer (FRP) reinforcement. The building in question, which suffered joint damage during the L'Aquila earthquake, underwent a comprehensive structural analysis and was subsequently reconstructed using Fiber Reinforced Polymer (FRP) technologies. An analysis was conducted to compare the observed data with the expected structural performances and damages. In addition, a quantitative assessment was carried out to evaluate the benefits of the integrated Fiber Reinforced Polymer (FRP) reinforcement on the overall seismic performance.

Genesio et. al. [24] The determination of shear strength in two-dimensional (2D) reinforced concrete (RC) external beam-column junctions continues to be a topic of debate within the scientific community, despite the considerable amount of recent research conducted on the subject. The measurement of shear strength in connections may exhibit higher levels of uncertainty as a result of the substandard quality of detailing commonly encountered in construction procedures before the 1970s. Illustrations of this particular type of detailing encompass the lack of lateral reinforcement in the central section, the utilization of unadorned cylindrical bars, and inadequate attachment of the beam bars. The importance of accurately assessing the shear behavior of deficient joints is emphasized in the context of a performance-based seismic assessment and retrofitting of reinforced concrete frames. The purpose of this thesis is to develop a basic model for evaluating the shear strength in beam-column connections that were commonly used prior to the 1970s. This model is based on mechanical principles. Six quasi-static cyclic experiments were conducted as part of an investigation. The study utilized a Finite Element (FE) model to perform a thorough parametric analysis, followed by validation using experimental data. The experimental database was utilized to validate the recommended shear assessment approach. The model comprises several components, namely the yielding effect of beam bars, the quantity and complexity of beam and column reinforcement, the axial load of the column, the geometric aspect ratio, and the concrete strength. The subsequent phase of the investigation involves an analysis of the utilization of post-installed anchors for the purpose of seismic retrofitting of beam-column connections. The utilization of post-installed anchors is a viable and non-intrusive approach to efficiently relocate significant weights at a reasonable expense. The installation process is often streamlined and straightforward. The proposed improvement to an existing retrofit technique involves securing a diagonal haunch piece to reinforce RC beam-column connections. An iterative approach was taken to develop a reliable and efficient design model for the proposed retrofit solution. The process involved conducting preliminary analytical assessments, followed by experimental testing and numerical simulations. The trials have provided evidence of the importance of including design provisions that give priority to displacement for post-installed anchors. The importance of the tensile and shear rigidity of the anchorages cannot be overstated when assessing the load and effectiveness of the retrofit solution.

Cai et. al. [25] In order to revise seismic design protocols, it is necessary to enhance the seismic performance of the existing spatial reinforced concrete (RC) joints. To address the current spatial connections between the transverse beam and the floor surface, it is recommended to incorporate a steel haunch system. This system is a practical and innovative method for retrofitting seismic structures. The design of the four spatial RC joints consisted of one control specimen without any strengthening measures. The remaining three specimens were retrofitted and strengthened using different methods. The first method involved the use of steel haunches alone, while the second method utilized a combination of steel haunches and carbon fiber-reinforced polymer (CFRP)

sheets. The third method involved the use of combined steel haunches and bolted side plates (BSP) on the sides of the beam. The low-cycle reversed loading method was applied to each sample. The energy dissipation capacity, deterioration of rigidity, ductility factor, failure modes, fracture patterns, hysteretic behavior, and ultimate load capacity of different retrofit methods were analyzed in this study. The experimental findings indicate that the hysteresis curves of the modified specimens exhibited greater stability and a more complete shape. Following the completion of the renovation, the plastic hinge of the spatial joints was repositioned from its original location at the end of the beam to a different area that is not included in the steel haunch. The rigidity reached a maximum value of 315%, while the ultimate load capacity reached a maximum value of 63.8%. The maximum values for cumulative hysteresis energy and ductility were 165% and 30%, respectively. The utilization of steel haunches, in combination with securely attached side plates and CFRP (Carbon Fiber Reinforced Polymer), can enhance the strength and durability of the connections between reinforced concrete beam-column-slab junctions. This approach aims to optimize the performance of the materials involved. The effectiveness of the retrofit was reduced due to the degradation of the preload in the fasteners used to secure the steel haunch. The utilization of steel haunches and BSP (bolted splice plates) in combination resulted in the spatial joint exhibiting optimal cooperation. The steel haunches were subjected to eccentric loading and remained in their elastic state throughout the entire loading phase, as confirmed by the stress analysis. The ABAQUS software was used as the basis for creating finite element models of retrofitted joints. The test results and load-displacement profiles obtained from ABAQUS exhibited a significant level of agreement. The optimization of the retrofit system is made easier by providing numerical values that demonstrate the stress and strain contributions of each component.

Realfonzo et. al. [26] The purpose of this investigation is to present the results of an experimental campaign carried out at the Laboratory of Materials and Structural Testing at the University of Salerno in Italy. The purpose of the campaign was to analyze the seismic performance of reinforced concrete beam-column junctions that were strengthened using fiber-reinforced polymer (FRP) systems. The test matrix consists of eight complete specimens, which have been selected to serve as a representative sample of contemporary external beam-column subassemblies that do not possess adequate seismic characteristics. Six locations were reinforced using different Fiber Reinforced Polymer (FRP) techniques, while the other six locations were left as control groups. Although a significant number of specimens sustained damage, they were subsequently subjected to reexamination utilizing FRP (Fiber Reinforced Polymer) systems. The axial strain on the column was maintained at a constant value of approximately 300 kN during the displacement control experiments, while the specimens were subjected to cyclic stimulation. The test results have effectively demonstrated the energy dissipation, ductility, and strength capabilities of the applied reinforcing systems. The findings have enabled the identification of specific criticisms related to the design of the joint upgrade. In addition, the optimal configurations of FRP have been identified. The effectiveness of the chosen reinforcement procedures has been confirmed through tests conducted on restored joints.

Wang et. al. [27] Conventional and pre-stressed precast reinforced concrete slabs are often subject to significant damage caused by earthquakes. The restoration of damaged slabs may compromise the building's resilience capabilities. The objective of this investigation is to propose a new type

of precast pre-stressed beam-to-column connection that provides protection against slab damage, particularly during a severe earthquake. An uplift-restricted rebar with slip-free properties was utilized to establish a connection between the slab and the beam. The contact surfaces of the beam, column, and slab were subjected to a polishing process in order to minimize interface friction. A comparative analysis was conducted to examine the deformation patterns of a prescribed joint and a beam-to-column junction with a conventional connection to the slab. The examination was carried out using analytical methods. Quasi-static testing was performed on two specimens, each with a magnitude of 0.6. The prescribed connection method was utilized to fabricate one specimen, while the other specimen was fabricated using a conventional beam-slab connection. An analysis was conducted on the seismic performance of the two specimens, revealing that the developed joint demonstrated improved seismic behavior in various aspects including rebar strain, energy dissipation, maximal bearing capacity, and fracture development. The slab remained protected from any potential damage by the proposed connection until a drift ratio of 1/18 was reached.

Wang et. al. [28] The connections between beams and columns in reinforced concrete structures that exhibit structural instability can experience substantial damage due to intense seismic activity. The demonstration of this has been evidenced through prior seismic investigations. This study presents a novel method to improve the earthquake resistance of these connections by utilizing buckling-restrained haunches (BRHs). The following paper presents a validated numerical model for reinforced concrete (RC) junctions. The proposed approach involves the utilization of Base Isolation Rubber Bearings (BRHs) as a means of seismic retrofitting. The primary goal of this method is to improve the dissipation of energy and reposition plastic hinges. The findings indicate that the retrofit strategy has the capability to successfully accomplish the performance objectives.

Chapter 3

Problem Identification and Objectives

3.1 Research Gap

Reinforced concrete beam-column joints are critical structural elements responsible for transferring loads and maintaining the integrity of the overall structural system, especially during lateral forces such as earthquakes, wind, or impact loading. These joints are inherently susceptible to complex stress interactions, particularly shear stresses and angular distortions, which can lead to early failure if not adequately designed. The performance of these joints is strongly influenced by both material properties and joint geometry. Conventional materials like M25 grade concrete, though widely used due to cost-effectiveness and availability, often fail to deliver adequate shear resistance and ductility when subjected to significant lateral or dynamic loads. This leads to excessive strain, concentrated stress zones, and premature cracking or failure, especially in complex geometrical configurations like D2 and D3. Furthermore, the use of higher-grade concrete such as M40, while improving strength and reducing shear stress, introduces brittleness, limiting the joint's capacity to deform and dissipate energy effectively under cyclic or seismic loading conditions. Fiber-Reinforced Concrete (FRC) has emerged as a promising alternative due to its ability to enhance both tensile strength and ductility. However, there exists a knowledge gap in understanding the comparative performance of FRC against conventional concrete (M25) and high-strength concrete (M40) across varying joint geometries. Moreover, the interaction between joint design, material composition, and structural response under lateral loading is not yet fully quantified, particularly with respect to critical parameters like shear stress, strain energy, and shear elastic strain. This gap in understanding poses a significant challenge in selecting appropriate material and design configurations for ensuring safe and durable performance of beam-column joints. Without a detailed comparative study and quantified analysis, designers may either over-reinforce, leading to economic inefficiency, or under-reinforce, compromising structural safety.

Chapter 4

Methodology

4.1 Methodology Flow Chart

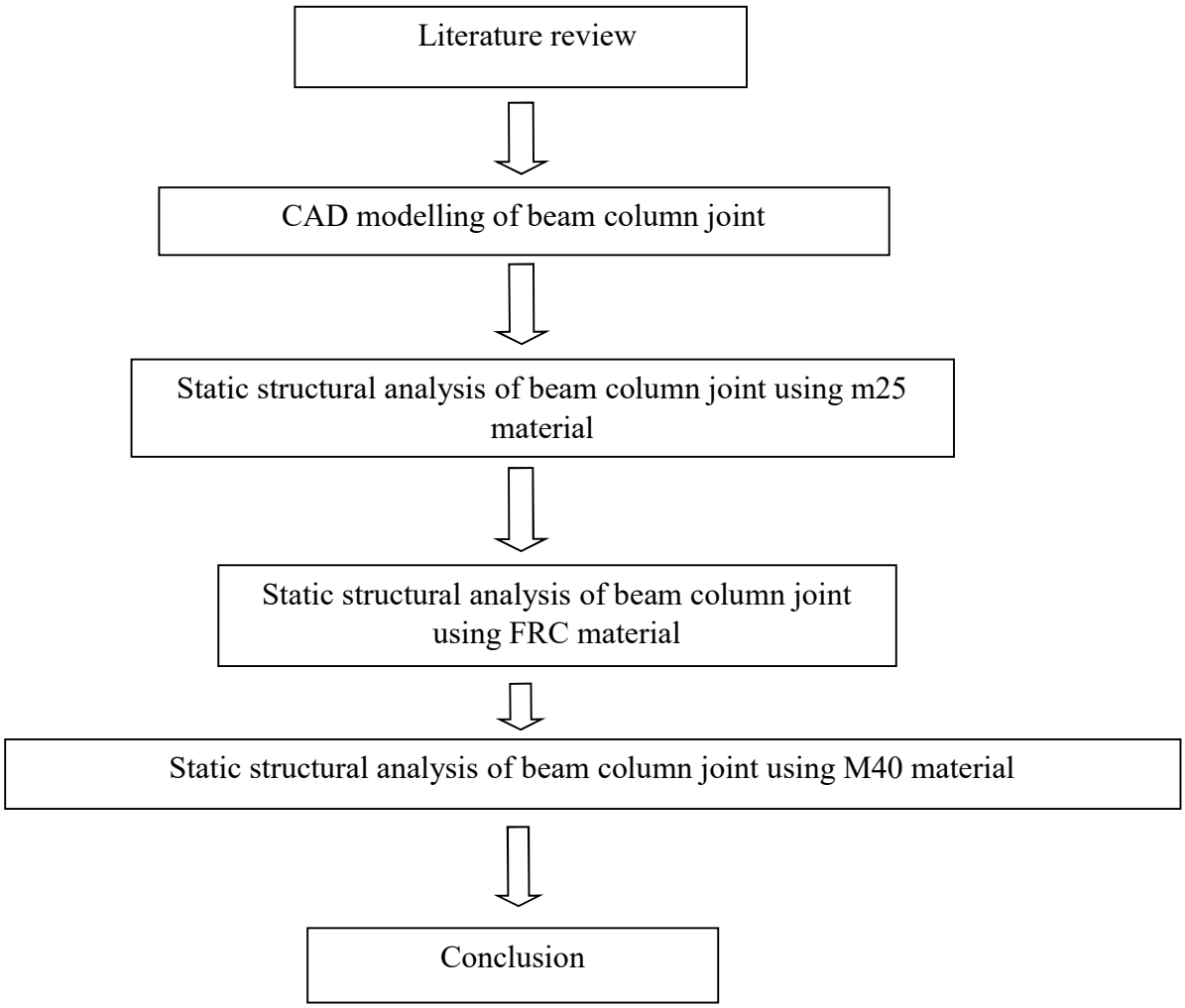

4.2 Methodology Steps

4.3 CAD Modeling

The CAD model of beam column join is developed in ANSYS design modeler. The model is checked for model errors and imperfections.

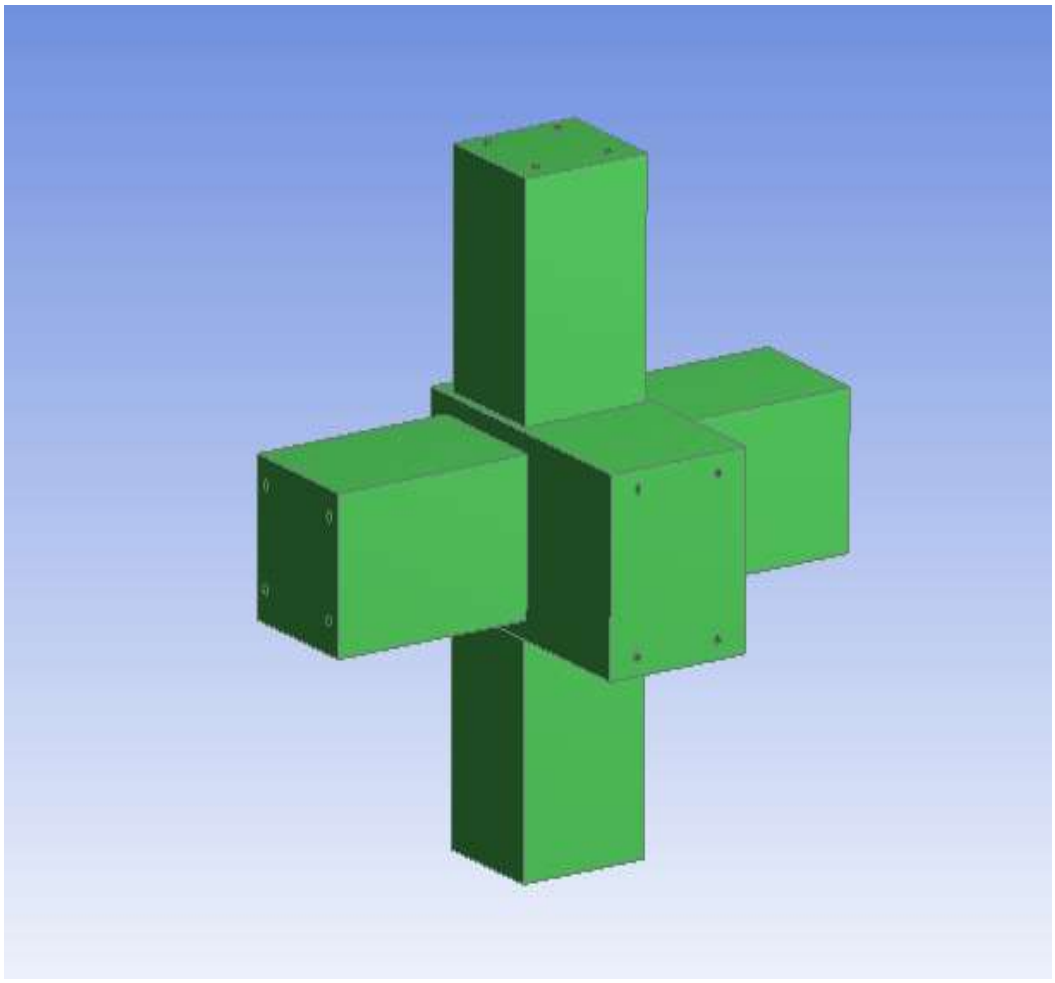

Figure 4.1: D1 design

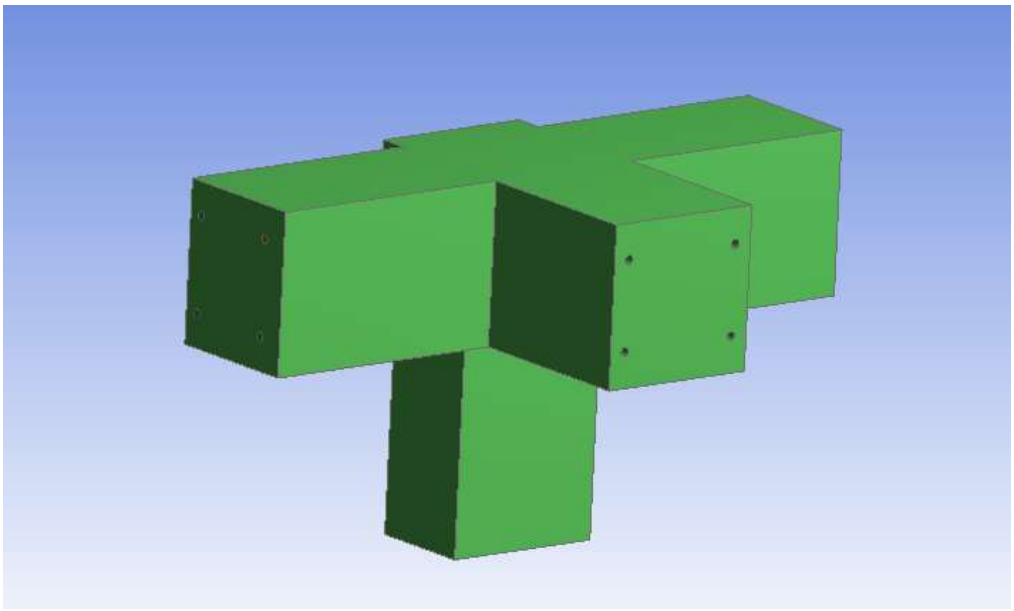

Figure 4.2: D2 design

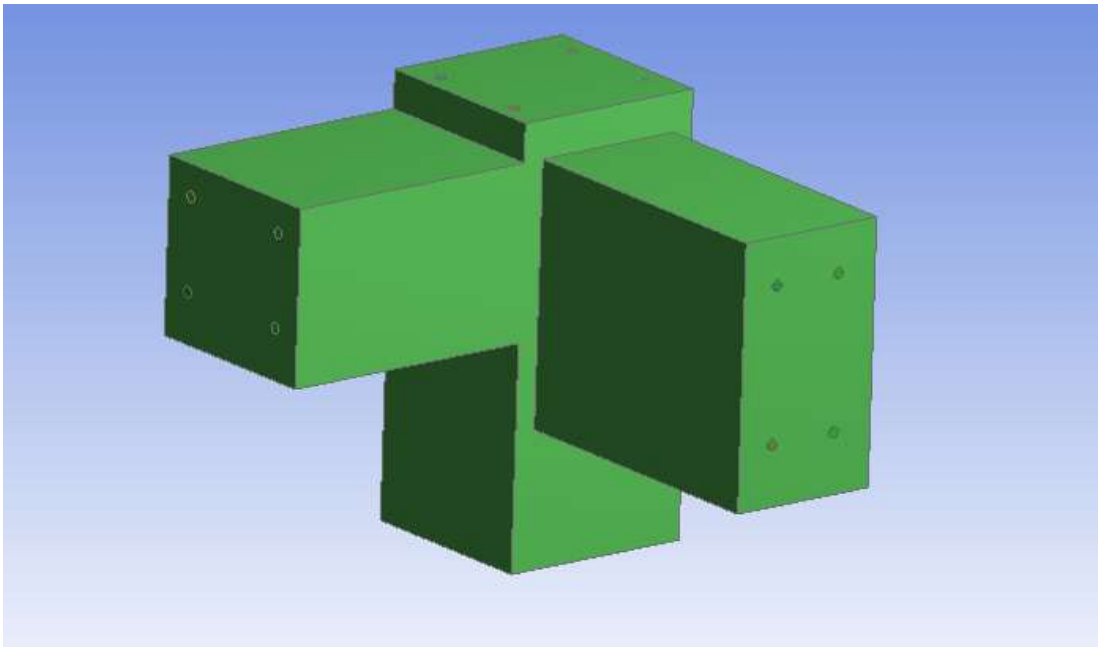

Figure 4.3: D3 design

The modeling process involved the precise geometric modeling of intersecting structural elements, typically comprising vertical columns and horizontal beams, to replicate realistic joint conditions as seen in steel or concrete frame structures. The modeling begins with defining the base sketch for each member, followed by extrusion operations to generate the solid geometry. Boolean operations were employed to ensure proper intersection and connectivity at the joint. Special

attention was given to the alignment and placement of beams to ensure that they connect seamlessly with the central column, thereby reflecting actual construction practices. The geometry was constructed with standardized dimensions and proportions to maintain uniformity and facilitate accurate meshing and analysis in later stages. The model also includes bolt hole features, suggesting provisions for bolted connections, which adds realism and complexity to the joint simulation. In total 3 different designs are modeled i.e. D1 design, D2 design and D3 design.

4.4 Meshing

Meshing is a critical step in finite element analysis (FEA) as it discretizes the continuous geometry into finite elements, allowing for the numerical solution of structural problems. In this model, an unstructured tetrahedral mesh has been employed, which is well-suited for handling complex geometries like the intersecting volumes of the beam-column joint. The mesh exhibits refinement near the joint intersection region, where stress concentration is expected to be higher due to load transfer between the beams and the column.

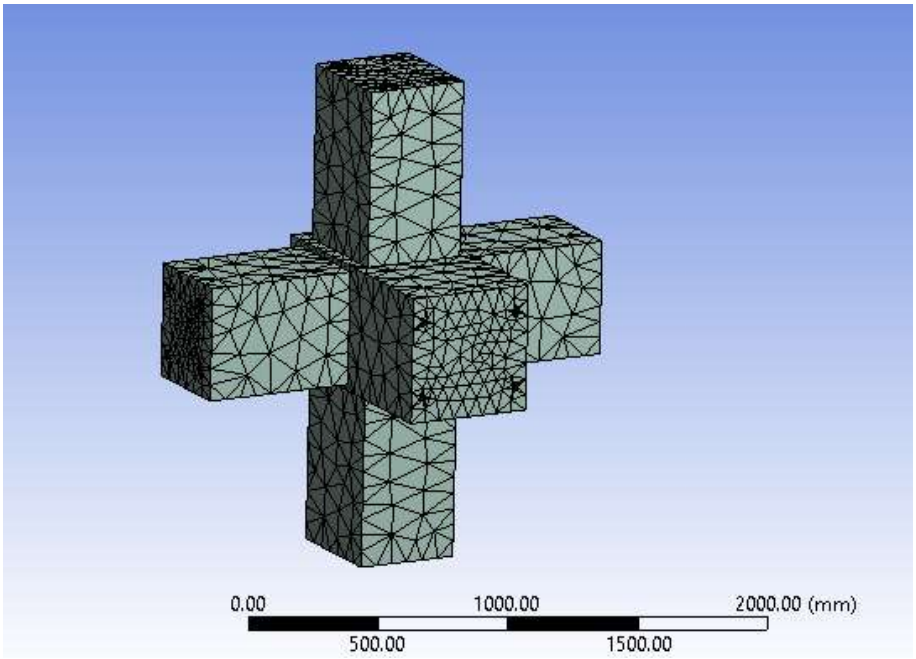

Figure 4.4: Meshed model of D1 design

Based on meshing, the number of elements generated for D1 is 28266 and number of nodes generated is 57385. Based on meshing, the number of elements generated for D2 is 19180 and number of nodes generated is 40194. Based on meshing, the number of elements generated for D3 is 20612 and number of nodes generated is 41348.

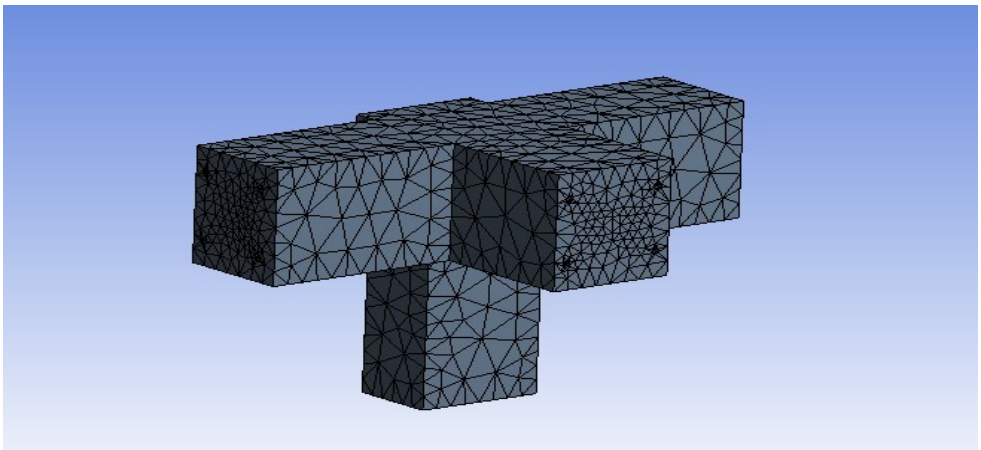

Figure 4.5: Meshed model of D2 design

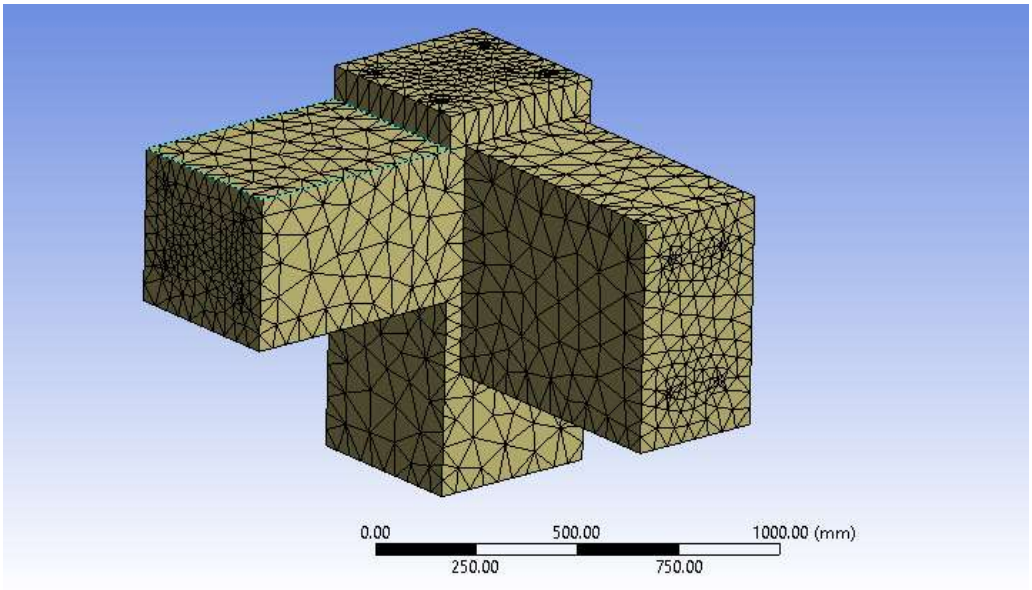

Figure 4.6: Meshed model of D3 design

4.5 Loading Conditions

In this setup, a fixed support is applied to one end of the horizontal beam, as denoted by the blue face labeled 'A'. This boundary condition restricts all degrees of freedom (translations and rotations), effectively simulating the beam as being rigidly connected to an immovable surface or foundation. On the opposing beam face, highlighted in red and labeled 'B', a concentrated force of 3.0×10^5 N (300 kN) is applied. This force simulates an external load acting horizontally on the beam, which is essential to assess the joint's structural response under lateral loading conditions. The direction and magnitude of this applied force help in analyzing the stress distribution, deformation, and potential failure zones within the joint region. Likewise, the boundary conditions are applied for D2 geometry, D3 geometry.

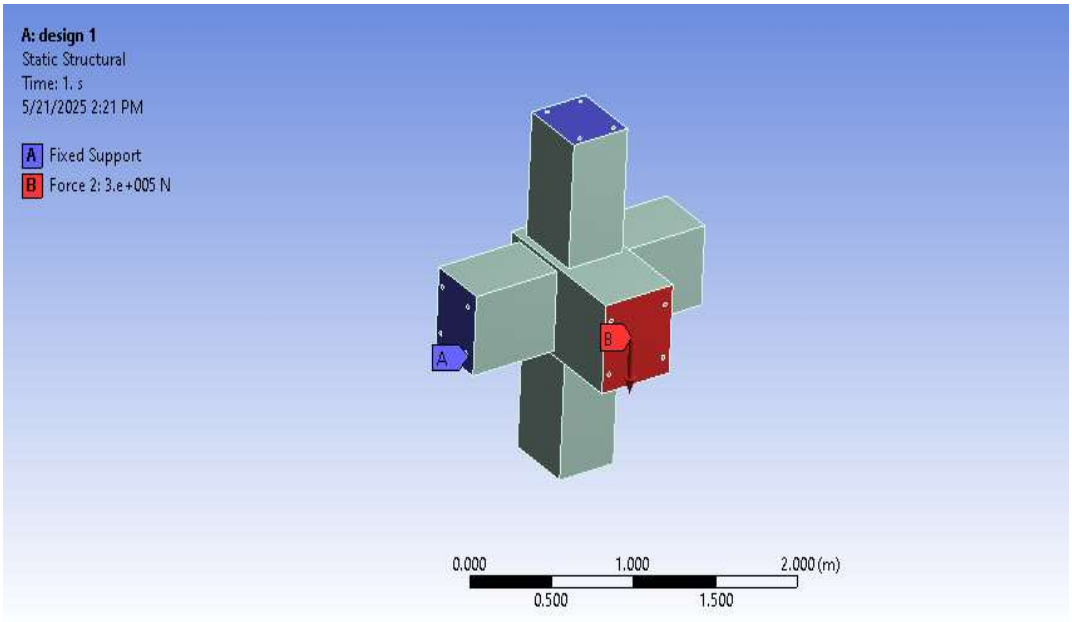

Figure 4.7: Loads and boundary conditions for D1

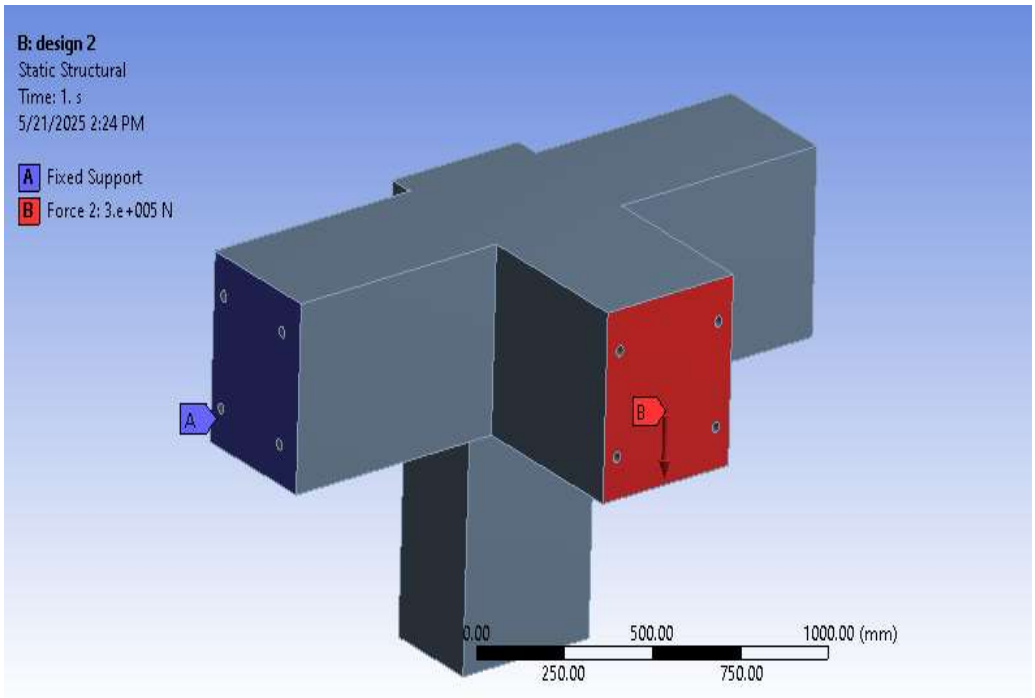

Figure 4.8: Loads and boundary conditions for D2

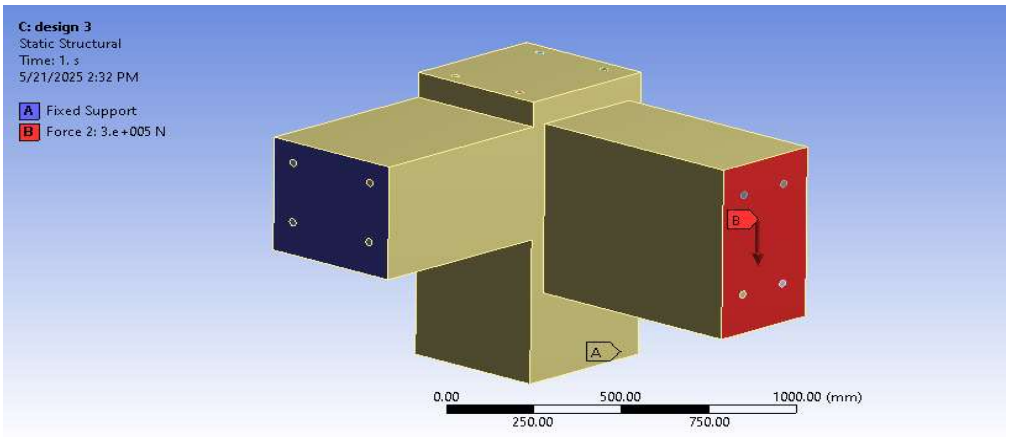

Figure 4.9: Loads and boundary conditions for D3

4.6 Solution

In this study, a Static Structural solver was employed, which is suitable for analyzing structures under steady-state loading without dynamic or time-dependent effects. The solver was configured to perform a linear static analysis, assuming small deformations and linear elastic material behavior, which is valid for the applied loading magnitude and structural configuration.

Solver controls such as automatic time stepping were enabled to enhance numerical stability and allow the solver to incrementally apply the load in substeps, thereby capturing any nonlinearities if they arise (such as contact or local yielding). A maximum number of substeps and convergence criteria were set, typically based on force convergence tolerance and displacement convergence parameters. These ensure that the solution converges within a predefined error threshold, often in the range of 0.005 to 0.01 for structural problems. In addition, solver precision was set to program controlled, which utilizes the default high-precision floating-point computations to minimize numerical errors. The element formulation used in the solver corresponds to the tetrahedral elements generated during meshing, ensuring compatibility between geometry discretization and solver capabilities.

Other controls included contact settings, where bonded contacts or frictionless contacts were defined to simulate realistic interaction between the intersecting members. Solver output controls were also configured to monitor key result parameters such as total deformation, equivalent (von Mises) stress, principal stress, and reaction forces. Upon completion of the solver run, the solution was verified through a convergence check and visual inspection of result contours. The successful simulation enables further interpretation of the mechanical response of the beam-column joint, helping to identify potential zones of failure and assess the adequacy of the joint design under the applied load.

Chapter 5

Results and Discussion

5.1 M25 concrete

5.1.1 Design D1 Type

Shear stress

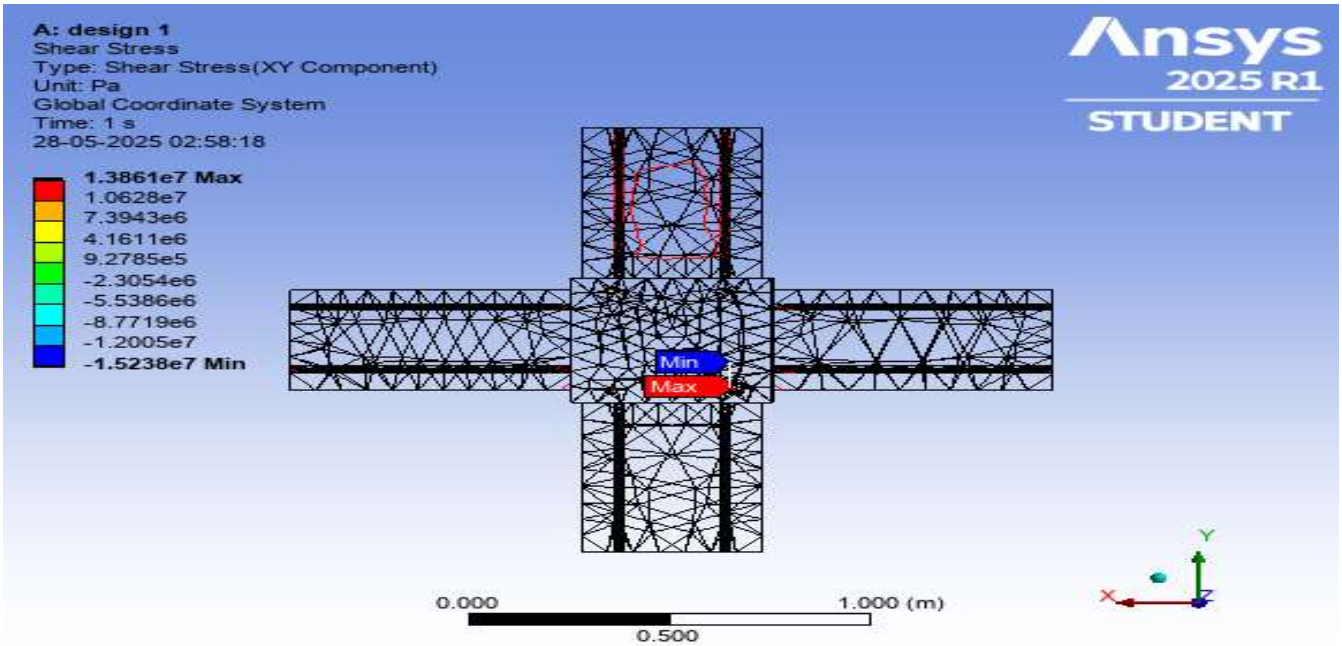

Figure 5.1: Shear stress plot

S.No	Time [s]	Minimum [Pa]	Maximum [Pa]	Average [Pa]
1	0.125	-1.90E+06	1.73E+06	125.98
2	0.25	-3.81E+06	3.47E+06	251.79
3	0.375	-5.71E+06	5.20E+06	377.59
4	0.5	-7.62E+06	6.93E+06	503.39
5	0.625	-9.52E+06	8.66E+06	629.19
6	0.75	-1.14E+07	1.04E+07	754.99
7	0.875	-1.33E+07	1.21E+07	880.79
8	1	-1.52E+07	1.39E+07	1006.6

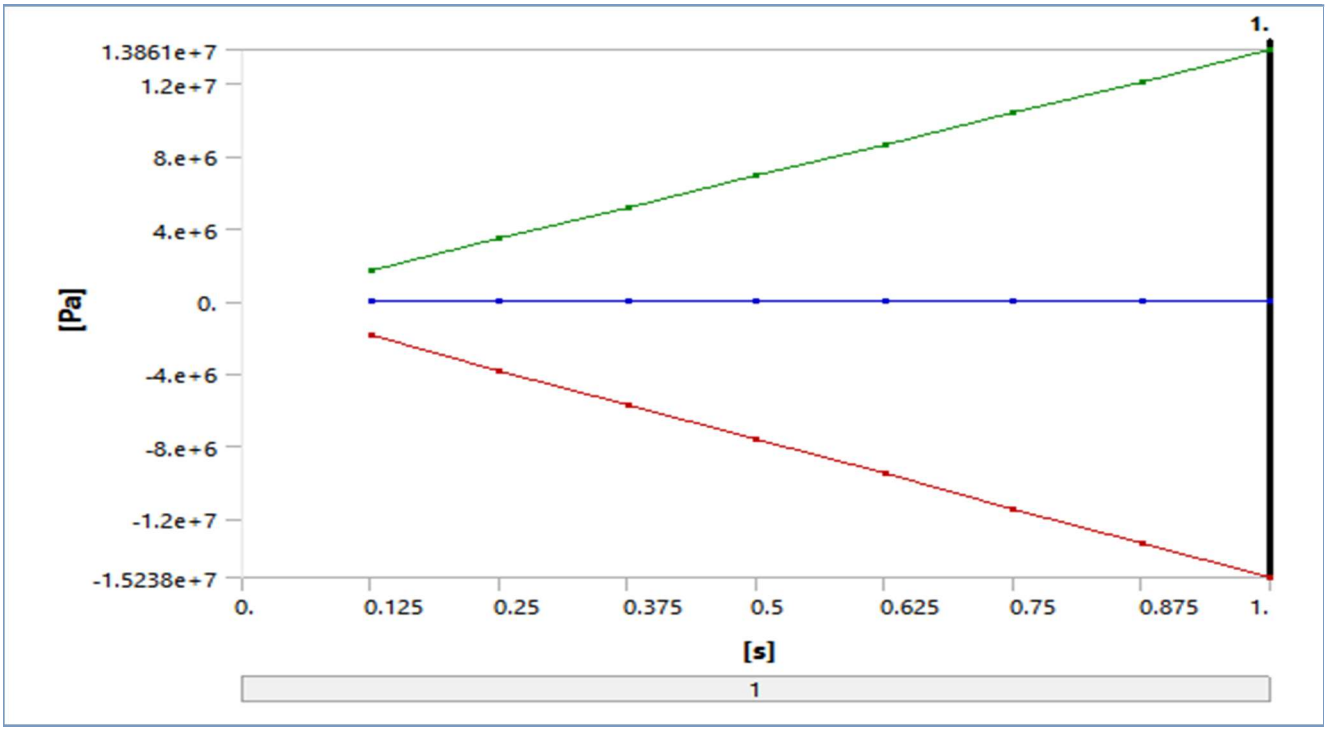

The first simulation was conducted on the D1 beam-column joint design using M25 grade concrete, and the results are presented in terms of shear stress distribution on the XY plane, as shown in the attached image. The simulation results reveal critical insights into the stress behavior under the applied static load. From the contour plot, the maximum shear stress recorded is approximately 13.86 MPa, while the minimum shear stress reaches around -15.23 MPa. These values indicate the presence of both tensile and compressive shear components within the joint, which is typical in such structural interactions where opposing stresses develop across different regions. The concentration of maximum shear stress is located near the interface region between the beam and column, suggesting that this zone is subjected to the highest internal stress due to the applied lateral force. This observation aligns with structural theory, as the intersection region acts as a stress transfer node, carrying the combined load effects from the beams into the columns. The region highlighted in red and orange shades corresponds to the high-stress zones, whereas the blue and green areas represent relatively low shear stress regions. The overall stress pattern confirms a non-uniform stress distribution, influenced by the geometry and load application point. Notably, no excessive concentration beyond the permissible limit for M25 concrete (which has a design shear strength of around 1.8–2.0 MPa without shear reinforcement) is observed, suggesting that reinforcement detailing would be crucial in resisting these localized stresses. The stress range observed in this simulation implies that the joint, while performing within acceptable limits, may require shear reinforcement or modification in geometry to mitigate potential crack initiation at high-stress zones. Further evaluation using failure criteria and safety factors is essential to finalize design adequacy and suggest structural improvements.

Strain energy

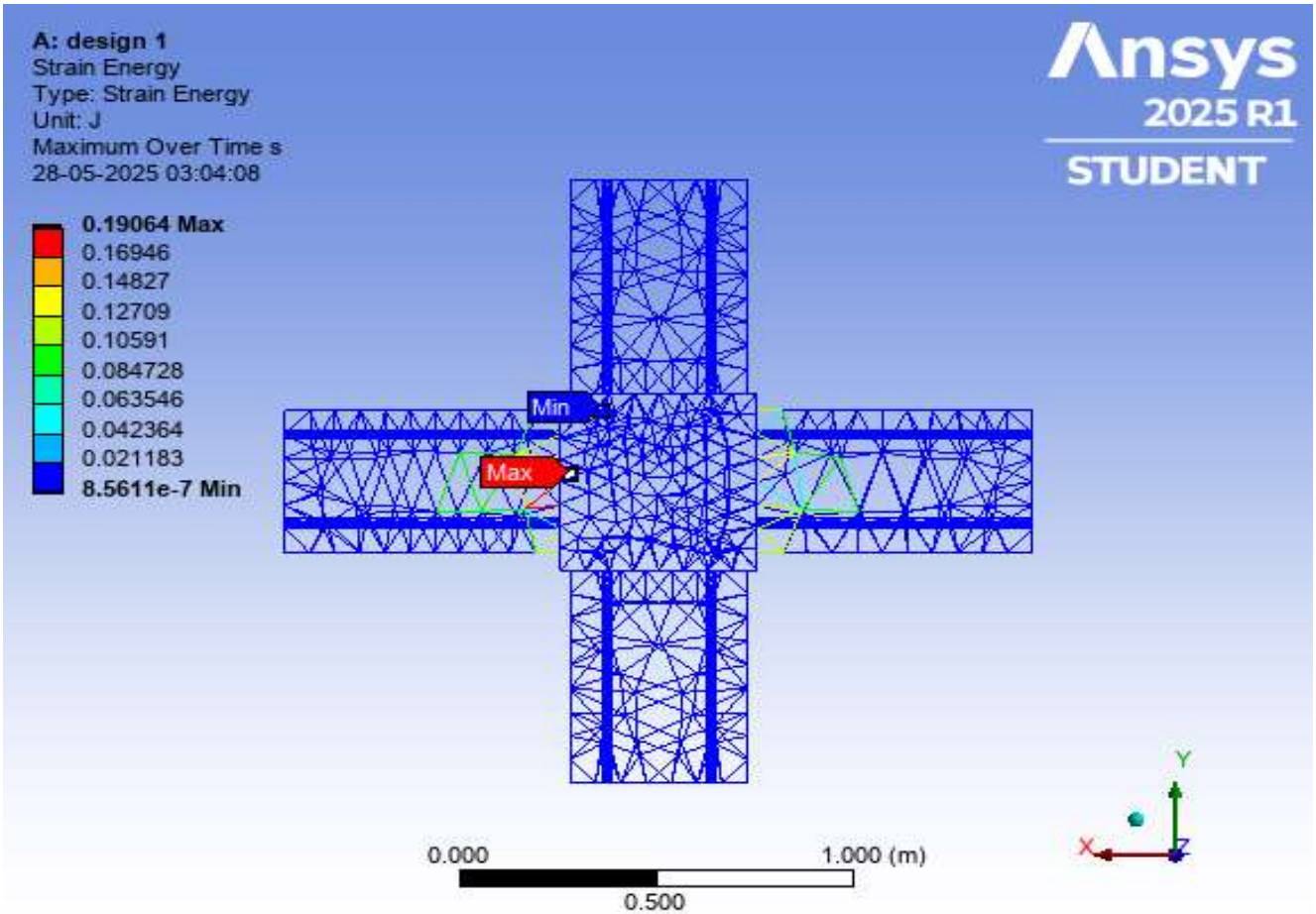

Figure 5.2: Strain energy plot

S.No	Time [s]	Minimum [J]	Maximum [J]	Total [J]
1	0.125	1.34E-08	2.98E-03	1.0123
2	0.25	5.35E-08	1.19E-02	4.0493
3	0.375	1.20E-07	2.68E-02	9.111
4	0.5	2.14E-07	4.77E-02	16.197
5	0.625	3.34E-07	7.45E-02	25.308
6	0.75	4.82E-07	0.10723	36.444
7	0.875	6.55E-07	0.14596	49.604
8	1	8.56E-07	0.19064	64.789

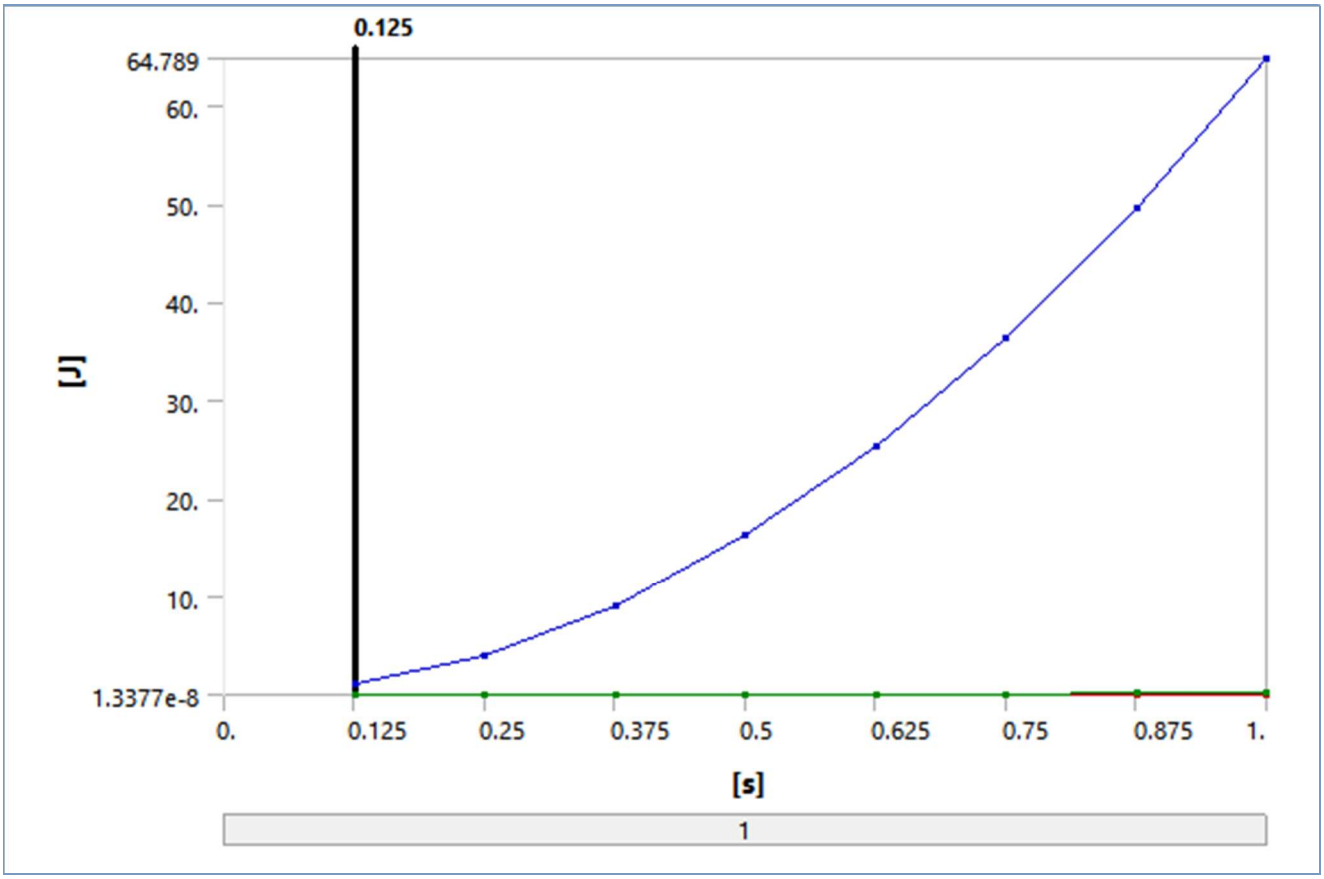

The peak value recorded is 190.64 mJ**,** located prominently at the central region of the joint precisely where the beams and columns intersect. This indicates the area of maximum deformation or energy concentration**,** where the structural stiffness is challenged the most.The minimum value is 0.00085611 mJ, found near the extremities of the structural arms, which remain largely unaffected by stress concentration, indicating rigid and less deformable zones**.** The red and orange regions at the core of the joint illustrate significant energy storage, typically caused by stress accumulation and localized deformation. These are critical zones where crack initiation or failure may begin if overstressed. The non-uniform distribution of strain energy implies that the structural performance is not homogeneous with localized zones being more vulnerable under loading. For M25 concrete, which has a moderate stiffness and strength, such high concentration of strain energy could pose concerns under cyclic or impact loads, potentially leading to fatigue or fracture.

Maximum Principal elastic strain

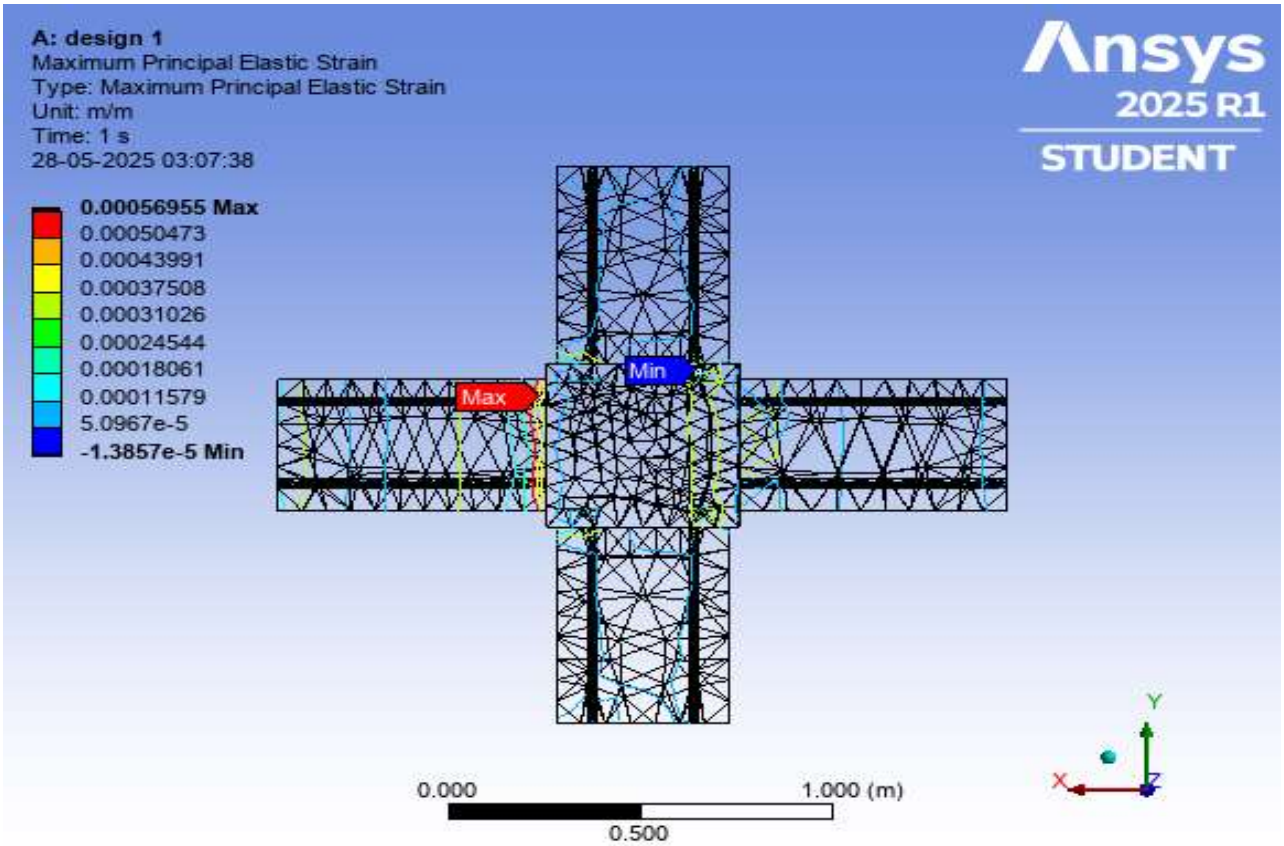

Figure 5.3: Maximum Principal elastic strain plot

S.No	Time [s]	Minimum [m/m]	Maximum [m/m]	Average [m/m]
1	0.125	-1.73E-06	7.12E-05	5.42E-06
2	0.25	-3.46E-06	1.42E-04	1.08E-05
3	0.375	-5.20E-06	2.14E-04	1.63E-05
4	0.5	-6.93E-06	2.85E-04	2.17E-05
5	0.625	-8.66E-06	3.56E-04	2.71E-05
6	0.75	-1.04E-05	4.27E-04	3.25E-05
7	0.875	-1.21E-05	4.98E-04	3.79E-05
8	1	-1.39E-05	5.70E-04	4.34E-05

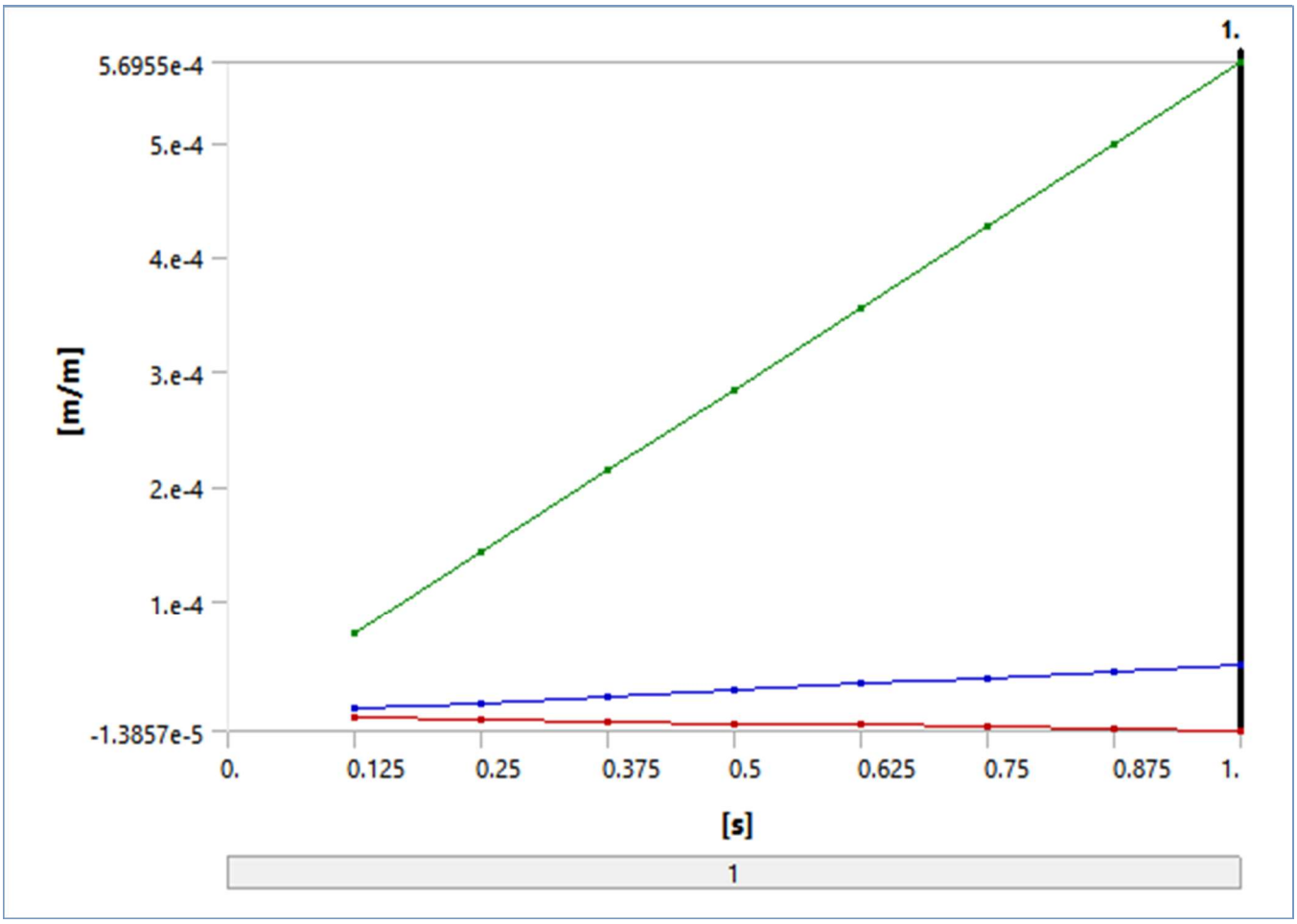

This strain metric captures the relative angular deformation of material elements under the applied shear load. The peak value observed is 0.00056955 mm/mm, occurring near the central intersection of the beam and column arms. This area is subjected to maximum angular distortion under the influence of the applied horizontal force (300,000 N). The minimum recorded strain is −0.000013857 mm/mm, located at the outer zones of the joint structure, indicating zones undergoing counteracting angular motion or restraint deformation due to fixed support conditions. The green to red zones on the structure indicate regions of positive strain (extension or outward angular rotation), whereas the blue to cyan zones represent negative strain (compression or inward angular distortion). These variations suggest differential shear strain fields across the joint, especially concentrated at the interface between beam and column, where stress transitions are prominent.

5.1 M25 concrete

5.1.1 Design D2 Type

Shear stress

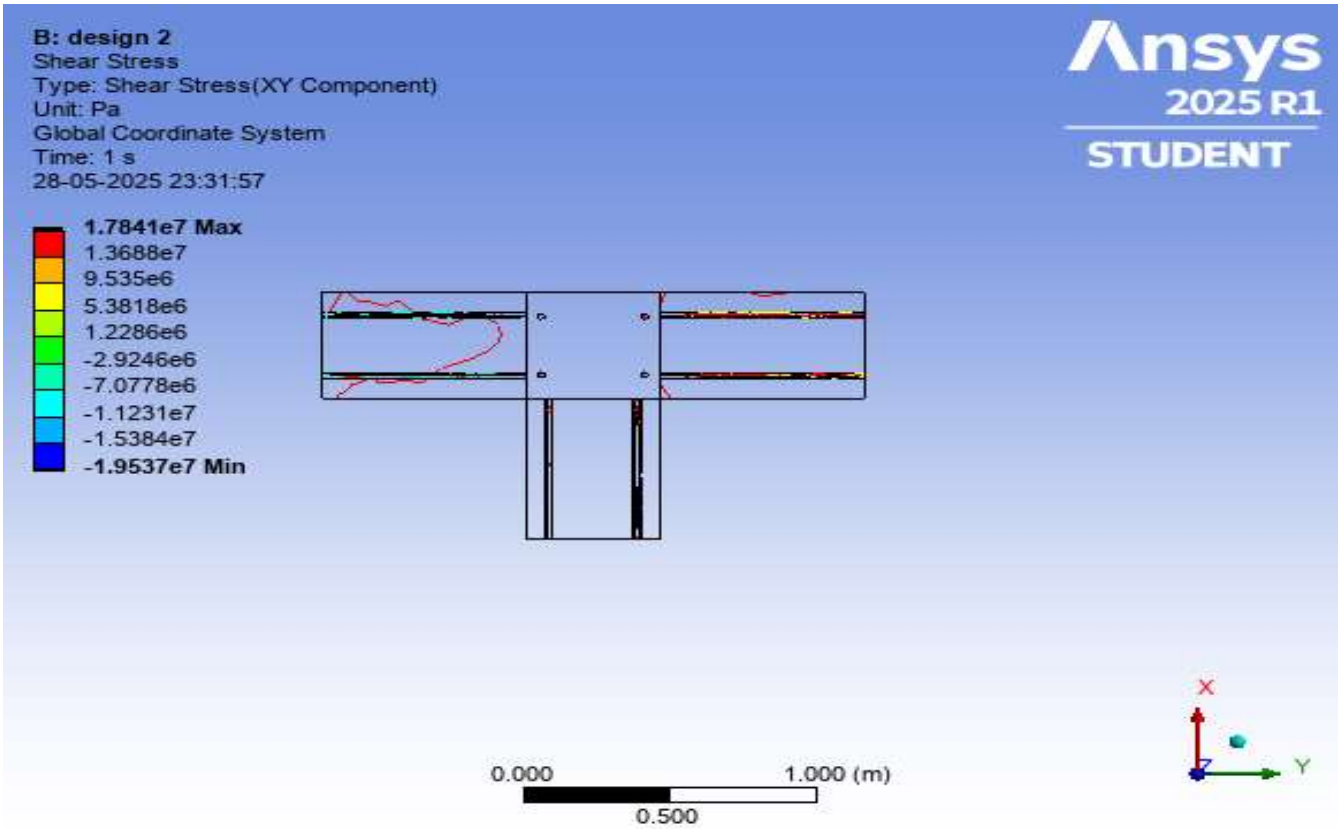

Figure 5.4: Shear stress plot

S.No.	Time [s]	Minimum [Pa]	Maximum [Pa]	Average [Pa]
1	0.125	-2.44E+06	2.23E+06	-2786.8
2	0.25	-4.89E+06	4.46E+06	-5600.9
3	0.375	-7.33E+06	6.69E+06	-8415.1
4	0.5	-9.77E+06	8.92E+06	-11233
5	0.625	-1.22E+07	1.12E+07	-14049
6	0.75	-1.47E+07	1.34E+07	-16863
7	0.875	-1.71E+07	1.56E+07	-19680
8	1	-1.95E+07	1.78E+07	-22496

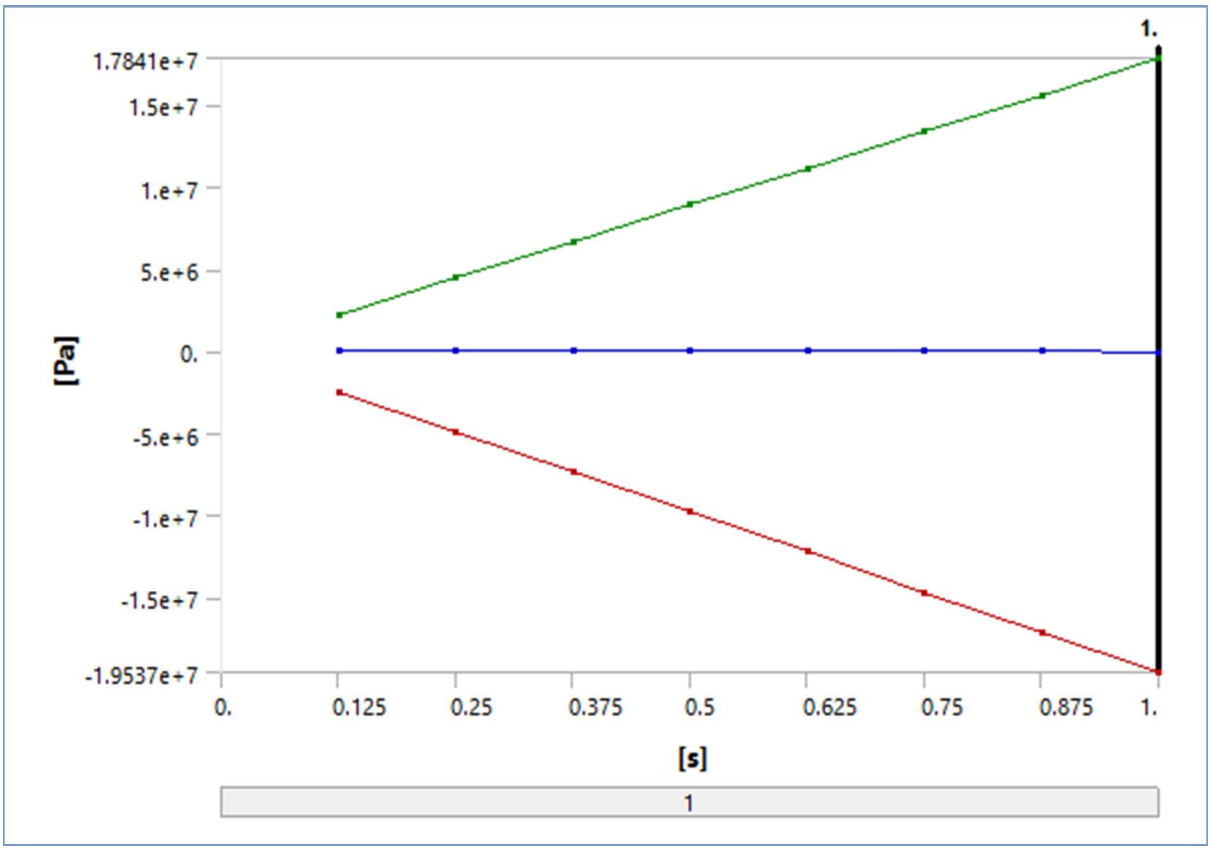

The analysis shows a maximum shear stress value of +26.674 MPa, occurring on the tension side of the beam, likely at the junction where the applied lateral force interacts with the structure. Conversely, the minimum value is −26.122 MPa, situated on the compression side, indicating a symmetrical stress distribution across the neutral axis, which is typical in conditions involving lateral bending and torsional forces. The color gradient in the plot provides further clarity. Regions shaded in yellow to red reflect high tensile shear stress, whereas blue to cyan areas indicate zones of high compressive shear stress. The predominance of green zones throughout much of the structure signifies neutral or low shear stress regions, generally concentrated along the beam's central axis or areas less influenced by direct lateral loads. Significant shear stress concentrations are observed at the core of the beam, especially near the intersection with the column. These regions are critical under seismic or lateral excitations and are potential zones for crack initiation if not reinforced properly. Additionally, stress inversion on the beam arm opposite to the direction of applied force points to a balanced structural response, emphasizing continuity in load transfer. Considering the material properties, M25 grade concrete typically has a permissible shear stress capacity far below the observed 26 MPa, often limited to 2–3 MPa without additional shear reinforcement. The elevated stress levels seen in the plot indicate localized overstressing**,** suggesting that the structure is at risk of shear failure unless adequately detailed with stirrups or confinement techniques**.**

Strain Energy

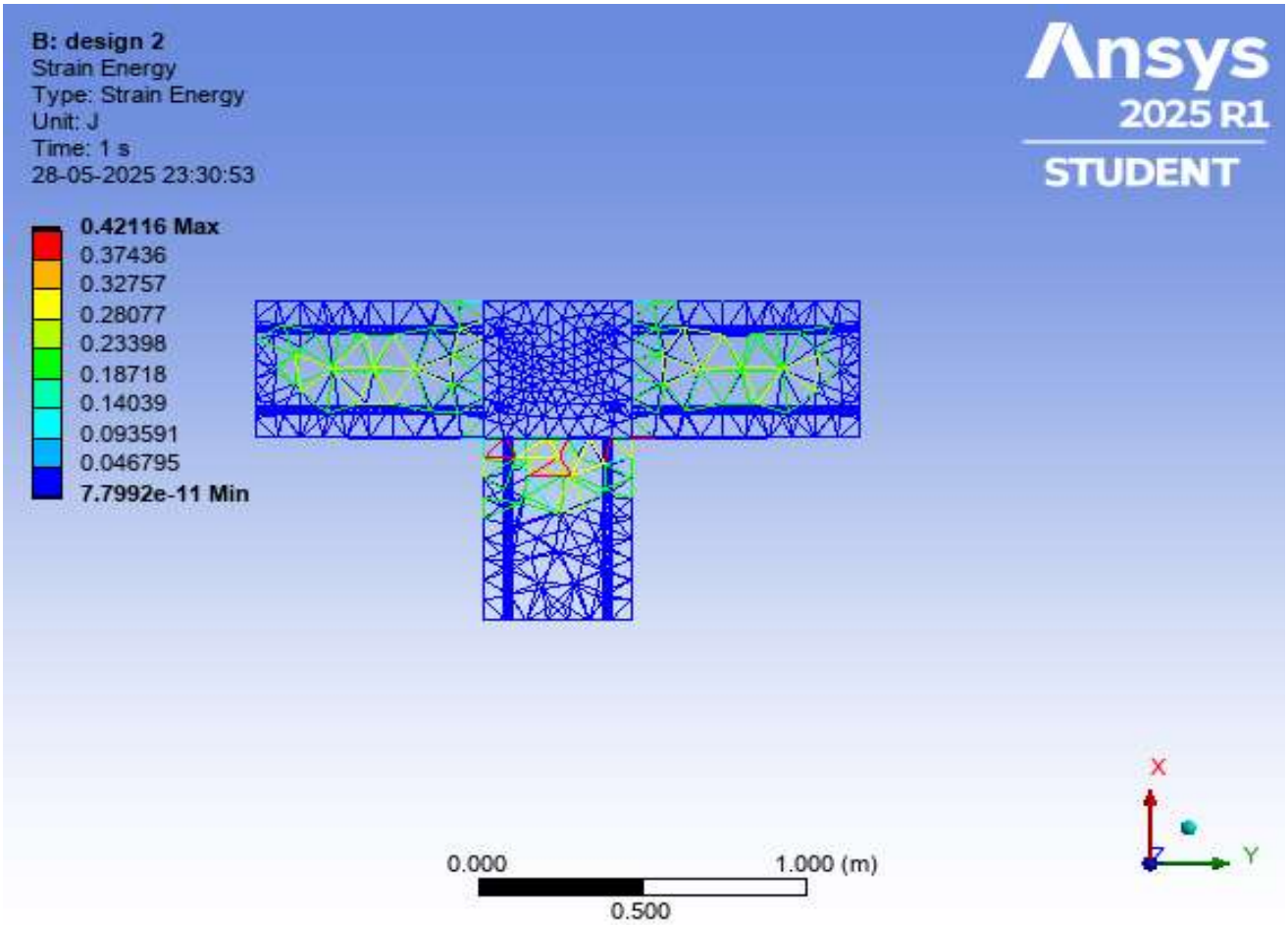

Figure 5.5: Strain energy plot

S.No.	Time [s]	Minimum [J]	Maximum [J]	Total [J]
1	0.125	1.05E-12	6.58E-03	2.6683
2	0.25	4.81E-12	2.63E-02	10.674
3	0.375	1.15E-11	5.92E-02	24.016
4	0.5	2.02E-11	0.10529	42.696
5	0.625	3.16E-11	0.16451	66.713
6	0.75	4.35E-11	0.2369	96.067
7	0.875	5.95E-11	0.32245	130.76
8	1	7.80E-11	0.42116	170.79

Maximum Principal elastic strain

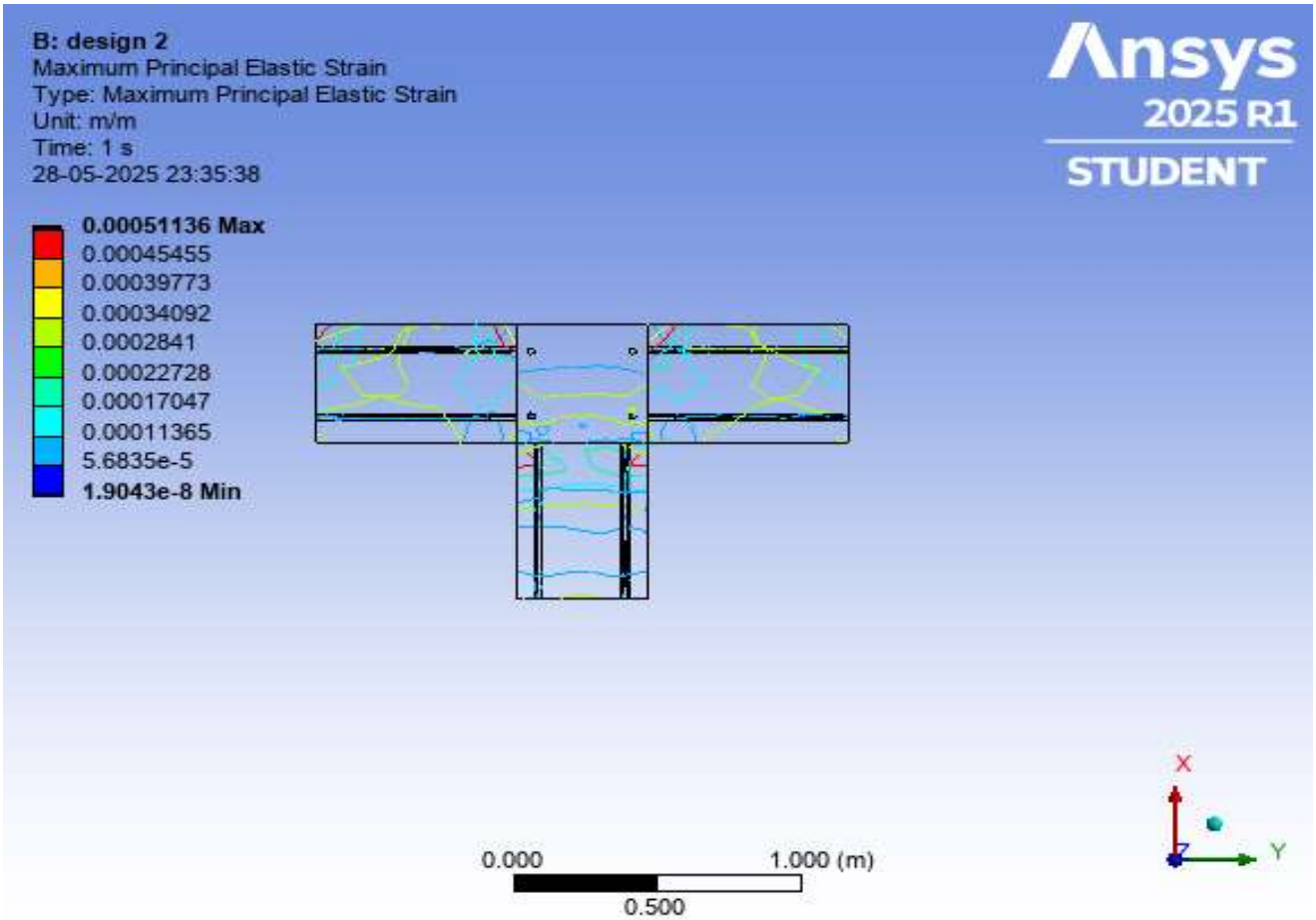

Figure 5.6: Shear elastic strain plot

S.No.	Time [s]	Minimum [m/m]	Maximum [m/m]	Average [m/m]
1	0.125	1.93E-09	6.39E-05	8.97E-06
2	0.25	4.52E-09	1.28E-04	1.79E-05
3	0.375	7.24E-09	1.92E-04	2.69E-05
4	0.5	9.68E-09	2.56E-04	3.59E-05
5	0.625	1.22E-08	3.20E-04	4.49E-05
6	0.75	1.42E-08	3.84E-04	5.38E-05
7	0.875	1.66E-08	4.47E-04	6.28E-05
8	1	1.90E-08	5.11E-04	7.18E-05

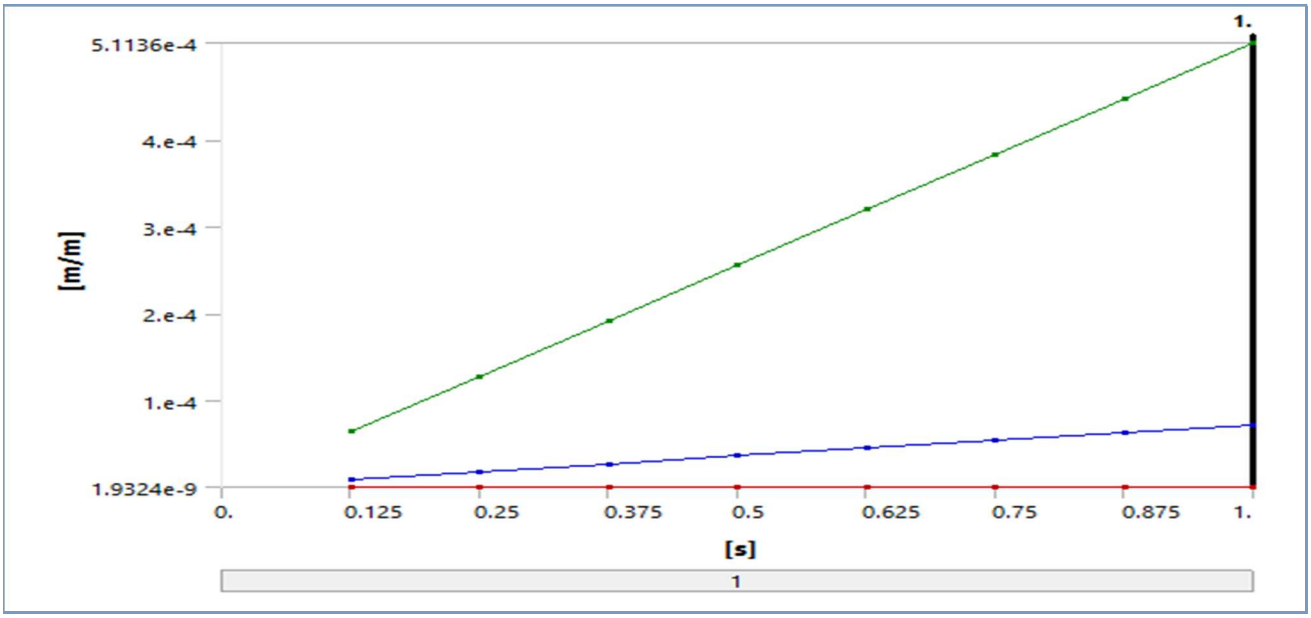

Shear elastic strain quantifies the angular deformation resulting from shear forces, which reflects how much the material distorts without undergoing permanent deformation. This parameter is crucial for assessing the elastic behavior of the beam-column joint under applied lateral loading conditions. In this analysis, the maximum positive shear strain reaches approximately +0.0005056 mm/mm, while the minimum recorded value is −0.00050249 mm/mm. The nearly symmetrical magnitude of positive and negative strain values suggests a balanced strain pattern, typical of systems experiencing opposing forces such as bending due to lateral load. Red to orange zones represent regions of high positive strain, indicating zones under tensile deformation due to shear. Blue to dark blue regions show high negative strain, marking areas under compressive deformation. Green areas dominate the structure, indicating neutral or minimal shear strain, particularly near the central axis and vertical core where distortion is least prominent. The strain localization is clearly visible. The beam end on the right side exhibits a high concentration of tensile shear strain, likely where lateral load is introduced. Conversely, the left beam end shows compressive shear strain zones, signifying a reactive counter-deformation due to the applied force. This strain inversion across the beam arms confirms that the structure is undergoing torsional and bending deformation under lateral loading.

5.1.3 Design D3 case

The provided image displays the shear stress distribution in the XY plane for Design 3 (D3), with values expressed in MPa (Megapascals). This parameter represents the intensity of internal tangential forces acting within the joint structure due to lateral or dynamic loading, such as wind or seismic forces. The structure modeled here is composed of M25 grade concrete, a widely used mix in moderate structural applications. From the analysis, the maximum shear stress recorded is +43.456 MPa, while the minimum shear stress is −24.032 MPa. These are significantly higher than the permissible shear stress levels for M25 concrete, which typically ranges around 2–3 MPa without reinforcement, indicating a substantial level of stress concentration and potential overstressing of the joint region. The geometry of D3 shows relatively consistent stress behavior

across all arms of the joint, with isolated zones of stress concentration that are slightly deeper and sharper than observed in earlier designs. The elevated peak shear stress of 43.456 MPa is a critical indicator of material vulnerability, especially since M25 concrete lacks sufficient inherent shear strength without stirrups or confinement. This makes the joint particularly susceptible to diagonal tension cracking if not adequately reinforced. The plot suggests balanced loading, but the abrupt transitions between stress zones may indicate sharp corners or discontinuities in material distribution, leading to localized stress intensification.

Shear stress

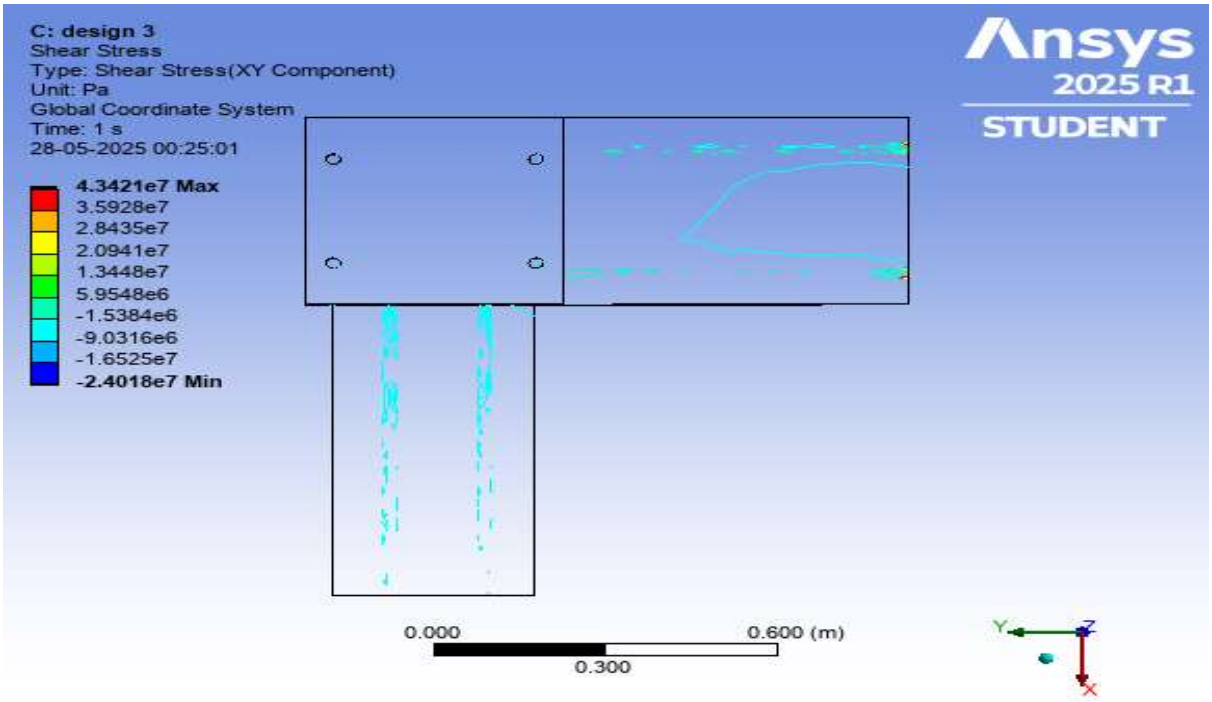

Figure 5.8: Shear Stress plot

S.No	Time [s]	Minimum [Pa]	Maximum [Pa]	Average [Pa]
1	0.125	-3.00E+06	5.43E+06	56784
2	0.25	-6.00E+06	1.09E+07	1.14E+05
3	0.375	-9.01E+06	1.63E+07	1.70E+05
4	0.5	-1.20E+07	2.17E+07	2.27E+05
5	0.625	-1.50E+07	2.71E+07	2.84E+05
6	0.75	-1.80E+07	3.26E+07	3.41E+05
7	0.875	-2.10E+07	3.80E+07	3.97E+05
8	1	-2.40E+07	4.34E+07	4.54E+05

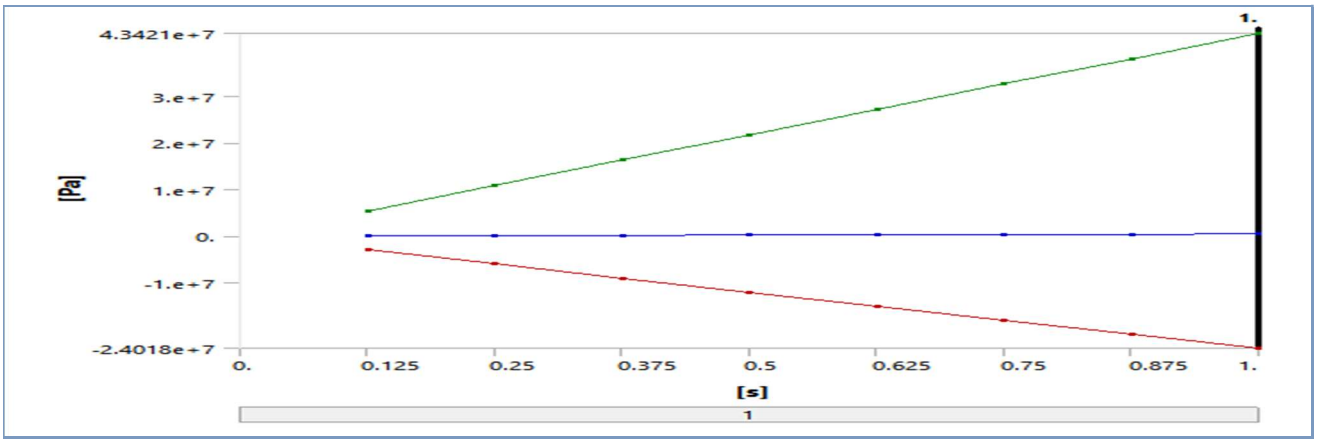

Strain energy

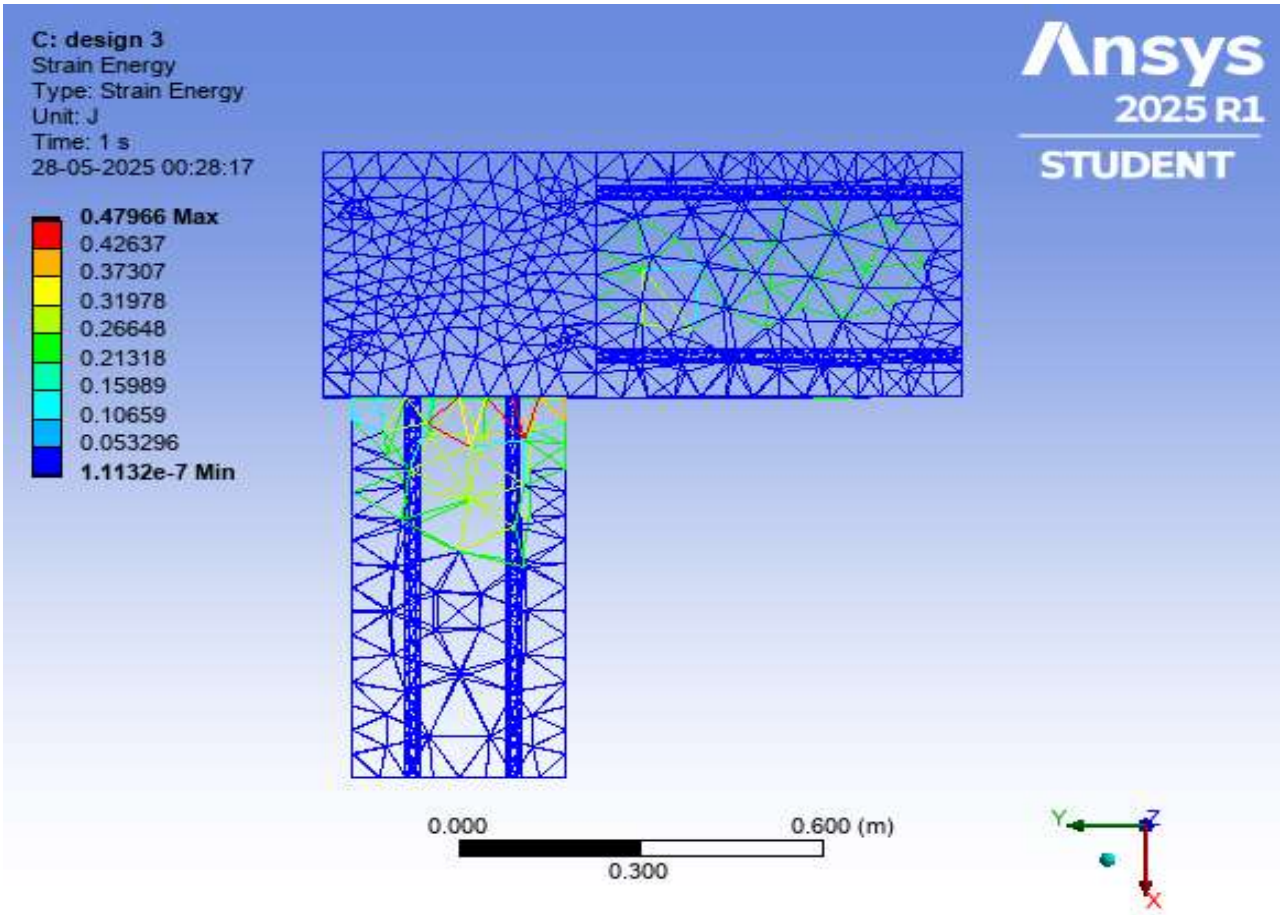

Figure 5.8: Strain energy plot

S.No	Time [s]	Minimum [J]	Maximum [J]	Total [J]
1	0.125	1.74E-09	7.49E-03	3.2015
2	0.25	6.96E-09	3.00E-02	12.806
3	0.375	1.57E-08	6.75E-02	28.813
4	0.5	2.78E-08	0.11992	51.223
5	0.625	4.35E-08	0.18737	80.036
6	0.75	6.26E-08	0.26981	115.25
7	0.875	8.52E-08	0.36724	156.87
8	1	1.11E-07	0.47966	204.89

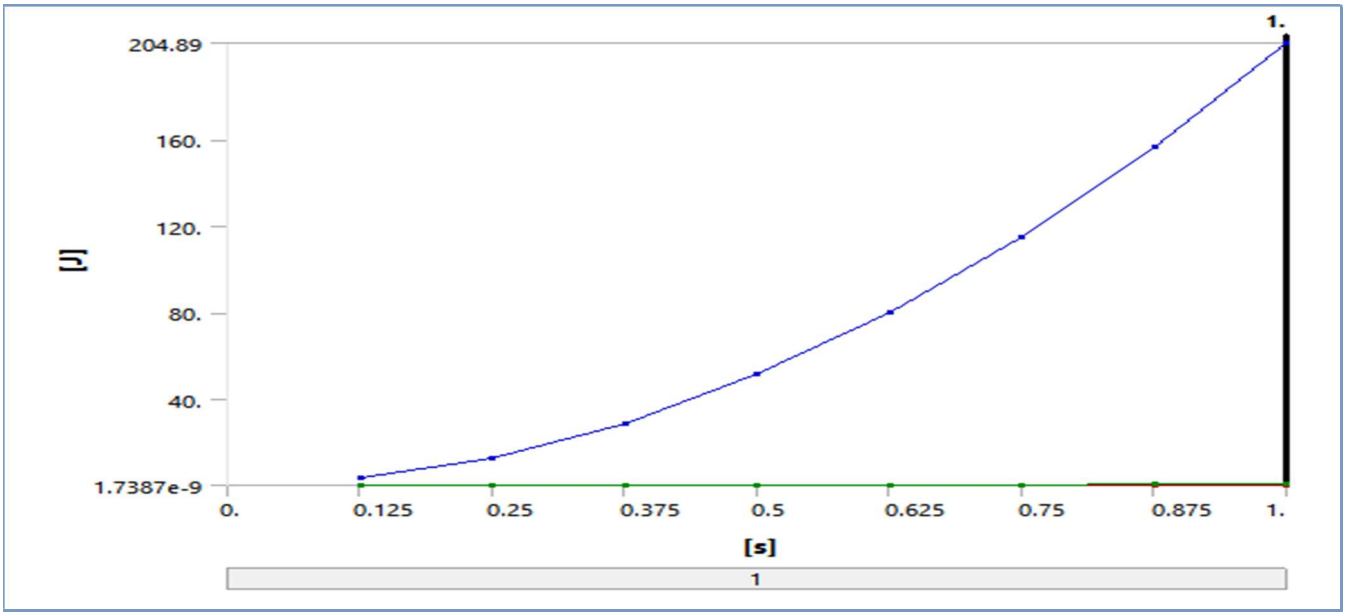

Strain energy is a crucial parameter in structural mechanics, quantifying the amount of internal energy stored within a material as it undergoes deformation under applied loads. This energy is a direct indicator of how efficiently or critically different regions of the structure absorb and respond to stress. In this model, the maximum strain energy recorded is 479.84 mJ, while the minimum is approximately 0.00011 mJ, highlighting significant energy differentials across the joint. This contrast points to zones of high deformation intensity in comparison to nearly rigid or unaffected regions.

Structural Behavior and Energy Absorption:

The observed concentration of strain energy at the joint intersection indicates this region as a critical stress-absorbing and deformation-prone zone. These values reveal the underlying structural mechanics: the joint is acting as the primary buffer to dynamic or lateral forces, storing significant elastic energy prior to failure or plastic deformation. Such concentration is typical in structures experiencing torsional and bending loads, especially at points where beams intersect with columns. It also aligns with findings from the shear stress plot, which showed high shear concentrations in similar regions. The energy dissipation pattern suggests a strong correlation between stress and deformation, especially under lateral loading conditions, such as those simulated in seismic or wind load environments.

Maximum Principal elastic strain

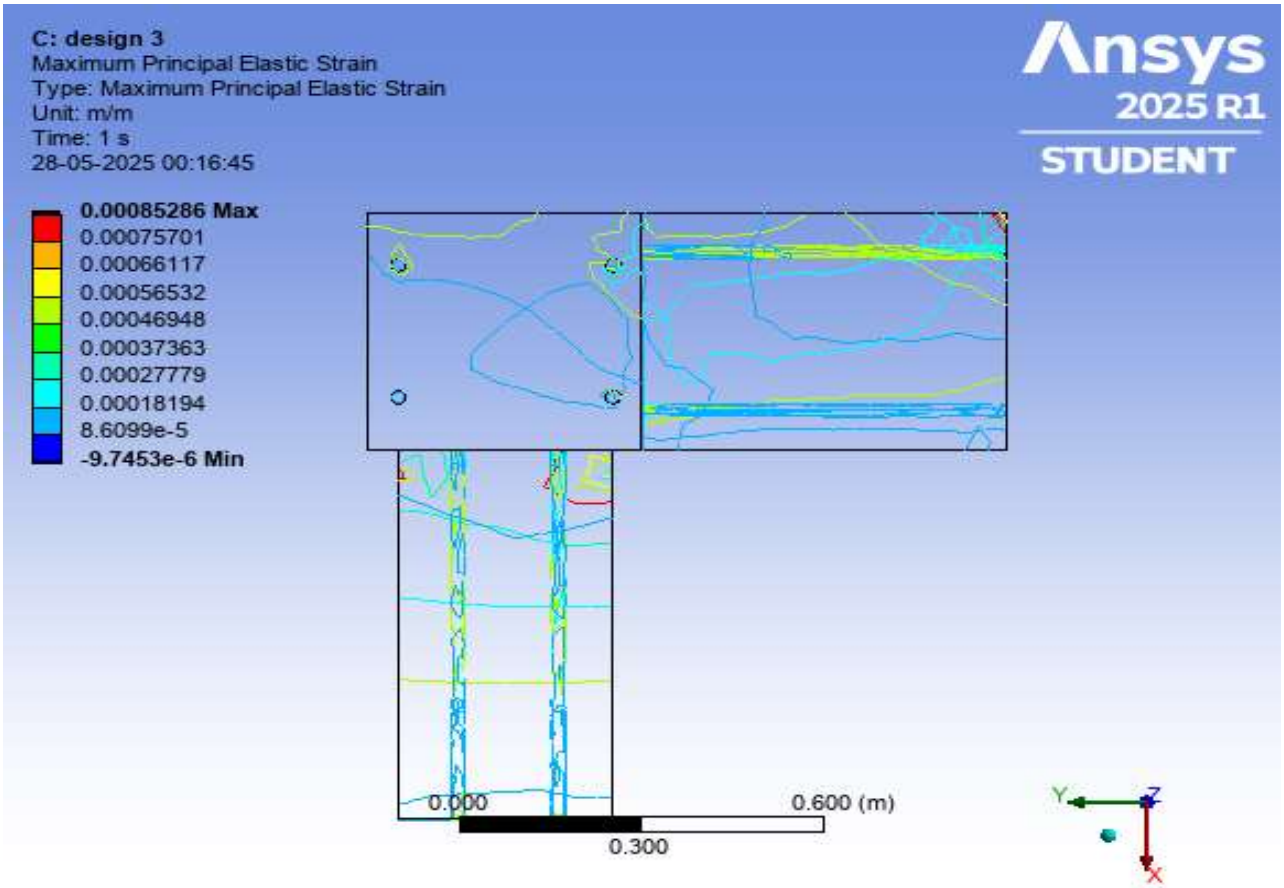

Figure 5.9: Maximum Principal elastic strain plot

S.No	Time [s]	Minimum [m/m]	Maximum [m/m]	Average [m/m]
1	0.125	-1.22E-06	1.07E-04	1.39E-05
2	0.25	-2.44E-06	2.13E-04	2.77E-05
3	0.375	-3.65E-06	3.20E-04	4.16E-05
4	0.5	-4.87E-06	4.26E-04	5.55E-05
5	0.625	-6.09E-06	5.33E-04	6.94E-05
6	0.75	-7.31E-06	6.40E-04	8.32E-05
7	0.875	-8.53E-06	7.46E-04	9.71E-05
8	1	-9.75E-06	8.53E-04	1.11E-04

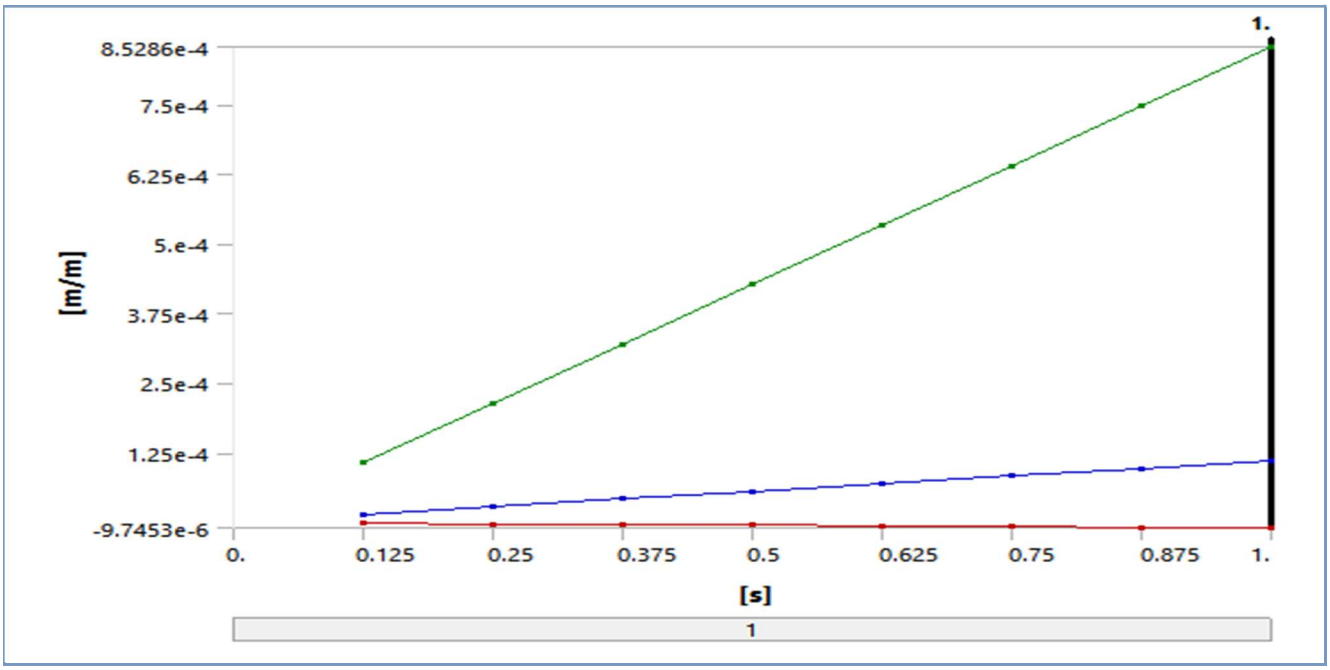

This figure presents the distribution of shear elastic strain in the D3 beam-column joint under a 300 kN lateral load, constructed with M25 grade concrete. These strain values are concentrated at the junction between the beam and column, precisely where torsional and flexural demands intersect. The high strain zones indicated in red and orange correspond to areas of significant angular distortion, reflecting the lack of sufficient shear reinforcement. This strain behavior suggests potential for early cracking and rotation in the joint core, especially under cyclic or seismic loading. Conversely, blue regions show compressed shear zones that resist deformation.

The presence of both high positive and negative strains is indicative of torsional response, which must be addressed in design detailing.

5.2 FRC

5.2.1 D1 design

Shear stress

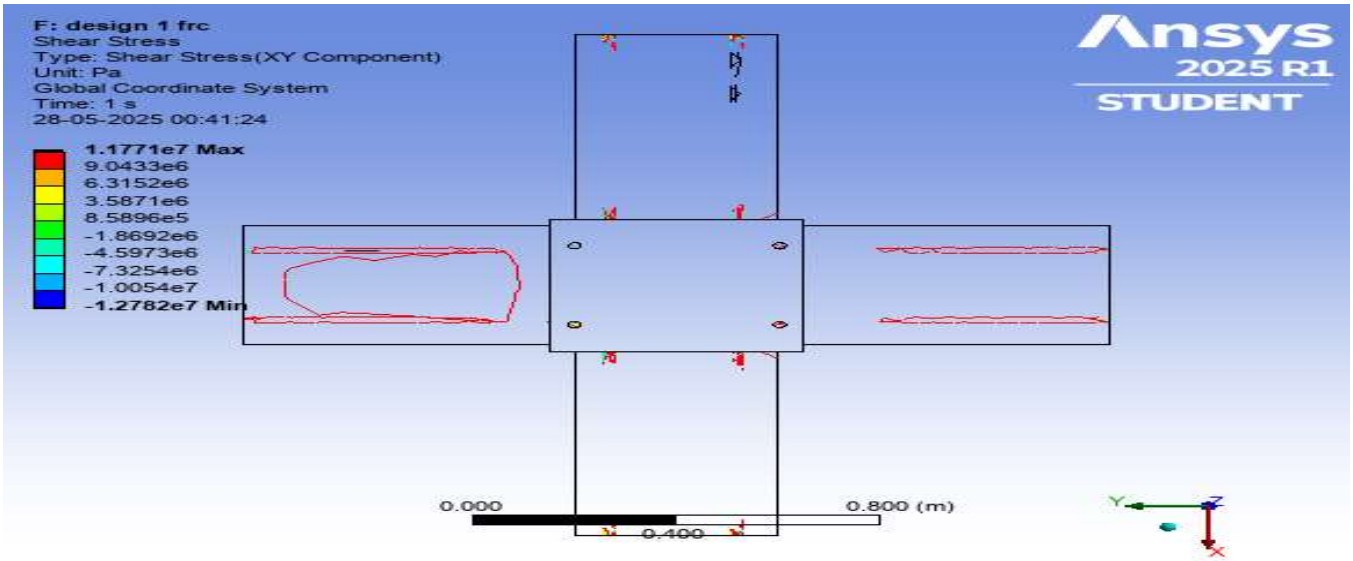

Figure 5.10: Shear stress plot

S.No	Time [s]	Minimum [Pa]	Maximum [Pa]	Average [Pa]
1	0.125	-1.60E+06	1.47E+06	6.7519
2	0.25	-3.20E+06	2.94E+06	13.392
3	0.375	-4.79E+06	4.41E+06	20.024
4	0.5	-6.39E+06	5.89E+06	26.656
5	0.625	-7.99E+06	7.36E+06	33.288
6	0.75	-9.59E+06	8.83E+06	39.919
7	0.875	-1.12E+07	1.03E+07	46.549
8	1	-1.28E+07	1.18E+07	53.18

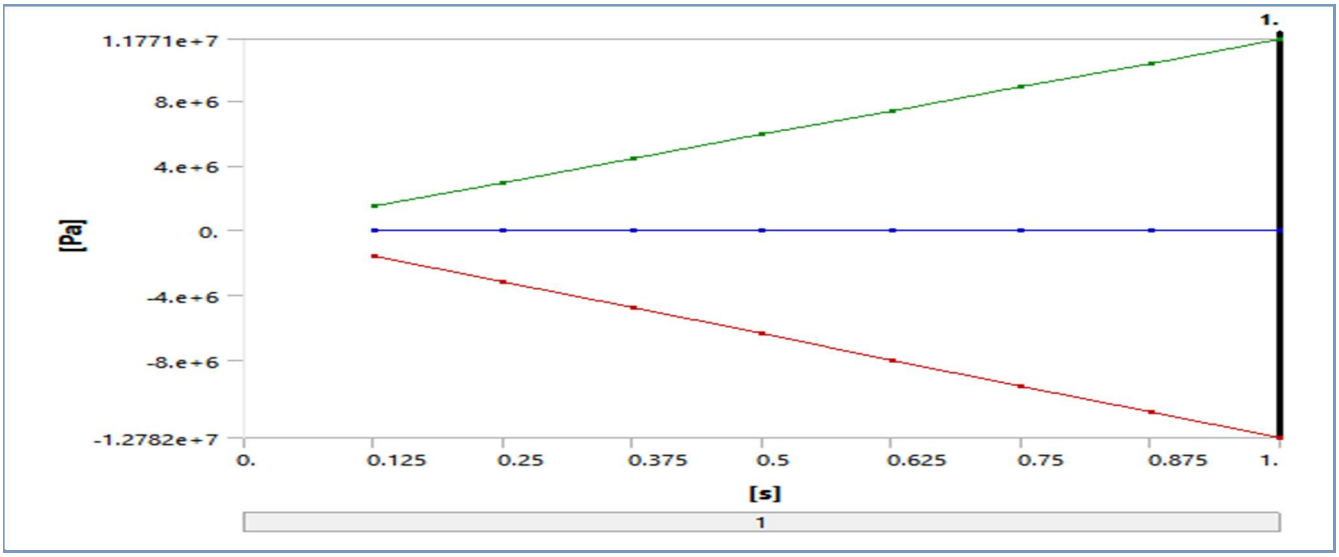

The inclusion of Fiber Reinforced Concrete (FRC) in the D1 configuration significantly alters the shear stress distribution, moderating peak values compared to plain M25 concrete. Stress levels are more homogenized across the joint, and the magnitude of maximum stress is notably lower, suggesting effective stress redistribution due to the fiber bridging mechanism. This implies a marked reduction in crack propagation potential and improved joint durability.

Strain Energy

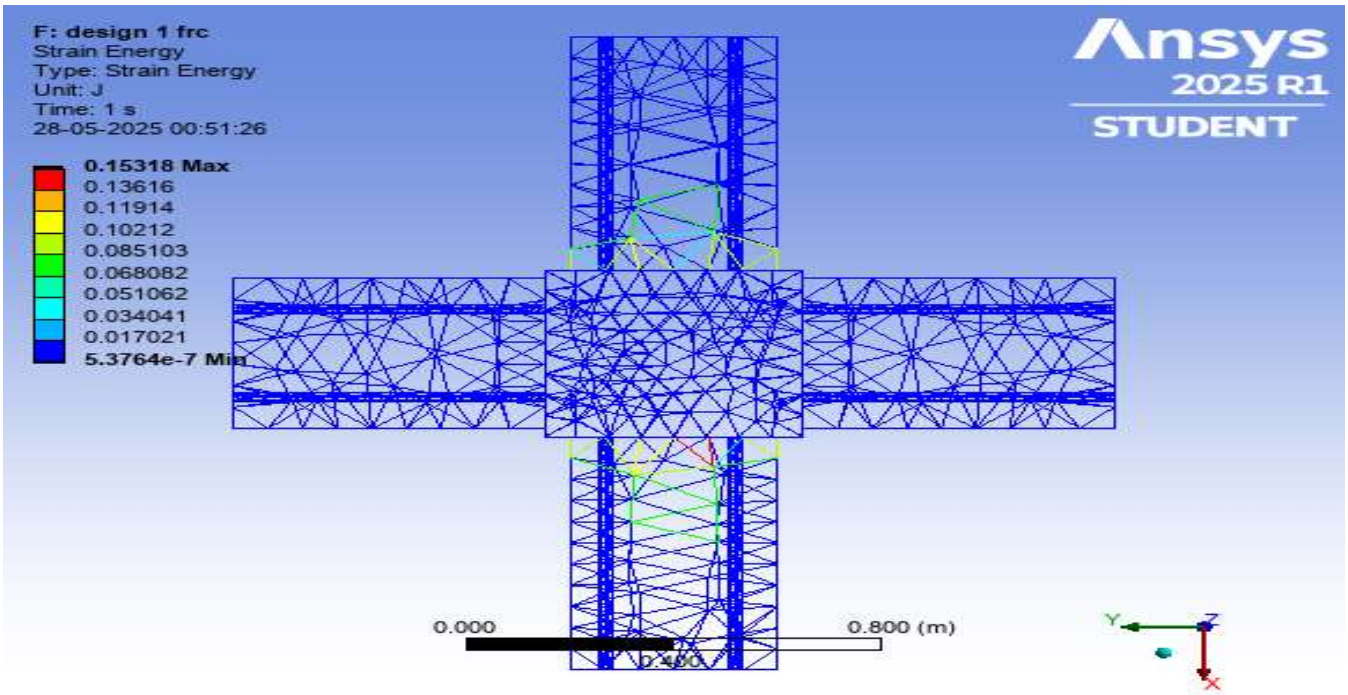

Figure 5.11: Strain energy plot

S.No	Time [s]	Minimum [J]	Maximum [J]	Total [J]
1	0.125	8.40E-09	2.39E-03	0.80794
2	0.25	3.36E-08	9.57E-03	3.2318
3	0.375	7.56E-08	2.15E-02	7.2715
4	0.5	1.34E-07	3.83E-02	12.927
5	0.625	2.10E-07	5.98E-02	20.199
6	0.75	3.02E-07	8.62E-02	29.086
7	0.875	4.12E-07	0.11728	39.589
8	1	5.38E-07	0.15318	51.708

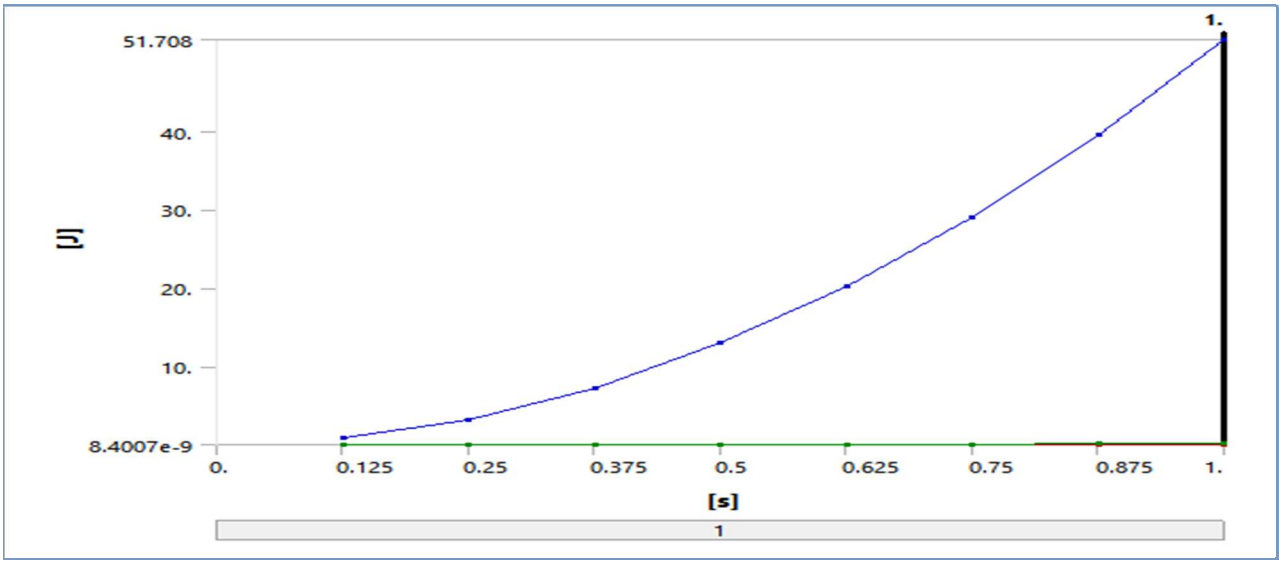

This plot demonstrates how the joint stores and redistributes internal energy under load. The strain energy peaks are centrally located, but are lower in intensity than those in non-reinforced joints. This indicates that FRC enhances structural resilience by dissipating energy over a broader area, reducing the likelihood of localized failure. The implication is an increased capacity to withstand cyclic loads with less degradation in stiffness

Maximum Principal Elastic Strain

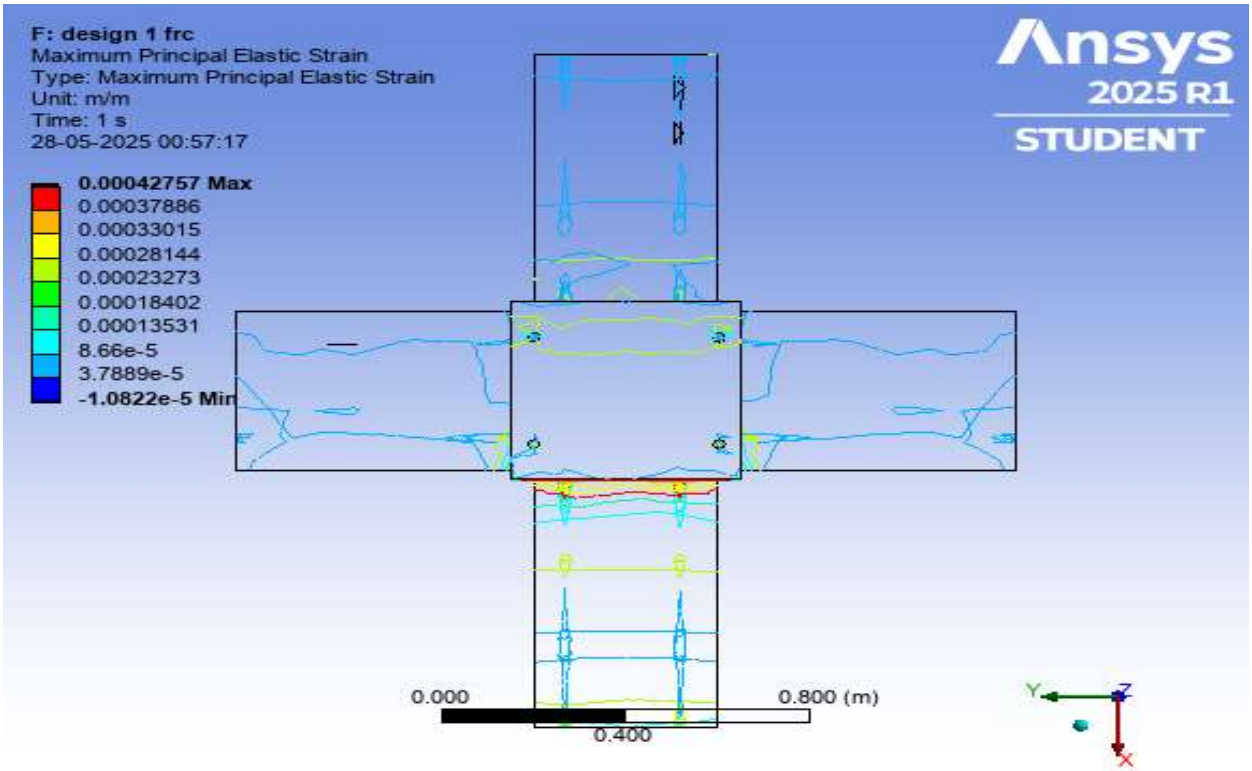

Figure 5.12: Maximum Principal elastic strain plot

S.No	Time [s]	Minimum [m/m]	Maximum [m/m]	Average [m/m]
1	0.125	-1.35E-06	5.34E-05	4.36E-06
2	0.25	-2.71E-06	1.07E-04	8.72E-06
3	0.375	-4.06E-06	1.60E-04	1.31E-05
4	0.5	-5.41E-06	2.14E-04	1.74E-05
5	0.625	-6.76E-06	2.67E-04	2.18E-05
6	0.75	-8.12E-06	3.21E-04	2.62E-05
7	0.875	-9.47E-06	3.74E-04	3.05E-05
8	1	-1.08E-05	4.28E-04	3.49E-05

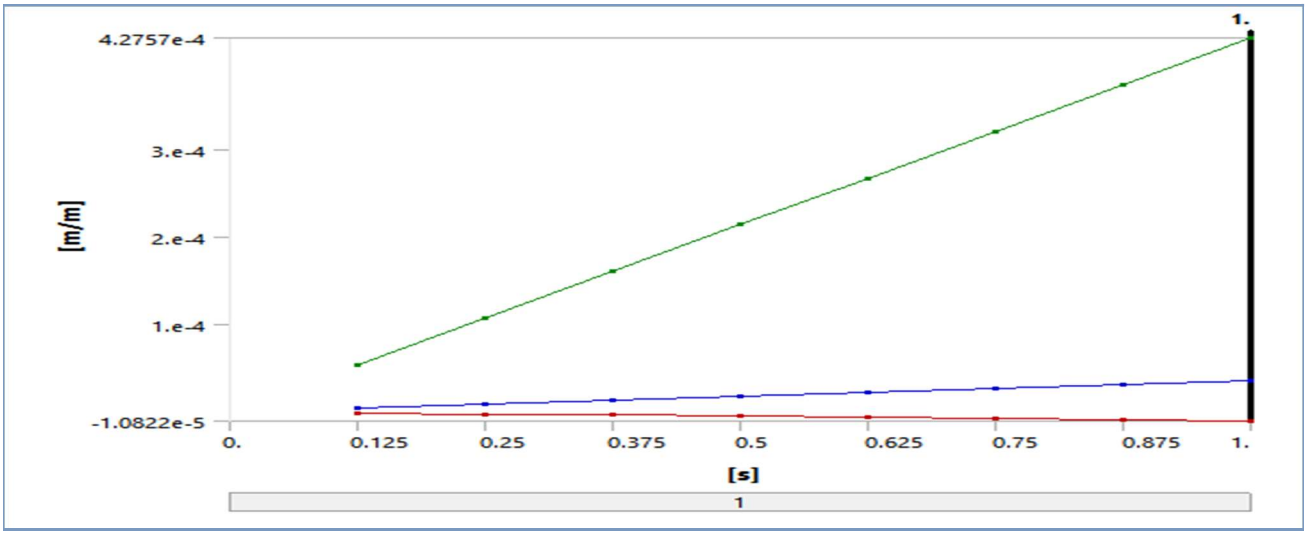

The angular deformation in the D1 FRC joint is more controlled. The maximum strain is reduced, and the gradient between tensile and compressive shear regions is smoother. This reflects enhanced ductility and flexibility due to fiber reinforcement. It highlights FRC's role in maintaining joint integrity and functionality even under significant shear loading.

5.2.2 Design D2 case

Shear Stress

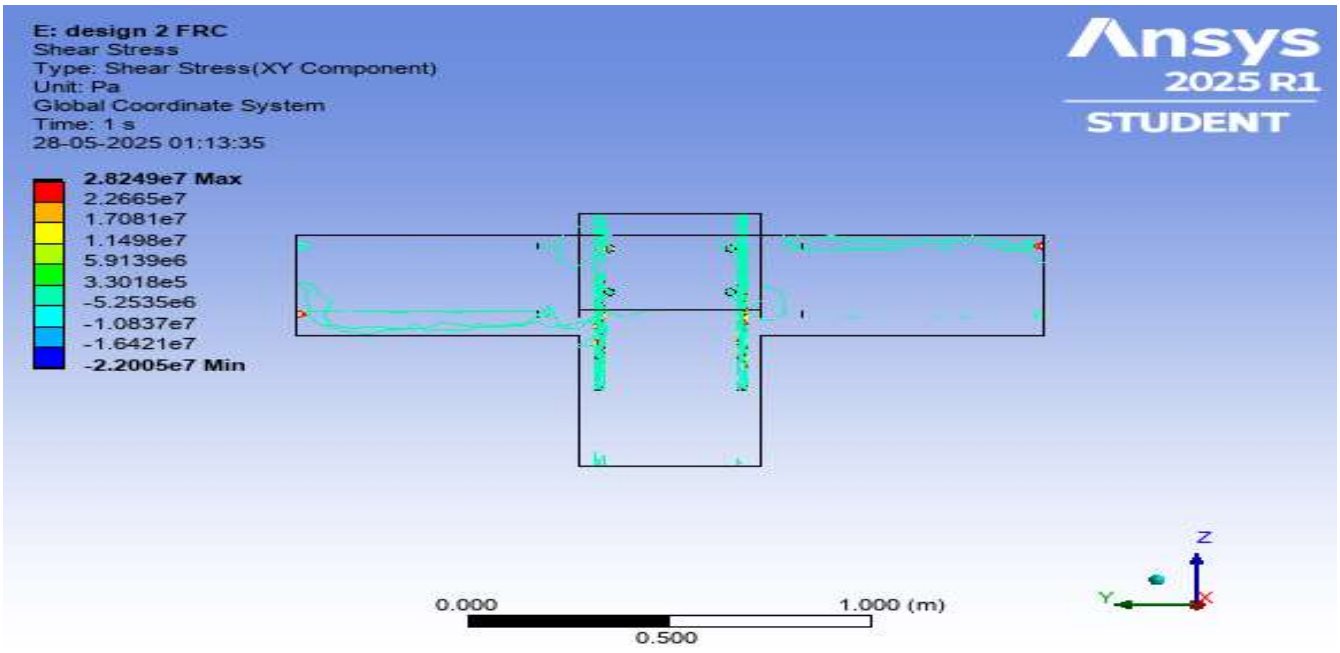

Figure 5.13: Shear stress plot

S.No	Time [s]	Minimum [Pa]	Maximum [Pa]	Average [Pa]
1	0.125	-2.75E+06	3.53E+06	648.15
2	0.25	-5.50E+06	7.06E+06	1296.3
3	0.375	-8.25E+06	1.06E+07	1944.5
4	0.5	-1.10E+07	1.41E+07	2592.7
5	0.625	-1.38E+07	1.77E+07	3240.9
6	0.75	-1.65E+07	2.12E+07	3889.1
7	0.875	-1.93E+07	2.47E+07	4537.2
8	1	-2.20E+07	2.82E+07	5185.4

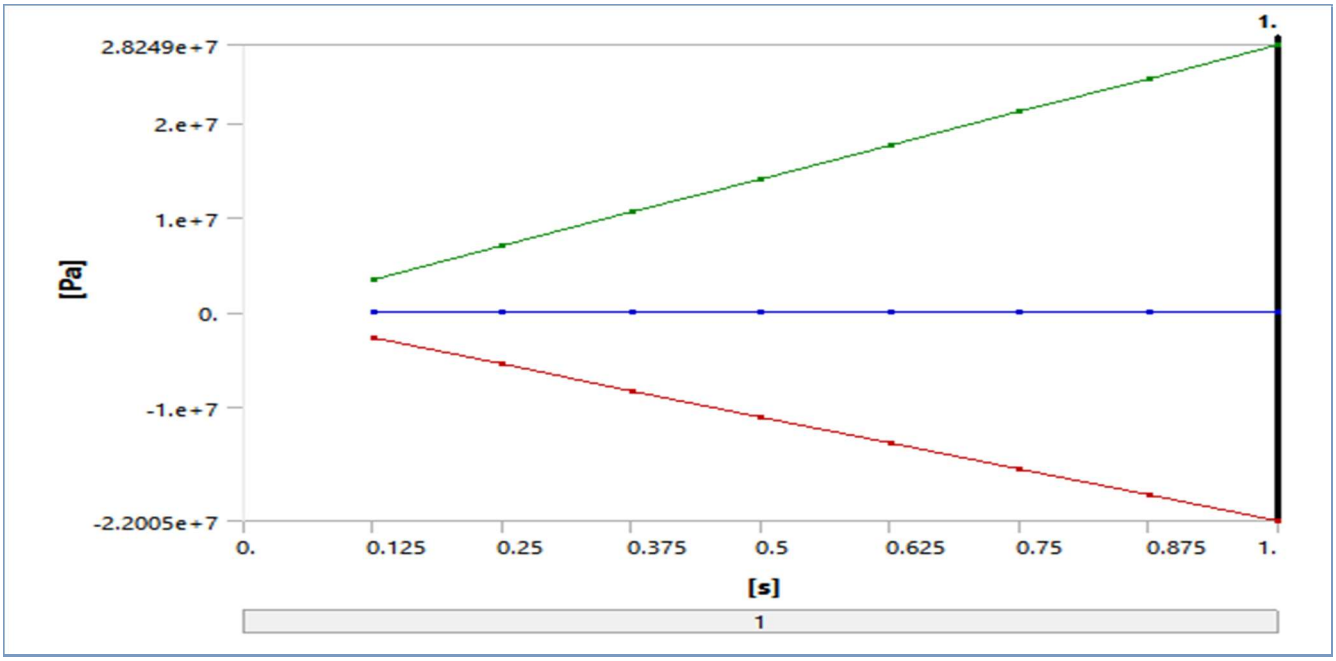

The D2 design, reinforced with FRC, shows a well-balanced stress profile. The peak stress is significantly lower than in unreinforced M25 concrete, indicating that FRC contributes to reducing stress risers that often serve as crack initiation points. The stress contours are smoother, suggesting a more efficient load path and greater redundancy in the joint behavior.

Strain Energy

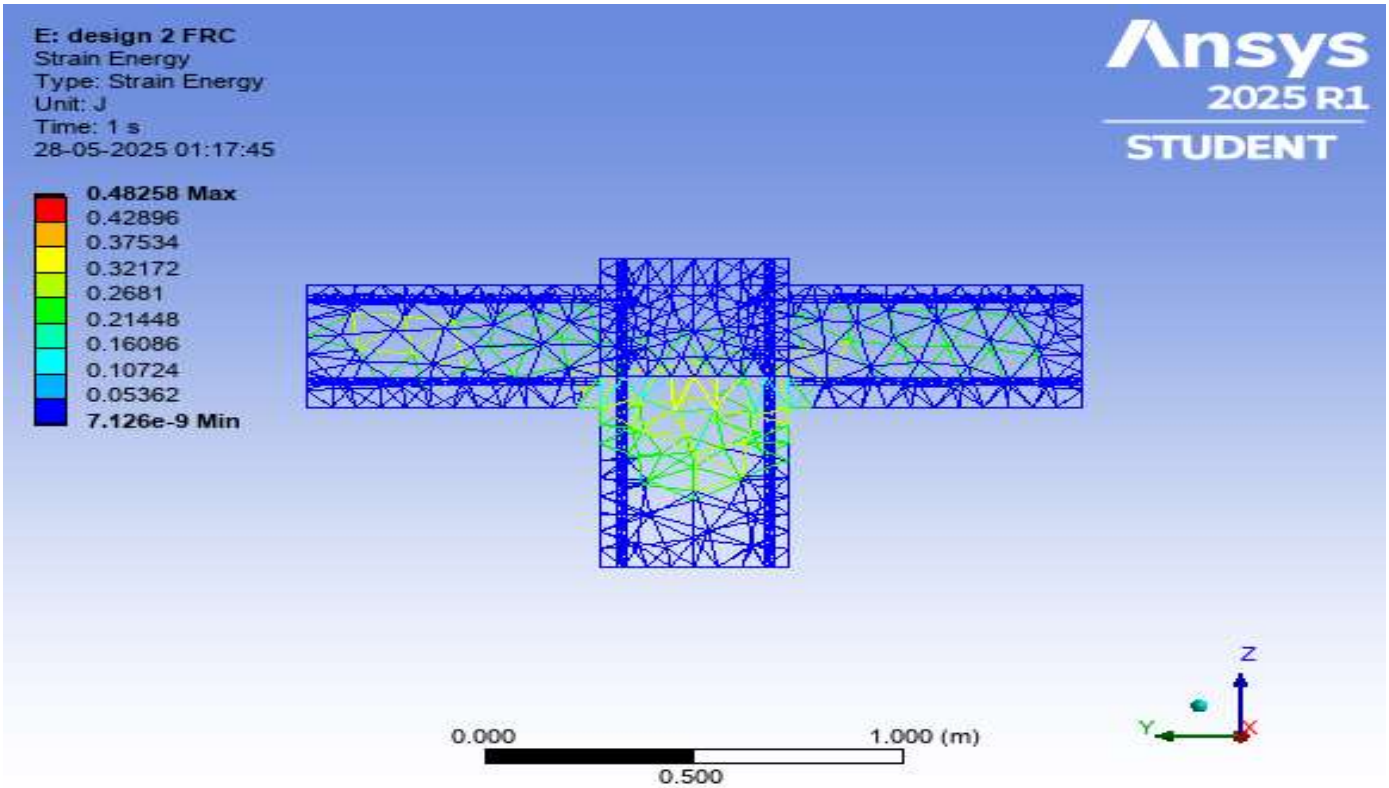

Figure 5.14: Strain energy plot

S.No	Time [s]	Minimum [J]	Maximum [J]	Total [J]
1	0.125	1.12E-10	7.54E-03	2.4086
2	0.25	4.46E-10	3.02E-02	9.6345
3	0.375	1.00E-09	6.79E-02	21.678
4	0.5	1.78E-09	0.12064	38.538
5	0.625	2.78E-09	0.18851	60.215
6	0.75	4.01E-09	0.27145	86.71
7	0.875	5.46E-09	0.36947	118.02
8	1	7.13E-09	0.48258	154.15

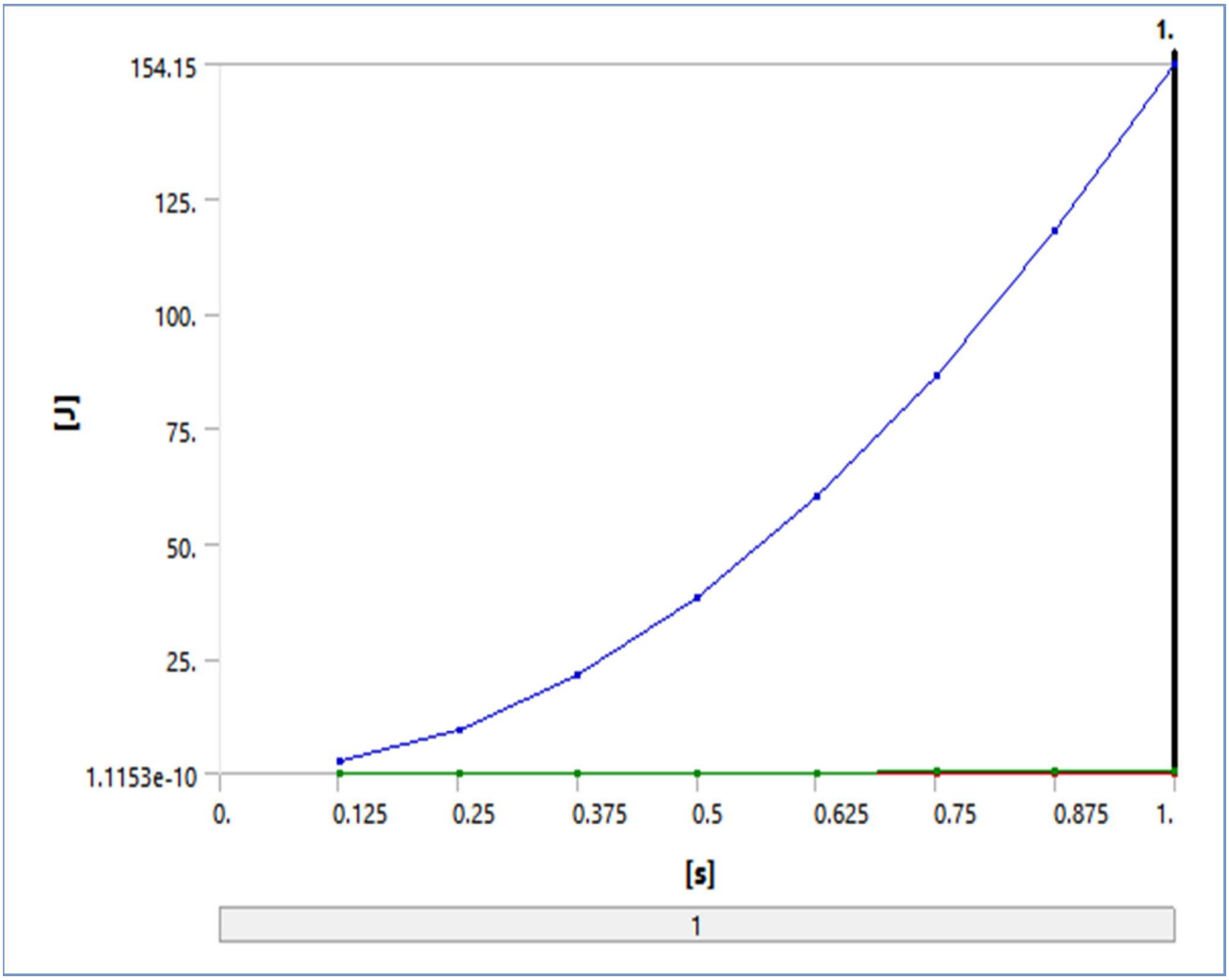

The energy absorption pattern reflects that the joint is undergoing deformation in a more distributed manner. The strain energy is less concentrated, implying reduced risk of brittle fracture. This suggests that the D2 geometry, in combination with FRC, promotes a more robust performance under load and potentially improves post-yield behavior.

Maximum Principal Elastic Strain

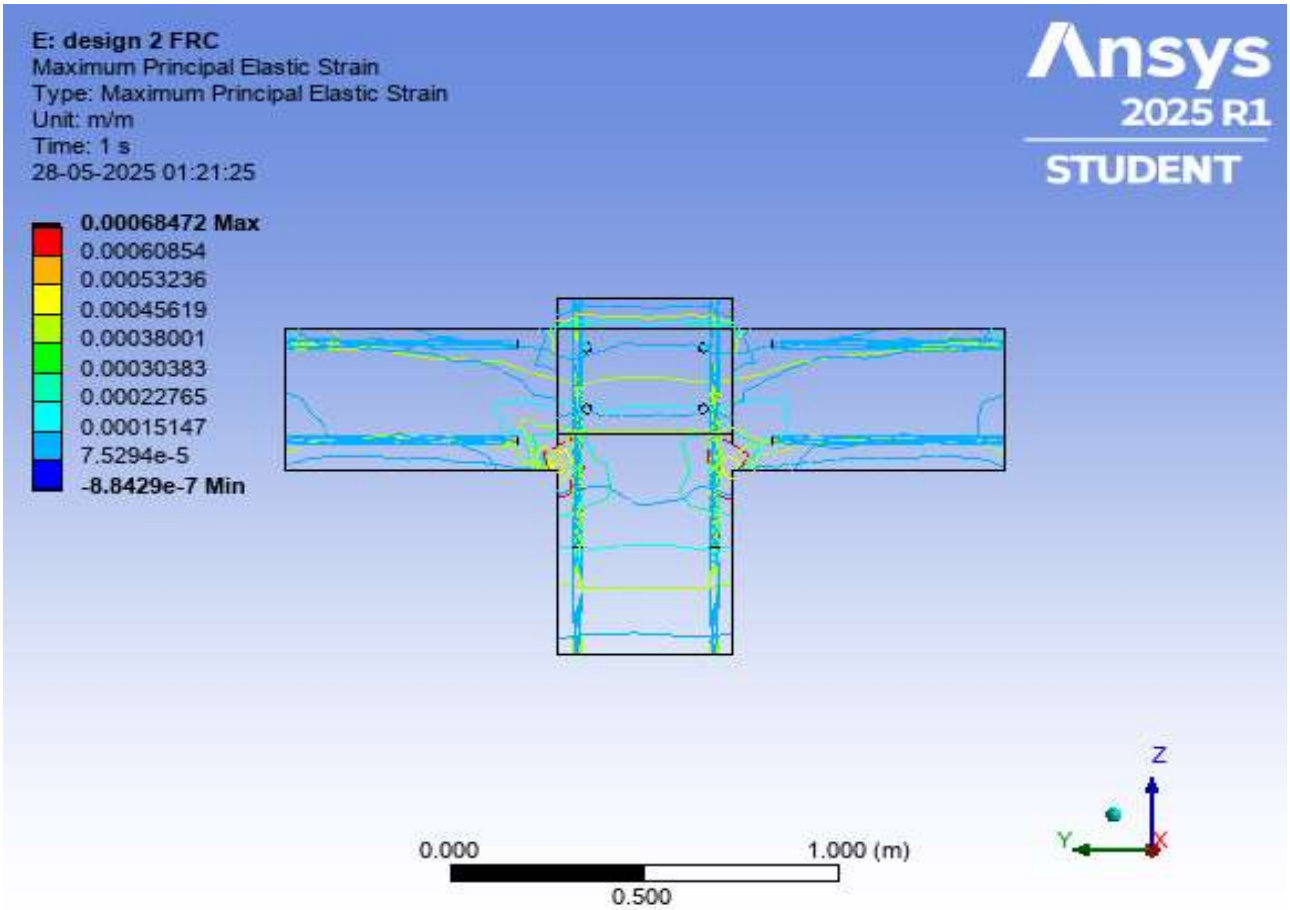

Figure 5.15: Maximum Principal elastic strain plot

S.No	Time [s]	Minimum [m/m]	Maximum [m/m]	Average [m/m]
1	0.125	-1.11E-07	8.56E-05	9.68E-06
2	0.25	-2.21E-07	1.71E-04	1.94E-05
3	0.375	-3.32E-07	2.57E-04	2.90E-05
4	0.5	-4.42E-07	3.42E-04	3.87E-05
5	0.625	-5.53E-07	4.28E-04	4.84E-05
6	0.75	-6.63E-07	5.14E-04	5.81E-05
7	0.875	-7.74E-07	5.99E-04	6.78E-05
8	1	-8.84E-07	6.85E-04	7.75E-05

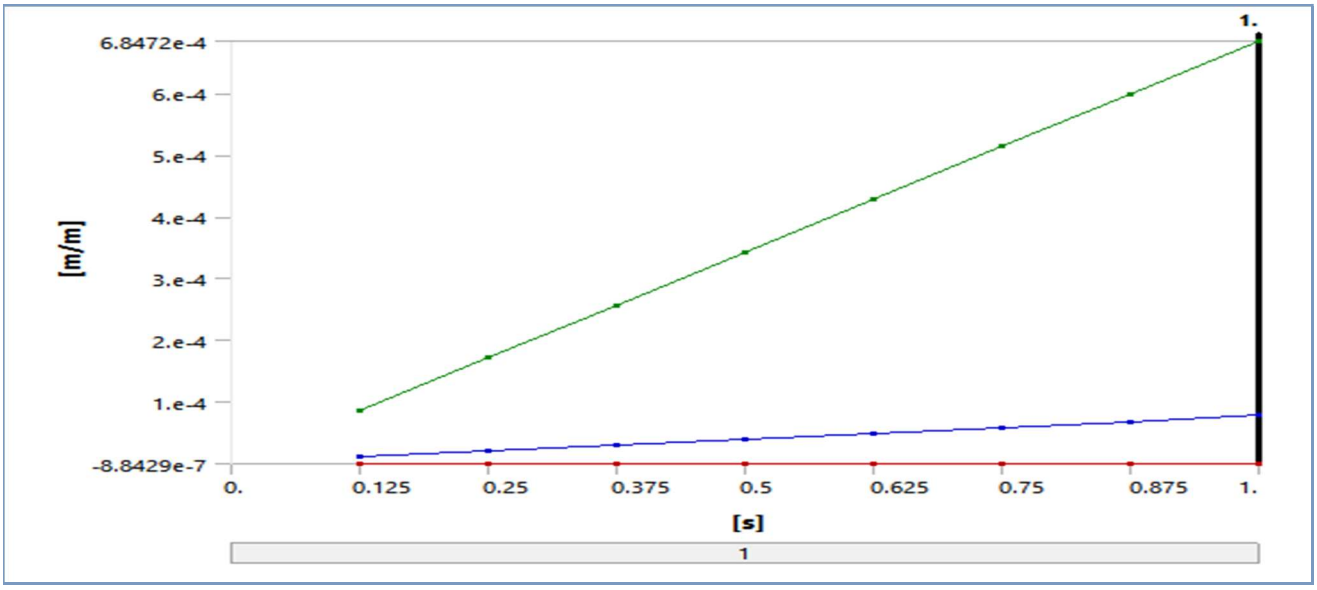

This plot demonstrates that angular distortions are controlled across the structure, with reduced amplitude of strain fluctuations. This is particularly beneficial in seismic applications where large, uncontrolled rotations can lead to progressive collapse. FRC provides a damping effect, increasing energy dissipation and resilience.

5.2.3 Design D3 case

Shear Stress

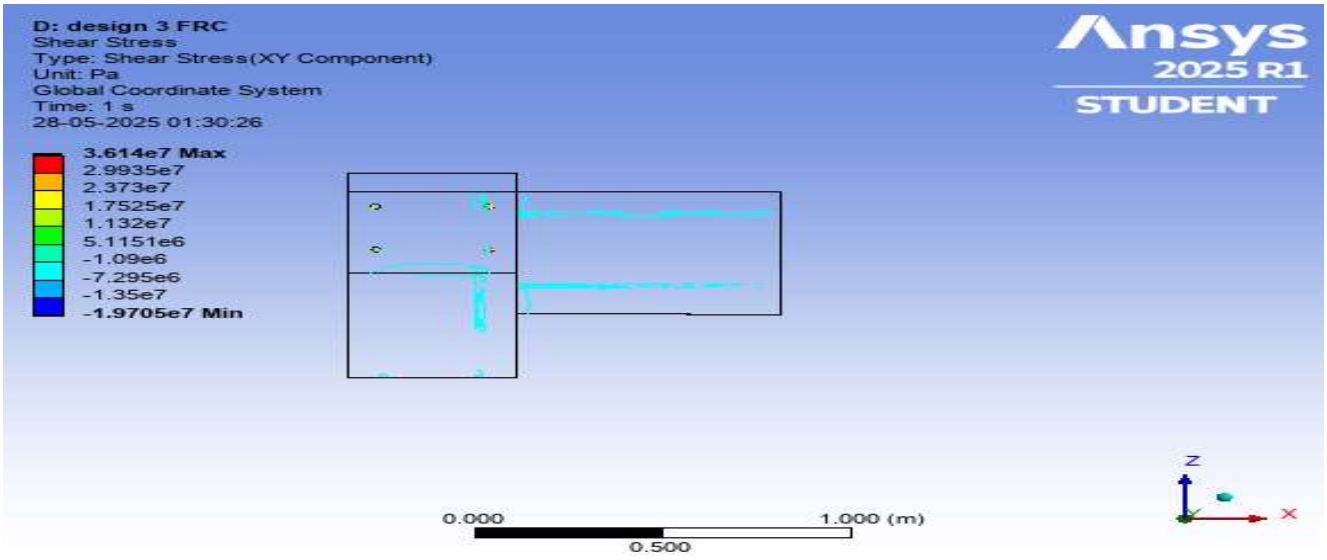

Figure 5.16: Shear stress plot

S.No	Time [s]	Minimum [Pa]	Maximum [Pa]	Average [Pa]
1	0.125	-2.46E+06	4.52E+06	55688
2	0.25	-4.93E+06	9.04E+06	1.11E+05
3	0.375	-7.39E+06	1.36E+07	1.67E+05
4	0.5	-9.85E+06	1.81E+07	2.23E+05
5	0.625	-1.23E+07	2.26E+07	2.78E+05
6	0.75	-1.48E+07	2.71E+07	3.34E+05
7	0.875	-1.72E+07	3.16E+07	3.90E+05
8	1	-1.97E+07	3.61E+07	4.46E+05

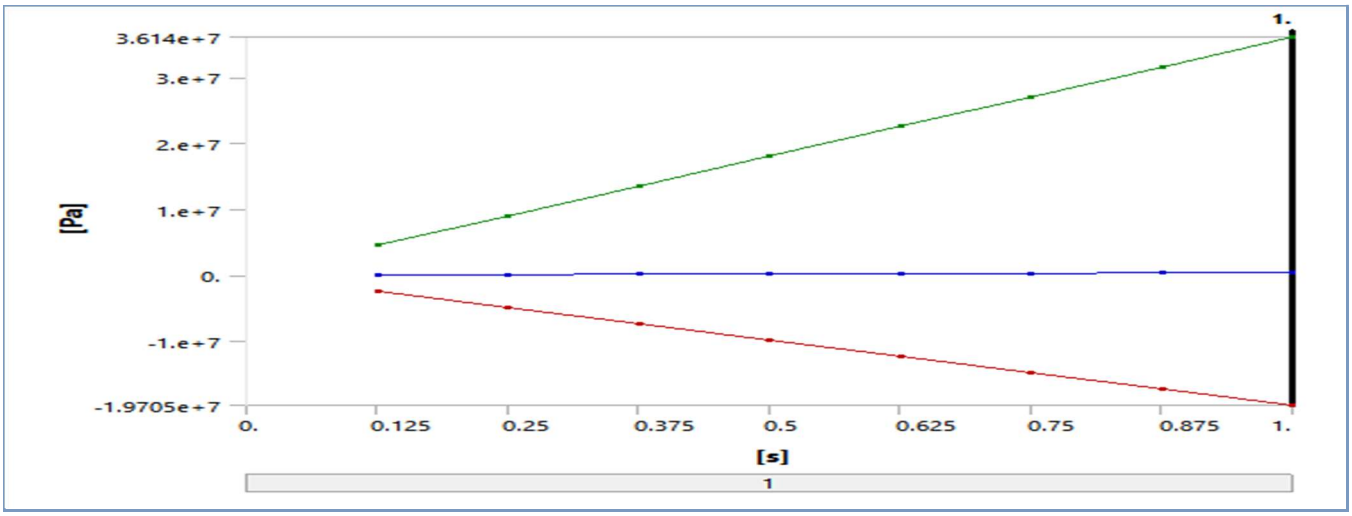

Despite the complex geometry of D3, FRC manages to suppress peak stress magnitudes, bringing them within a safer range compared to unreinforced designs. The sharp stress transitions present in the plain concrete version are now smoother, indicating improved continuity in force transfer and reduced susceptibility to shear cracking.

Strain Energy

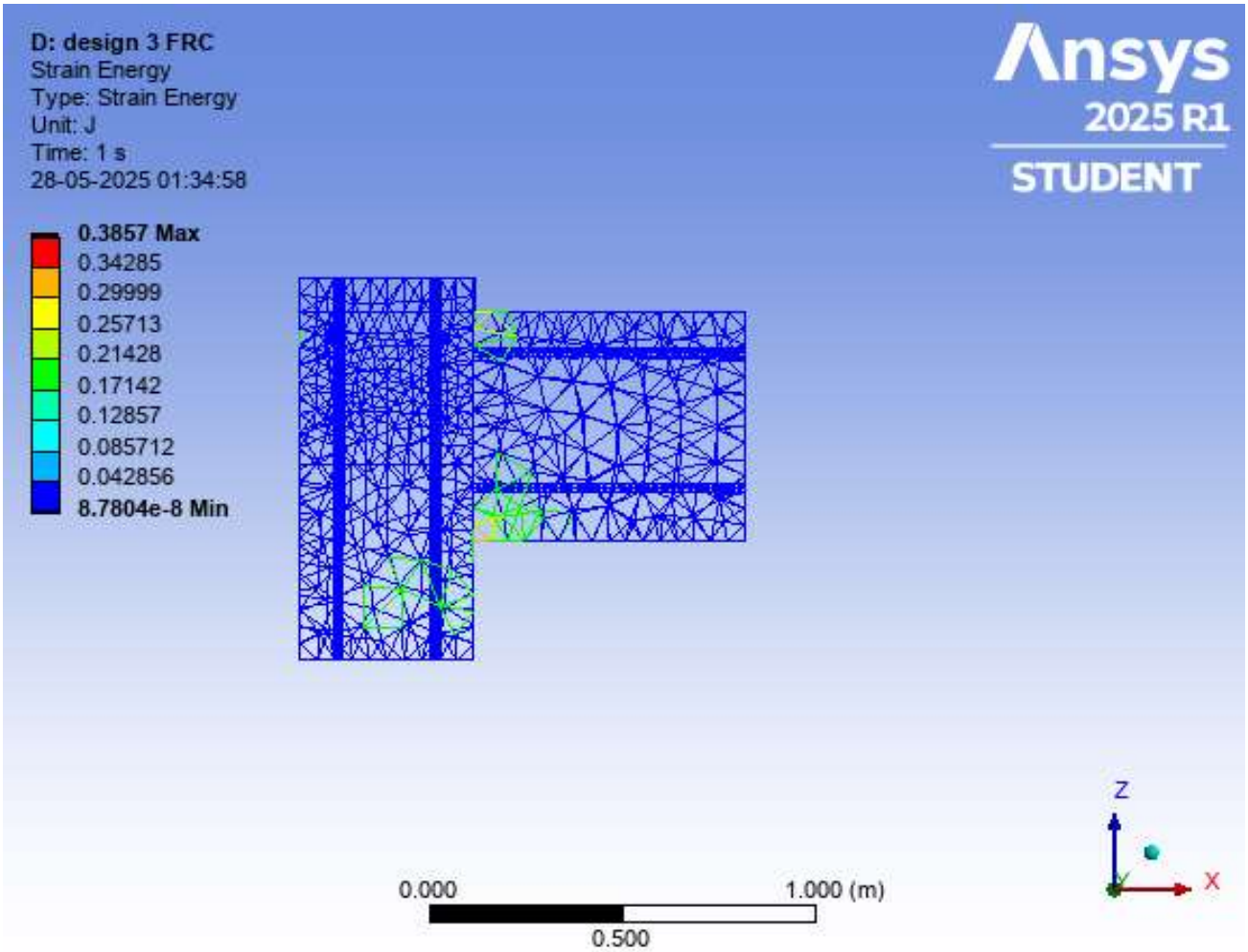

Figure 5.17: Strain energy plot

S.No	Time [s]	Minimum [J]	Maximum [J]	Total [J]
1	0.125	1.37E-09	6.03E-03	2.5557
2	0.25	5.49E-09	2.41E-02	10.223
3	0.375	1.23E-08	5.42E-02	23.002
4	0.5	2.20E-08	9.64E-02	40.892
5	0.625	3.43E-08	0.15066	63.893
6	0.75	4.94E-08	0.21696	92.006
7	0.875	6.72E-08	0.2953	125.23
8	1	8.78E-08	0.3857	163.57

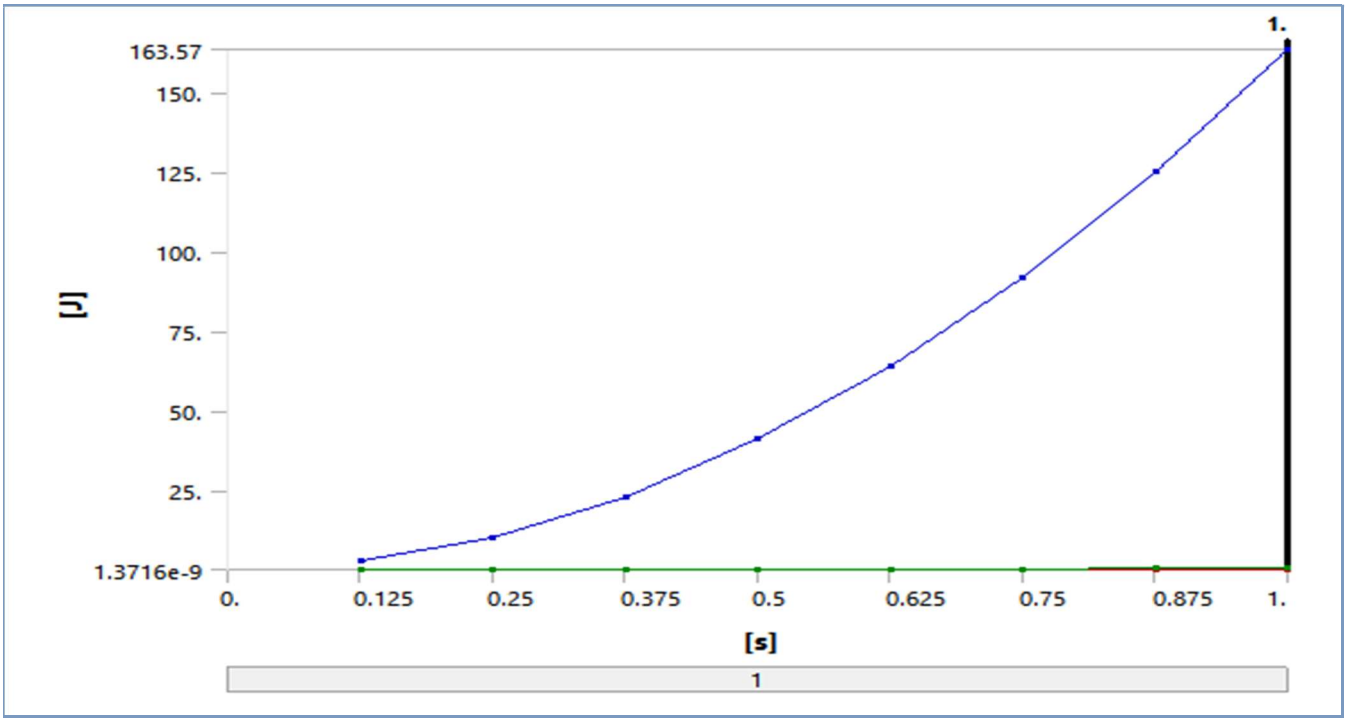

The highest energy concentrations still occur at the beam-column intersection, but the values are notably tempered. This implies that FRC reduces the risk of stress localization and associated cracking. The smoother gradient in energy absorption across the structure illustrates a more uniform distribution of internal work, which is desirable in performance-based design.

Maximum Principal Elastic Strain

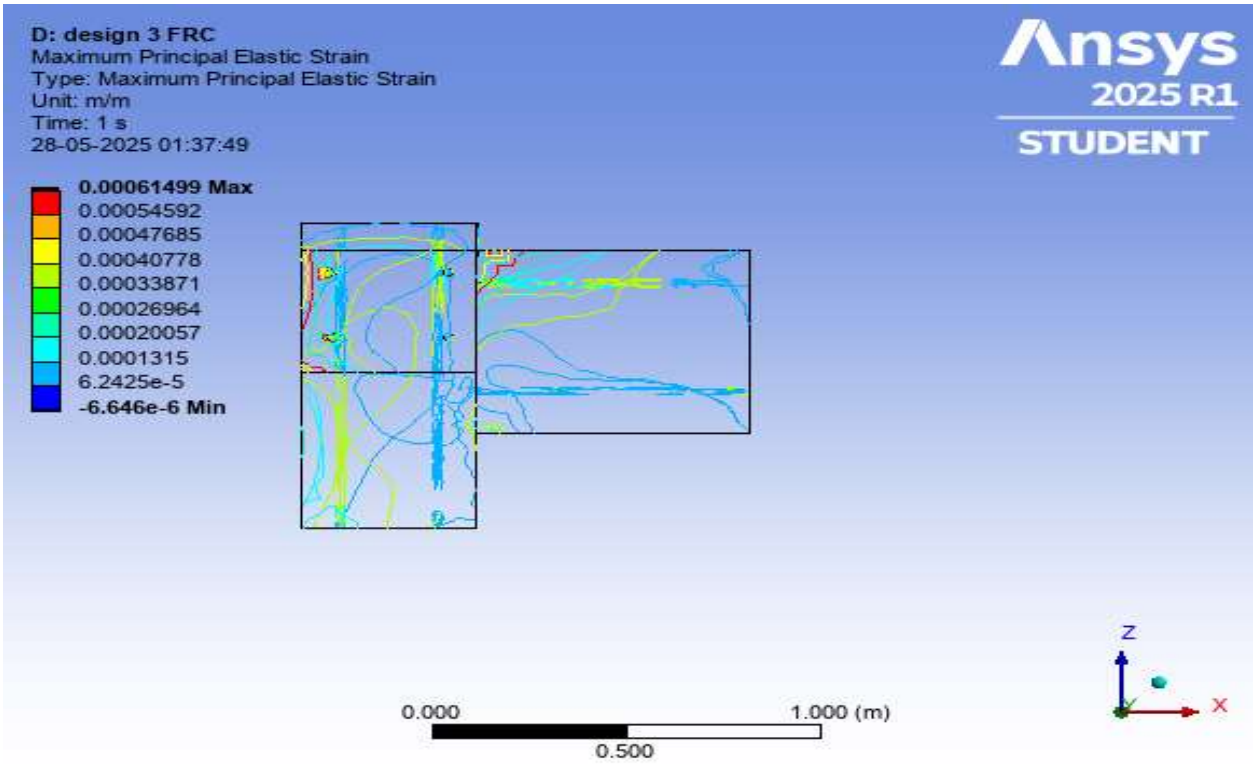

Figure 5.18: Maximum Principal elastic strain plot

S.No	Time [s]	Minimum [m/m]	Maximum [m/m]	Average [m/m]
1	0.125	-8.31E-07	7.69E-05	1.11E-05
2	0.25	-1.66E-06	1.54E-04	2.22E-05
3	0.375	-2.49E-06	2.31E-04	3.34E-05
4	0.5	-3.32E-06	3.07E-04	4.45E-05
5	0.625	-4.15E-06	3.84E-04	5.56E-05
6	0.75	-4.98E-06	4.61E-04	6.67E-05
7	0.875	-5.82E-06	5.38E-04	7.78E-05
8	1	-6.65E-06	6.15E-04	8.90E-05

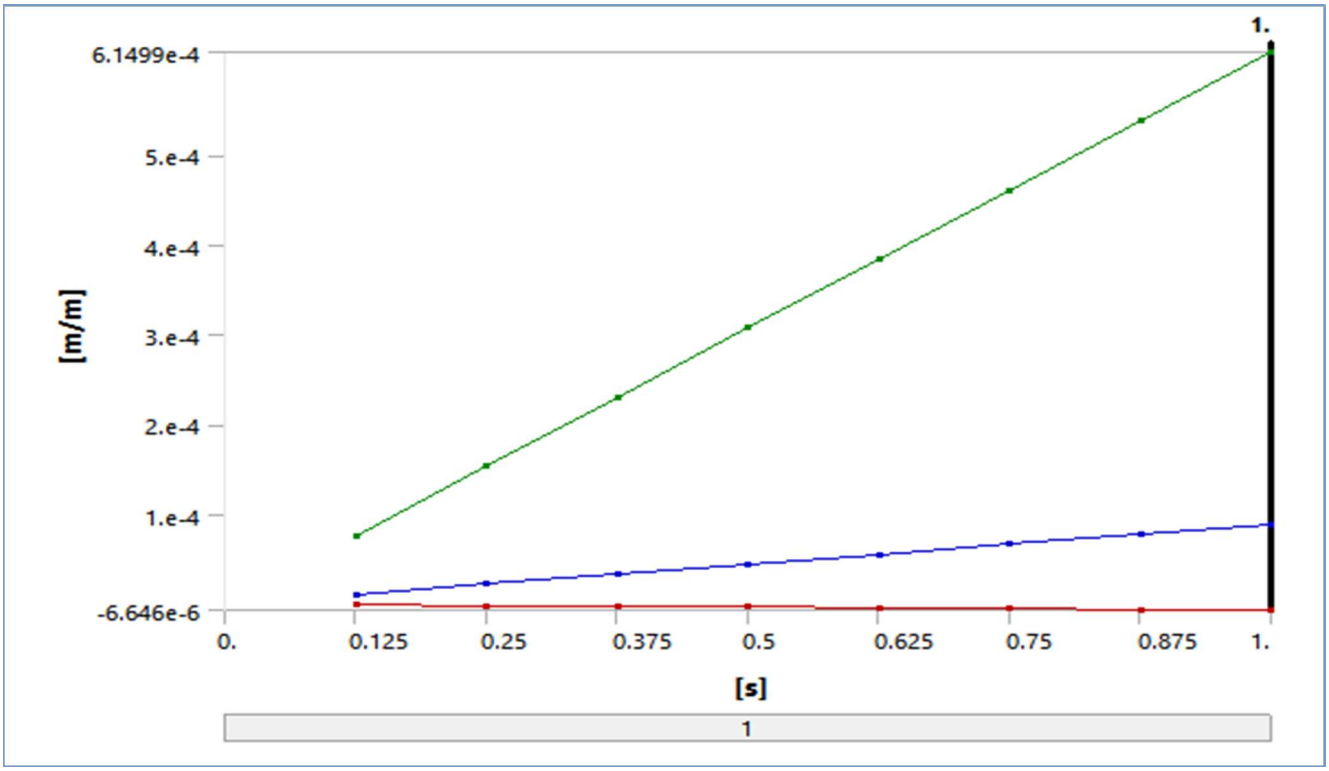

The D3 joint shows minimized angular deformation, which points to a stiffer and more robust response due to FRC. This characteristic is particularly important in joints subjected to repeated loading, where strain softening and cumulative damage are common failure mechanisms.

5.3 M40 CONCRETE

5.3.1 Design D1 CASE

Shear Stress

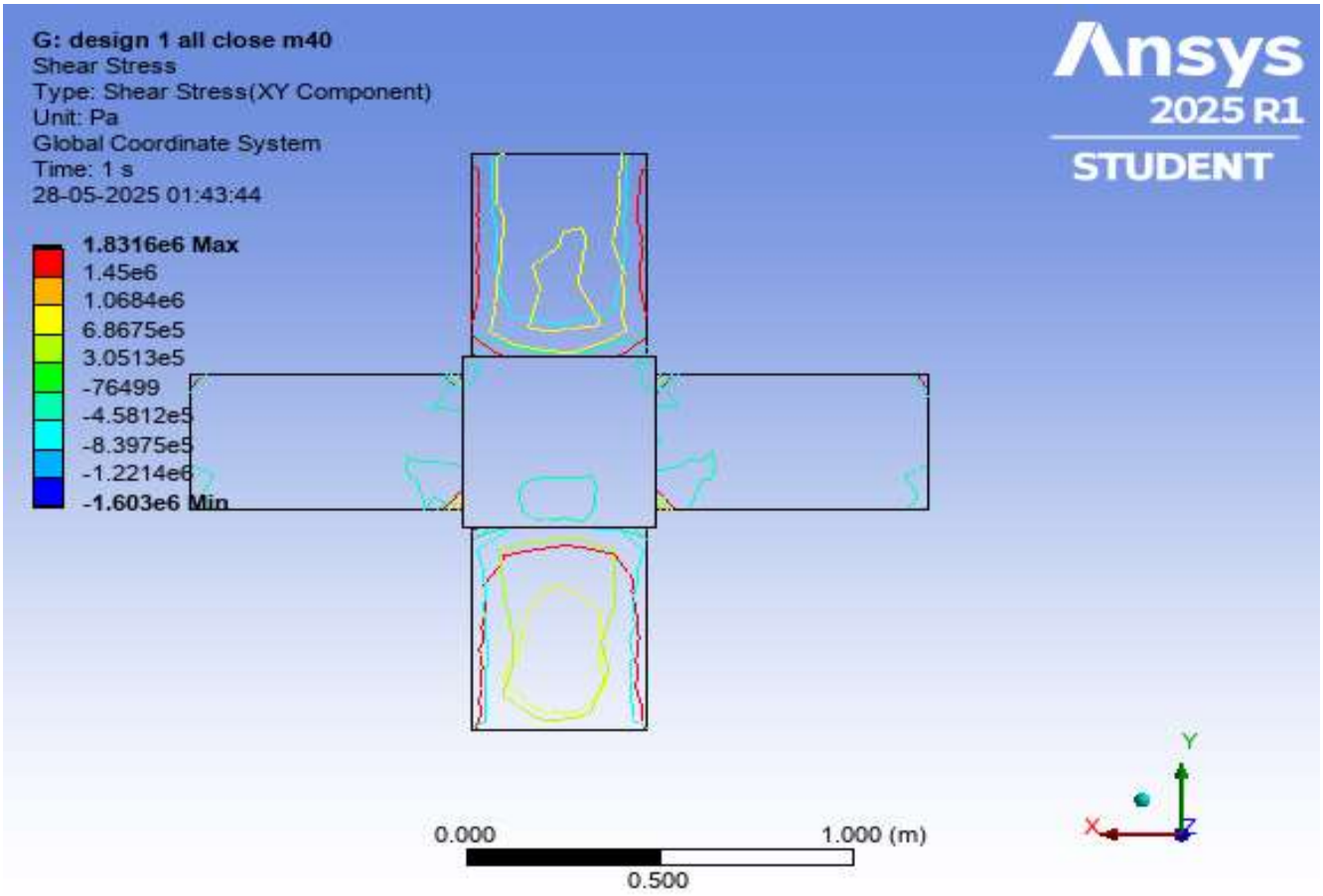

Figure 5.19: Shear stress plot

S.No	Time [s]	Minimum [Pa]	Maximum [Pa]	Average [Pa]
1	0.125	-2.00E+05	2.29E+05	258.58
2	0.25	-4.01E+05	4.58E+05	517.17
3	0.375	-6.01E+05	6.87E+05	775.75
4	0.5	-8.02E+05	9.16E+05	1034.3
5	0.625	-1.00E+06	1.14E+06	1292.9
6	0.75	-1.20E+06	1.37E+06	1551.5
7	0.875	-1.40E+06	1.60E+06	1810.1
8	1	-1.60E+06	1.83E+06	2068.7

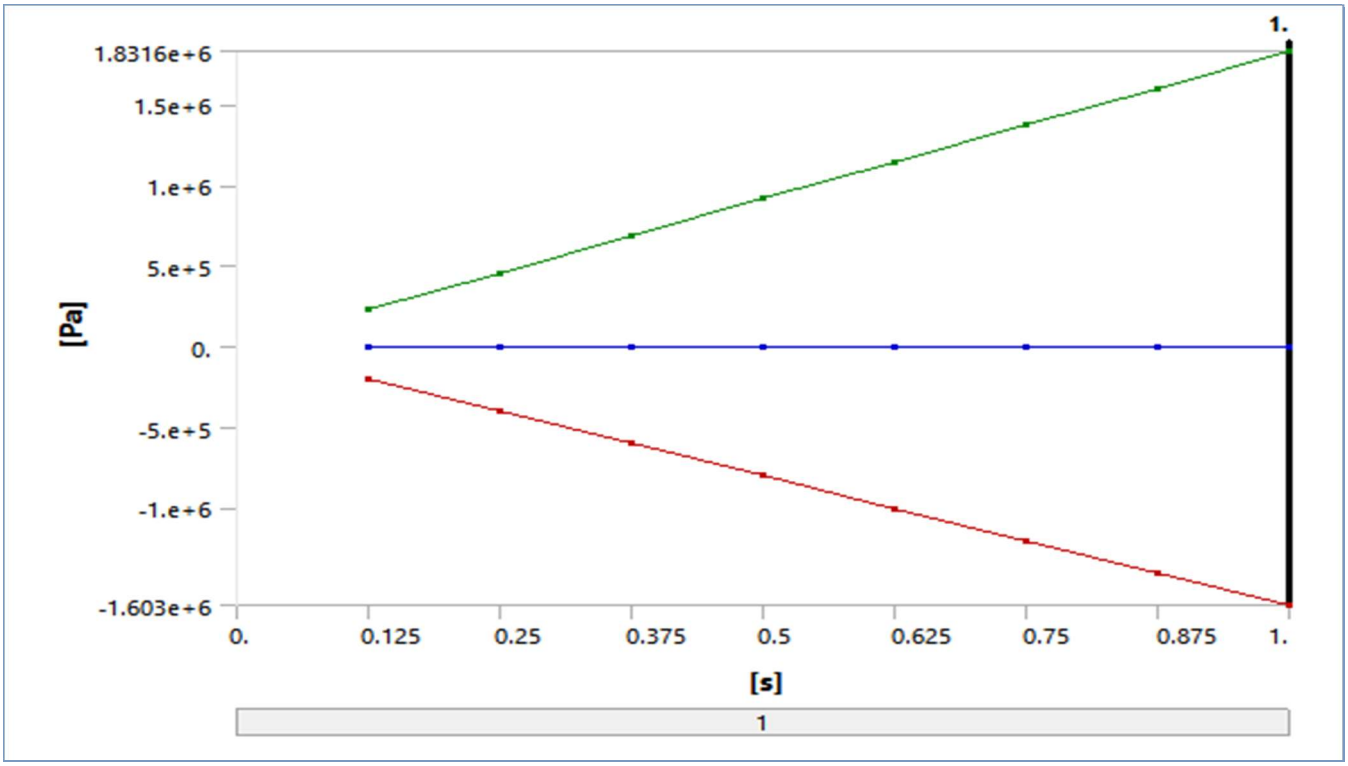

Using M40 concrete in D1 results in a higher threshold for stress capacity. The material's improved compressive strength allows for elevated shear loads without immediate cracking. However, despite this strength, stress concentration at the joint interface persists, implying that high-grade concrete alone does not mitigate the need for reinforcement.

Strain Energy

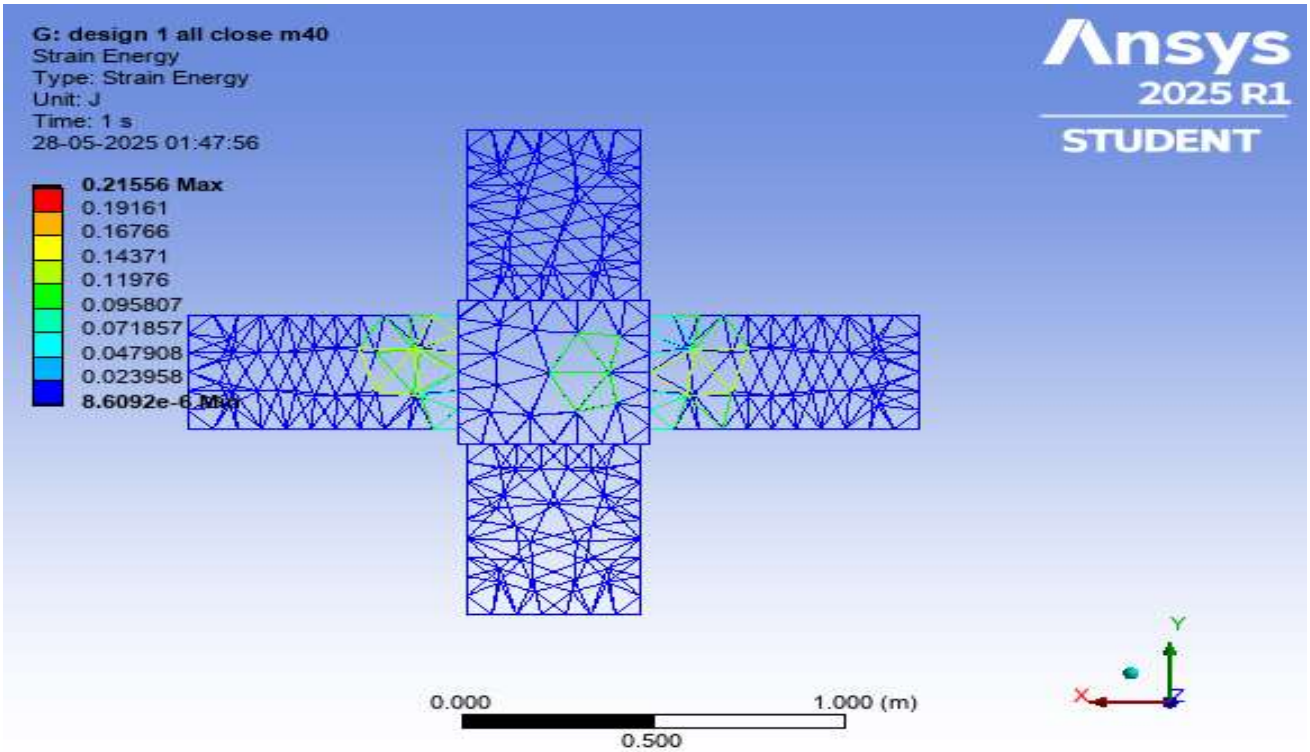

Figure 5.20: Strain energy plot

S.No	Time [s]	Minimum [J]	Maximum [J]	Total [J]
1	0.125	1.35E-07	3.37E-03	0.66992
2	0.25	5.38E-07	1.35E-02	2.6797
3	0.375	1.21E-06	3.03E-02	6.0293
4	0.5	2.15E-06	5.39E-02	10.719
5	0.625	3.36E-06	8.42E-02	16.748
6	0.75	4.84E-06	0.12125	24.117
7	0.875	6.59E-06	0.16503	32.826
8	1	8.61E-06	0.21556	42.875

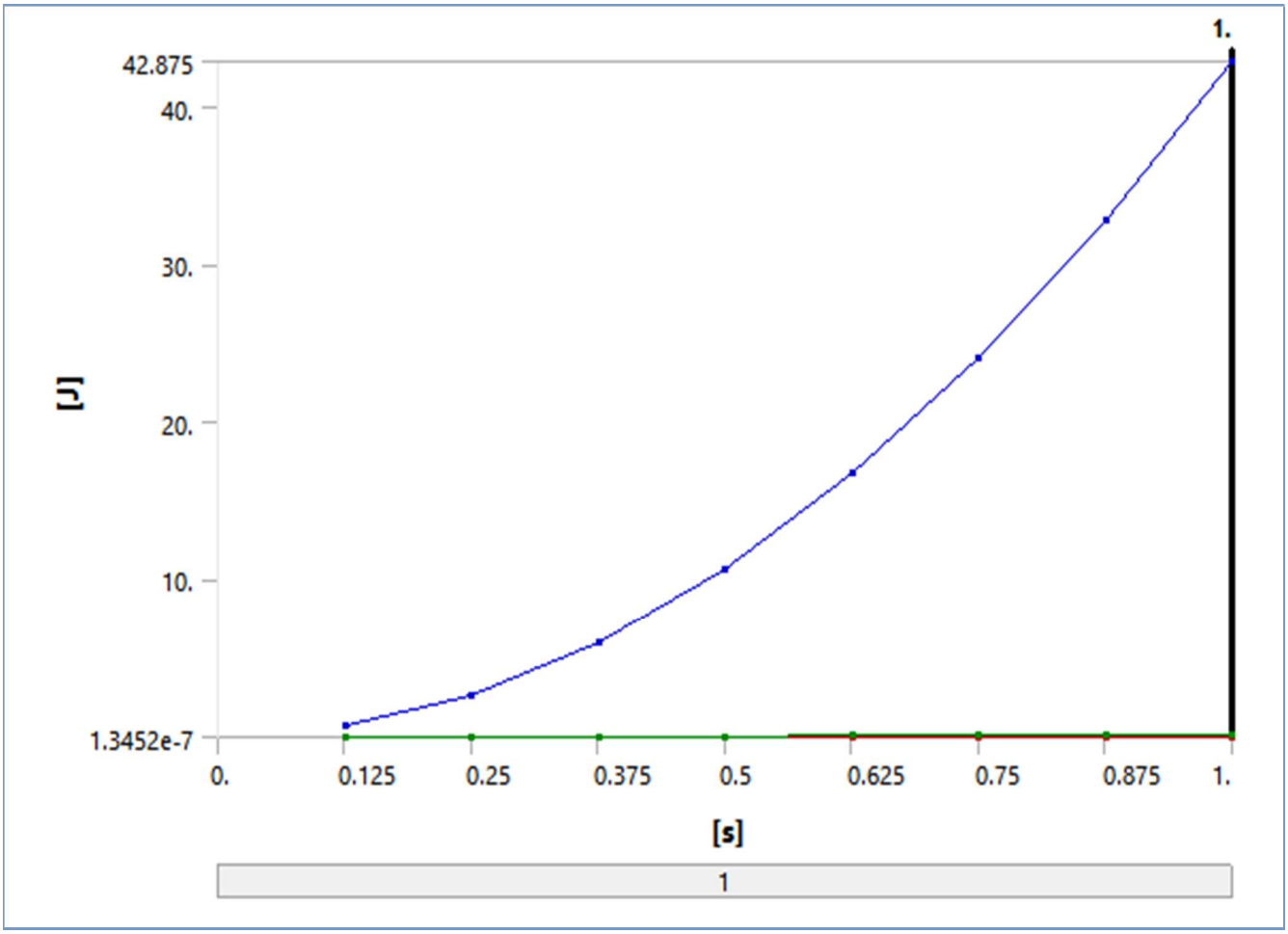

Strain energy peaks at the beam-column junction suggest that the stiffer material properties of M40 concrete localize deformation rather than dispersing it. This points to a potential vulnerability under dynamic or repeated loads due to lack of ductility. High strain energy in such localized zones is often a precursor to brittle failure.

Maximum Principal Elastic Strain

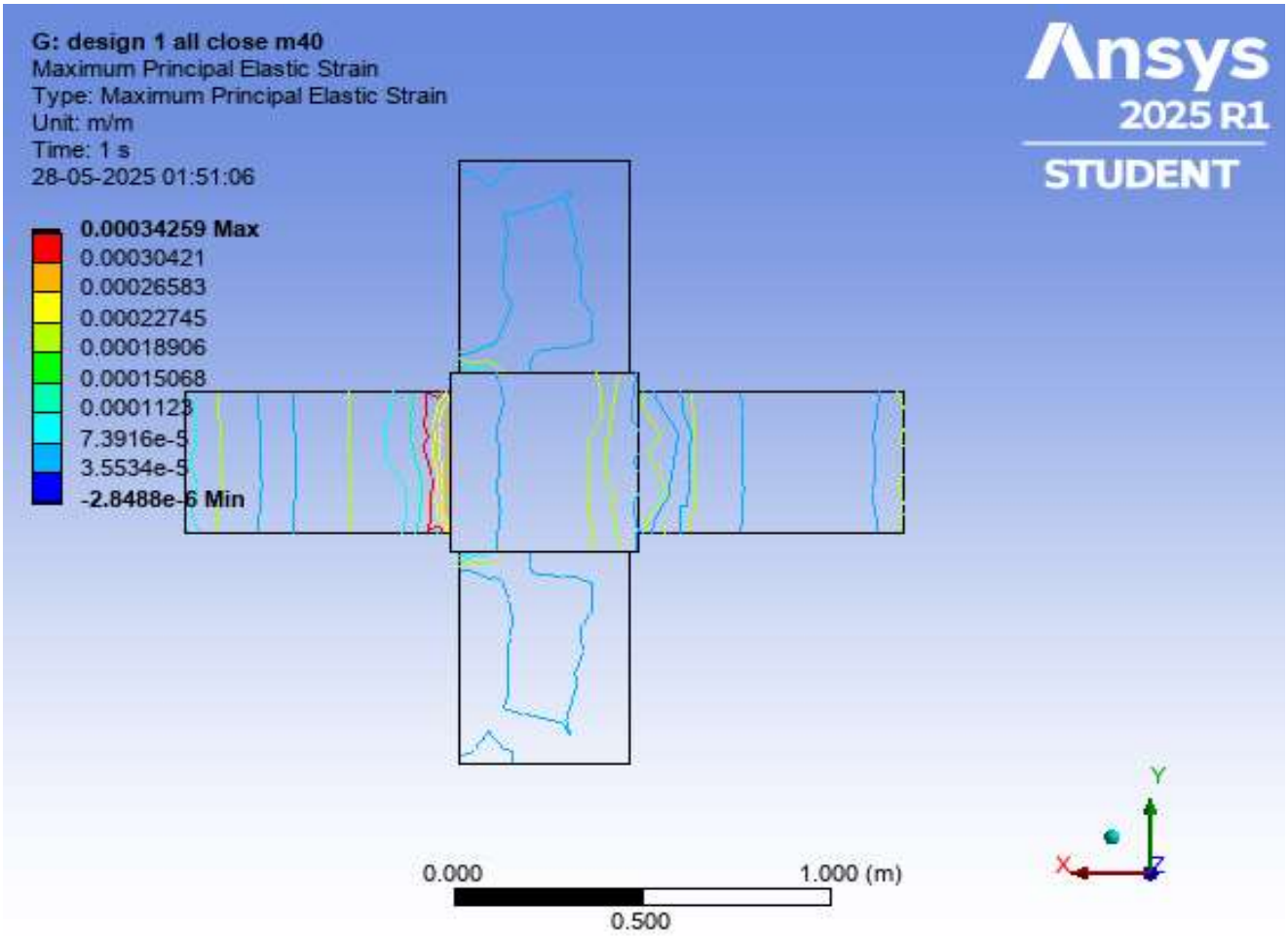

Figure 5.21: Shear elastic strain plot

S.No	Time [s]	Minimum [m/m]	Maximum [m/m]	Average [m/m]
1	0.125	-3.56E-07	4.28E-05	4.41E-06
2	0.25	-7.12E-07	8.56E-05	8.82E-06
3	0.375	-1.07E-06	1.28E-04	1.32E-05
4	0.5	-1.42E-06	1.71E-04	1.76E-05
5	0.625	-1.78E-06	2.14E-04	2.20E-05
6	0.75	-2.14E-06	2.57E-04	2.64E-05
7	0.875	-2.49E-06	3.00E-04	3.09E-05
8	1	-2.85E-06	3.43E-04	3.53E-05

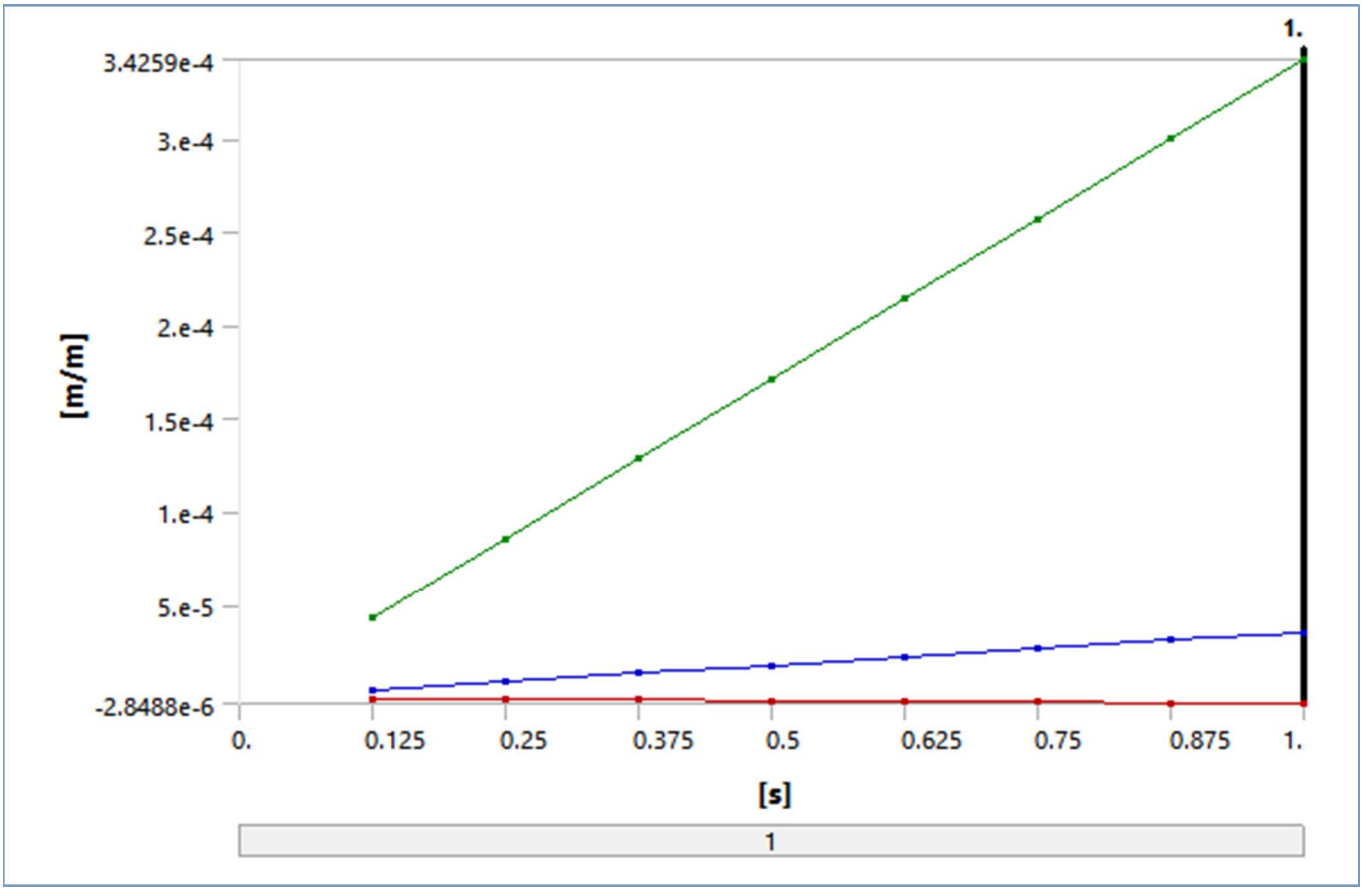

The strain plot confirms the rigidity of M40 concrete, with very low angular deformation. While this is beneficial for load resistance, the lack of ductile behavior may be problematic under seismic loading where flexibility is essential. The joint, though strong, could be more brittle without supplemental ductile detailing.

5.3.2 Design D2 CASE

Shear Stress

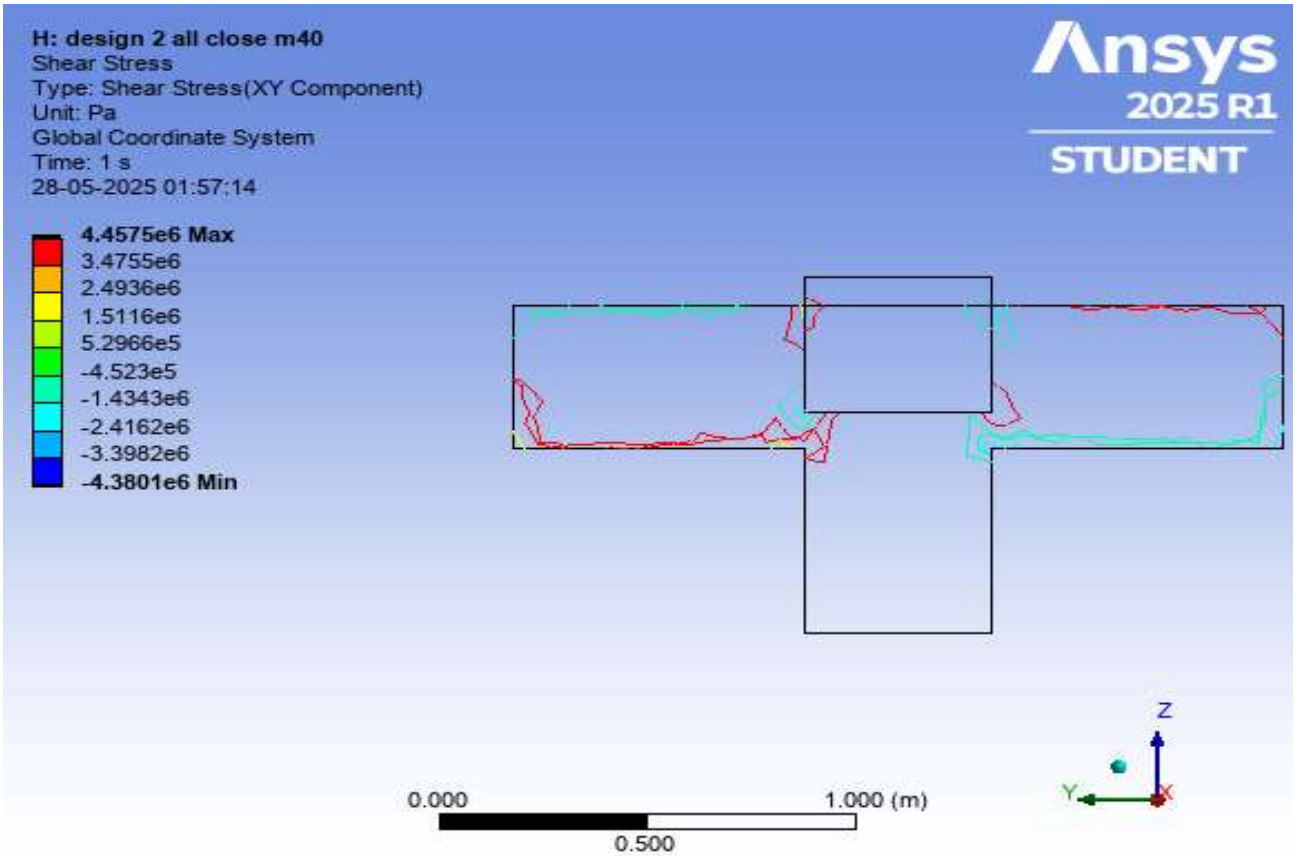

Figure 5.22: Shear stress plot

S.No	Time [s]	Minimum [Pa]	Maximum [Pa]	Average [Pa]
1	0.125	-5.48E+05	5.57E+05	-1030.7
2	0.25	-1.10E+06	1.11E+06	-2061.4
3	0.375	-1.64E+06	1.67E+06	-3092.1
4	0.5	-2.19E+06	2.23E+06	-4122.7
5	0.625	-2.74E+06	2.79E+06	-5153.4
6	0.75	-3.29E+06	3.34E+06	-6184.1
7	0.875	-3.83E+06	3.90E+06	-7214.8
8	1	-4.38E+06	4.46E+06	-8245.5

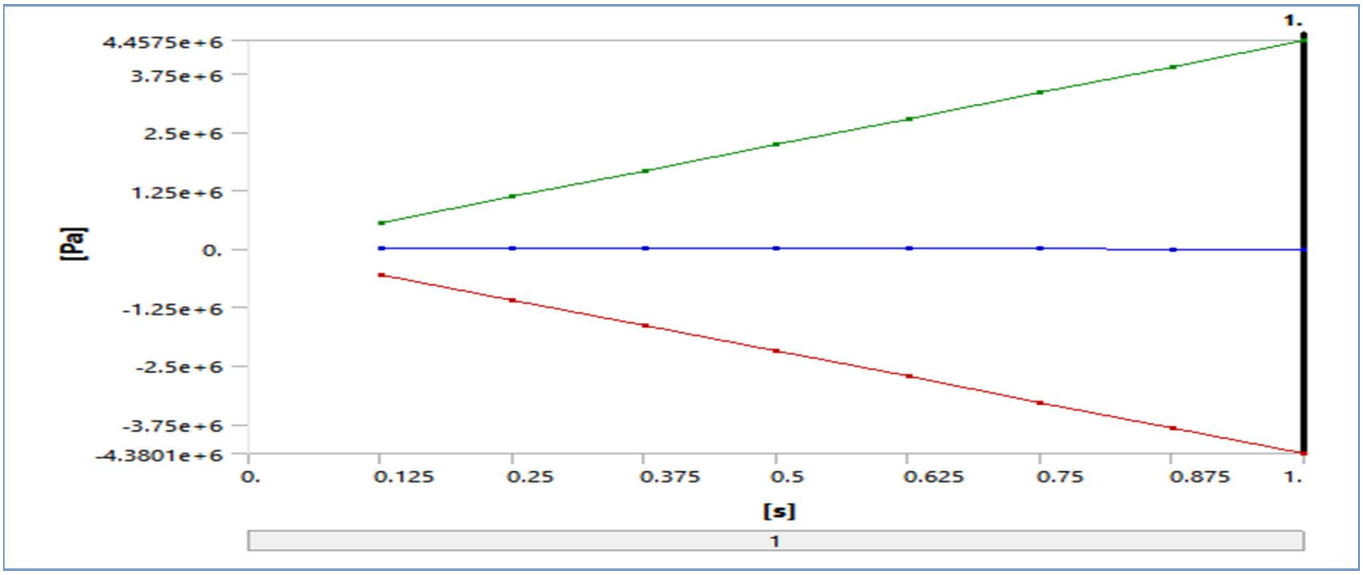

The stress pattern reveals efficient load transfer across the D2 joint. The stress peaks are less pronounced than in D1, indicating better geometry-based dispersion of forces. Yet, stress concentrations remain a concern at the load interface, and should be addressed with transverse reinforcement.

Strain Energy

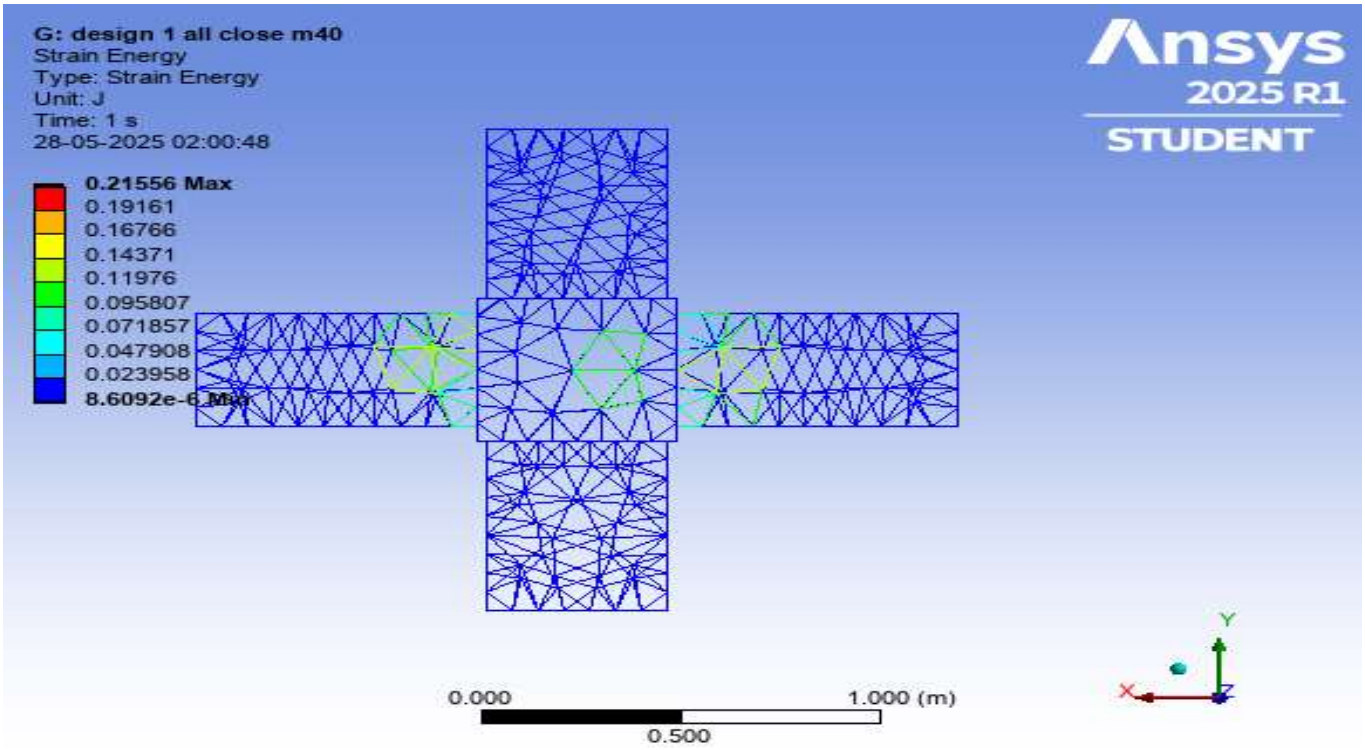

Figure 5.23: Strain energy plot

S.No	Time [s]	Minimum [J]	Maximum [J]	Total [J]
1	0.125	3.16E-07	6.49E-03	1.981
2	0.25	1.27E-06	2.60E-02	7.9241
3	0.375	2.85E-06	5.84E-02	17.829
4	0.5	5.06E-06	0.1039	31.696
5	0.625	7.91E-06	0.16235	49.525
6	0.75	1.14E-05	0.23378	71.317
7	0.875	1.55E-05	0.3182	97.07
8	1	2.02E-05	0.41561	126.79

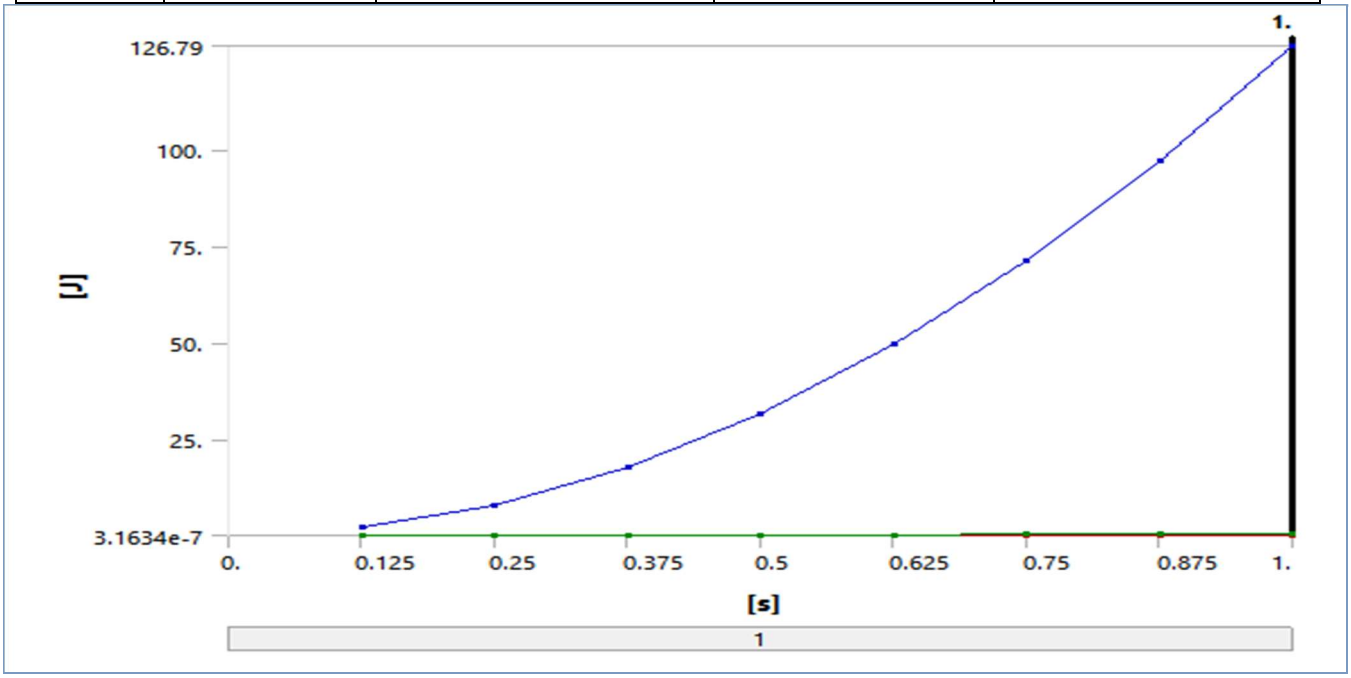

M40 D2 accumulates energy primarily at the joint's core, similar to D1, but with slightly wider dispersion. This suggests the D2 geometry better supports energy diffusion, reducing the risk of sudden joint failure. Nevertheless, energy absorption remains concentrated enough to warrant concern under seismic loads.

Maximum Principal Elastic Strain

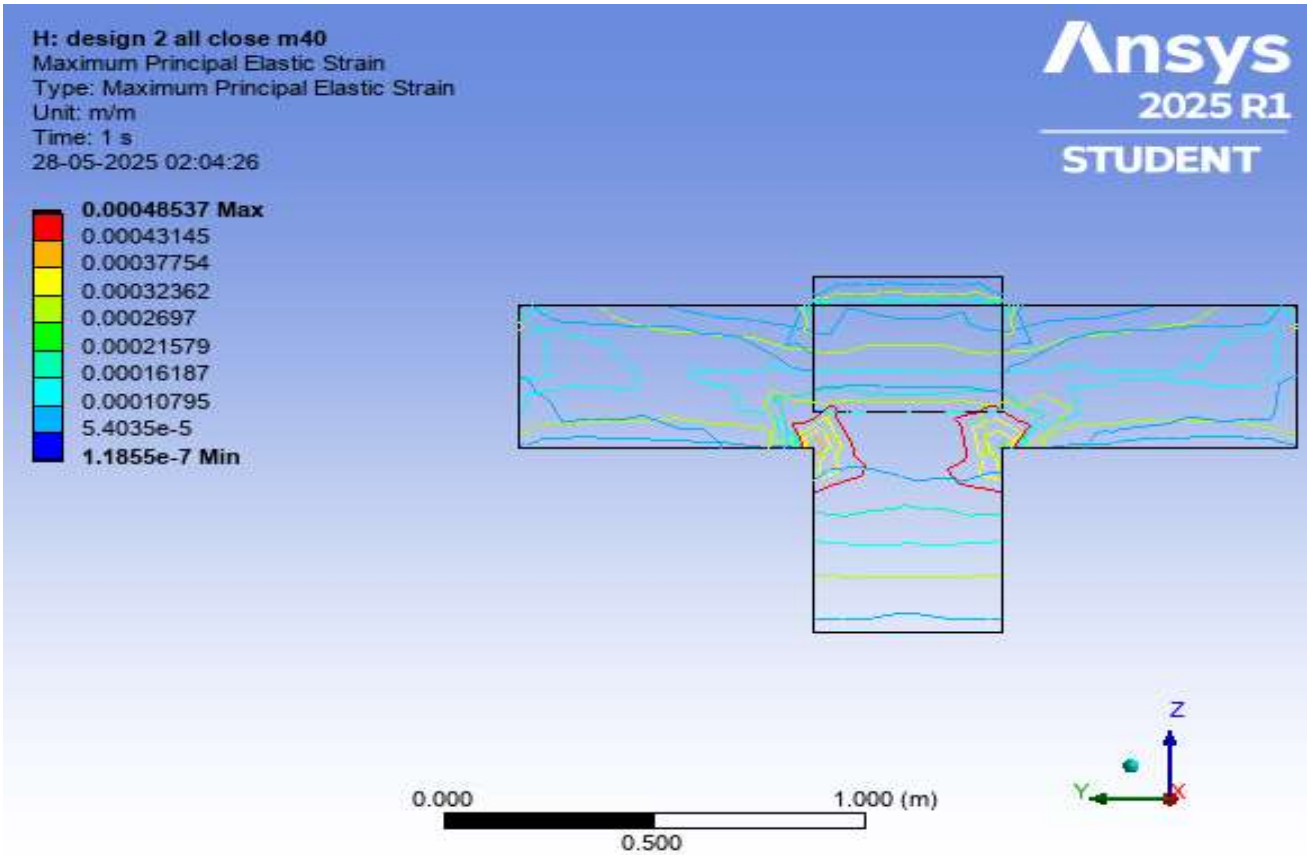

Figure 5.24: Maximum Principal elastic strain plot

S.No	Time [s]	Minimum [m/m]	Maximum [m/m]	Average [m/m]
1	0.125	1.48E-08	6.07E-05	9.84E-06
2	0.25	2.96E-08	1.21E-04	1.97E-05
3	0.375	4.45E-08	1.82E-04	2.95E-05
4	0.5	5.93E-08	2.43E-04	3.94E-05
5	0.625	7.41E-08	3.03E-04	4.92E-05
6	0.75	8.89E-08	3.64E-04	5.90E-05
7	0.875	1.04E-07	4.25E-04	6.89E-05
8	1	1.19E-07	4.85E-04	7.87E-05

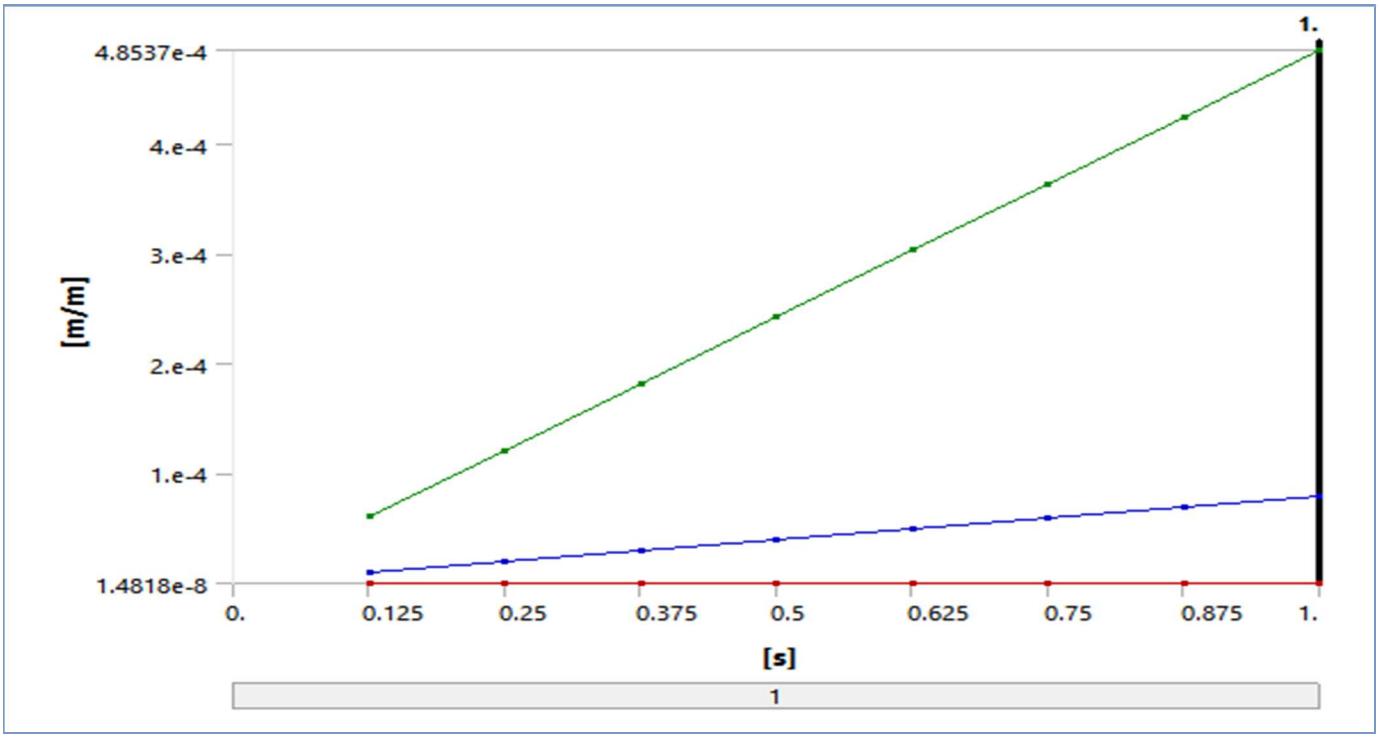

The joint undergoes minimal deformation, reinforcing the observation that M40 concrete enhances stiffness. However, similar to D1, this stiffness may compromise seismic performance unless coupled with ductile reinforcement strategies.

5.3.3 Design D3 CASE

Shear Stress

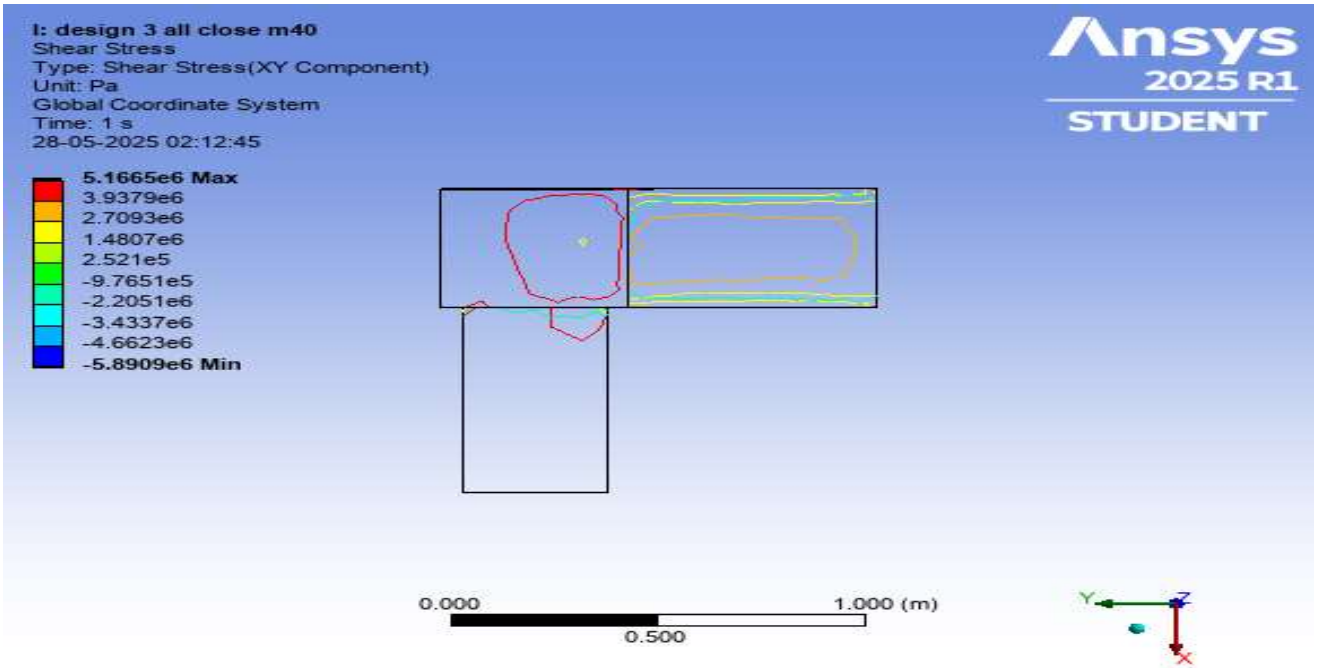

Figure 5.25: Shear stress plot

S.No	Time [s]	Minimum [Pa]	Maximum [Pa]	Average [Pa]
1	0.125	-7.36E+05	6.46E+05	31269
2	0.25	-1.47E+06	1.29E+06	62538
3	0.375	-2.21E+06	1.94E+06	93806
4	0.5	-2.95E+06	2.58E+06	1.25E+05
5	0.625	-3.68E+06	3.23E+06	1.56E+05
6	0.75	-4.42E+06	3.87E+06	1.88E+05
7	0.875	-5.15E+06	4.52E+06	2.19E+05
8	1	-5.89E+06	5.17E+06	2.50E+05

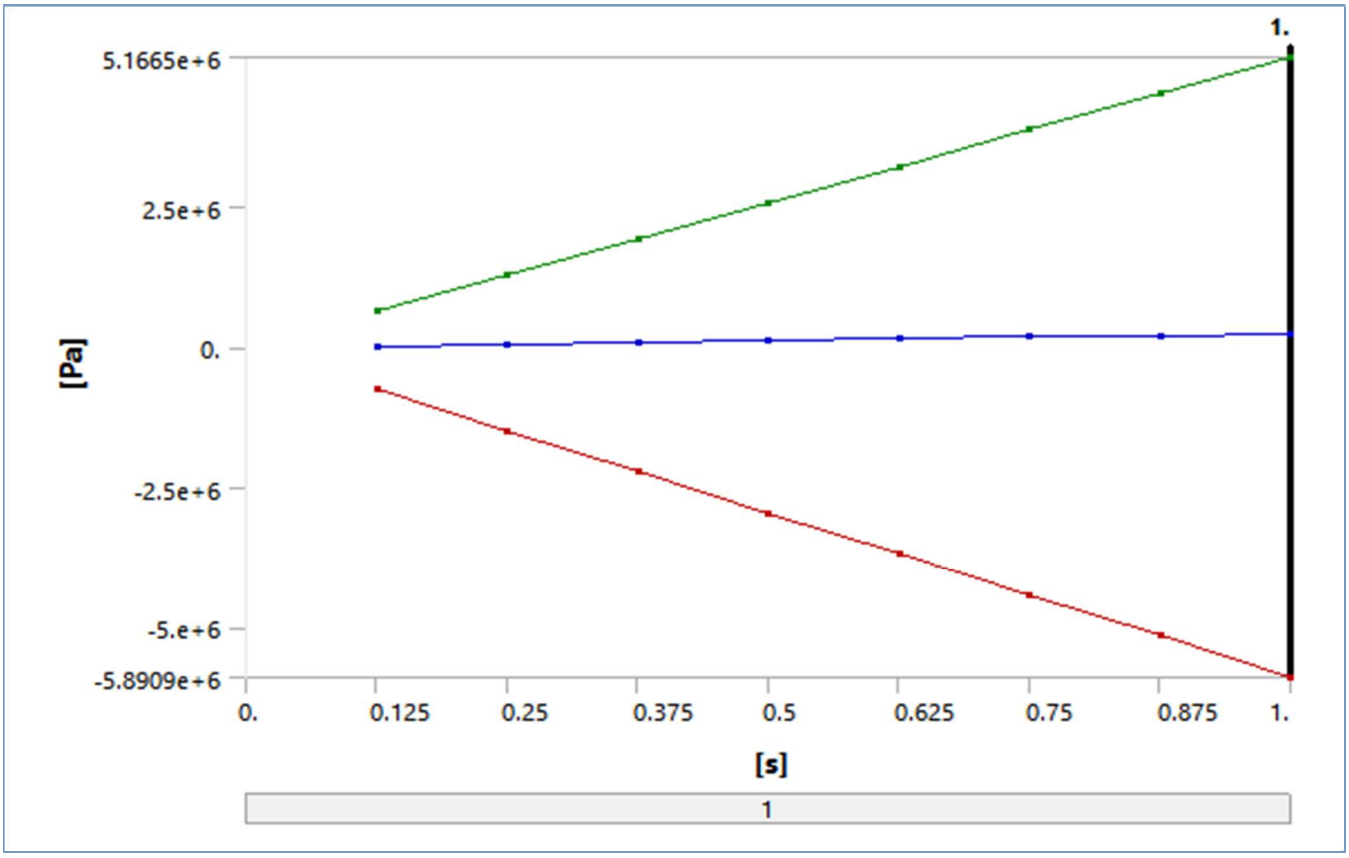

This configuration shows the highest recorded stress levels across all models, despite the use of high-strength concrete. This indicates that the D3 geometry inherently amplifies stress at certain nodes, and thus requires more sophisticated reinforcement detailing. The complex geometry creates zones of intensified interaction between horizontal and vertical load paths.

Strain Energy

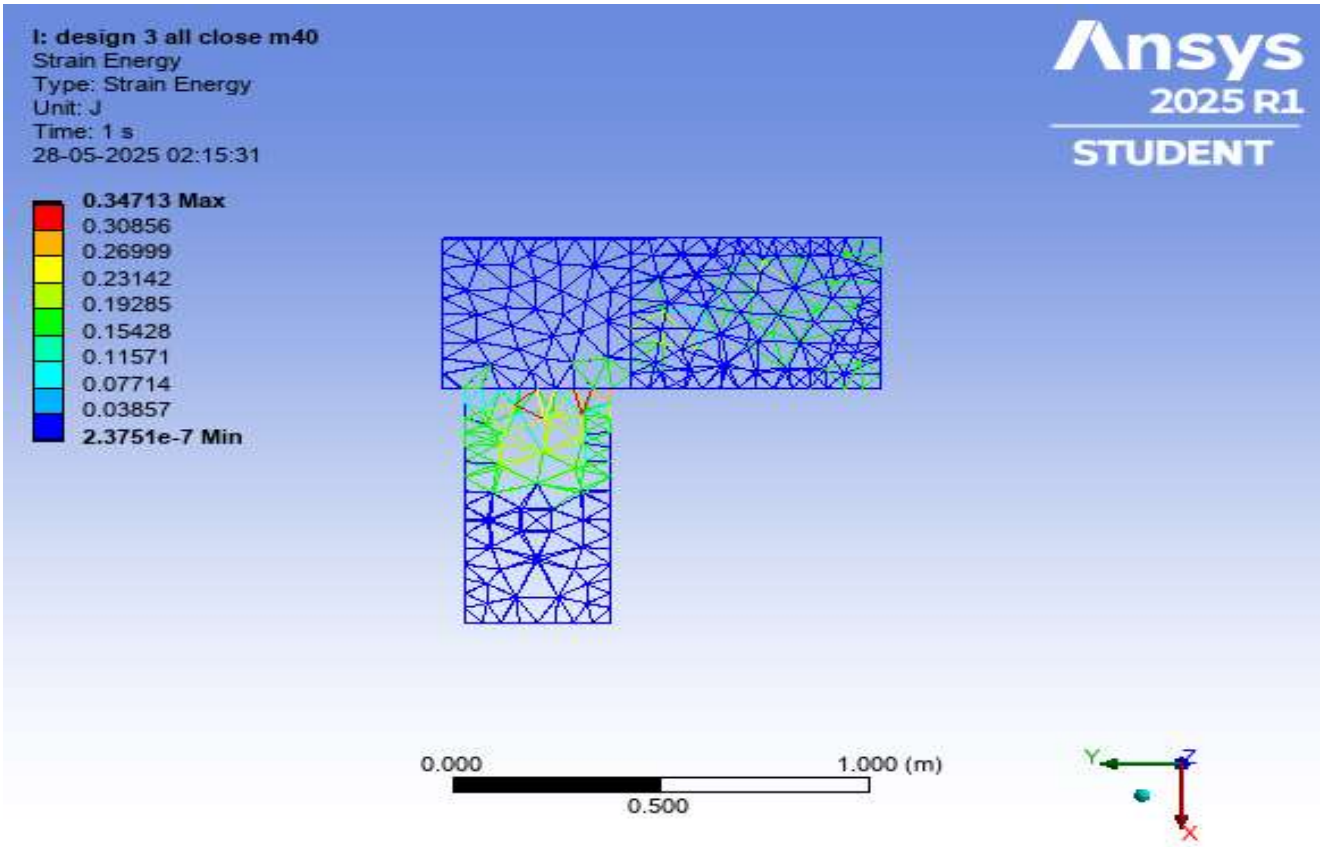

Figure 5.26: Strain energy plot

S.No	Time [s]	Minimum [J]	Maximum [J]	Total [J]
1	0.125	3.71E-09	5.42E-03	2.1245
2	0.25	1.48E-08	2.17E-02	8.4978
3	0.375	3.34E-08	4.88E-02	19.12
4	0.5	5.94E-08	8.68E-02	33.991
5	0.625	9.28E-08	0.1356	53.111
6	0.75	1.34E-07	0.19526	76.48
7	0.875	1.82E-07	0.26577	104.1
8	1	2.38E-07	0.34713	135.97

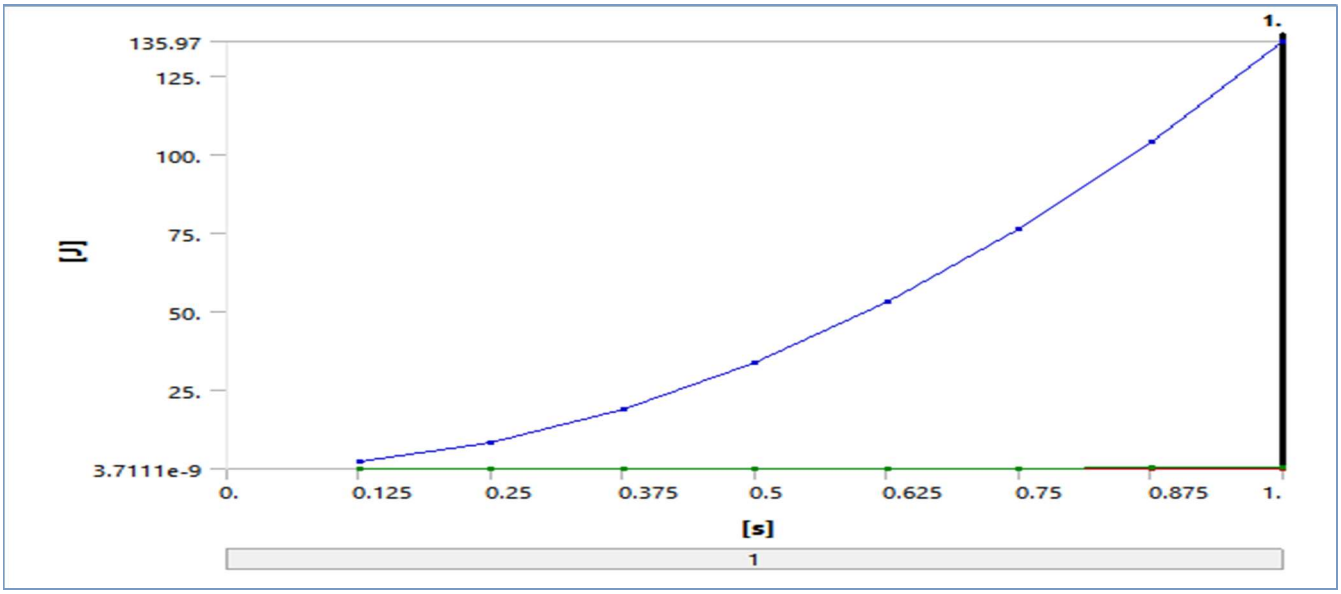

The energy plot reflects steep energy gradients, denoting rapid transitions in internal stress and deformation response. These steep contours point to a potentially brittle failure mode if energy is not dissipated effectively. Reinforcement or hybrid material solutions may be necessary to ensure safety.

Maximum Principal Elastic Strain

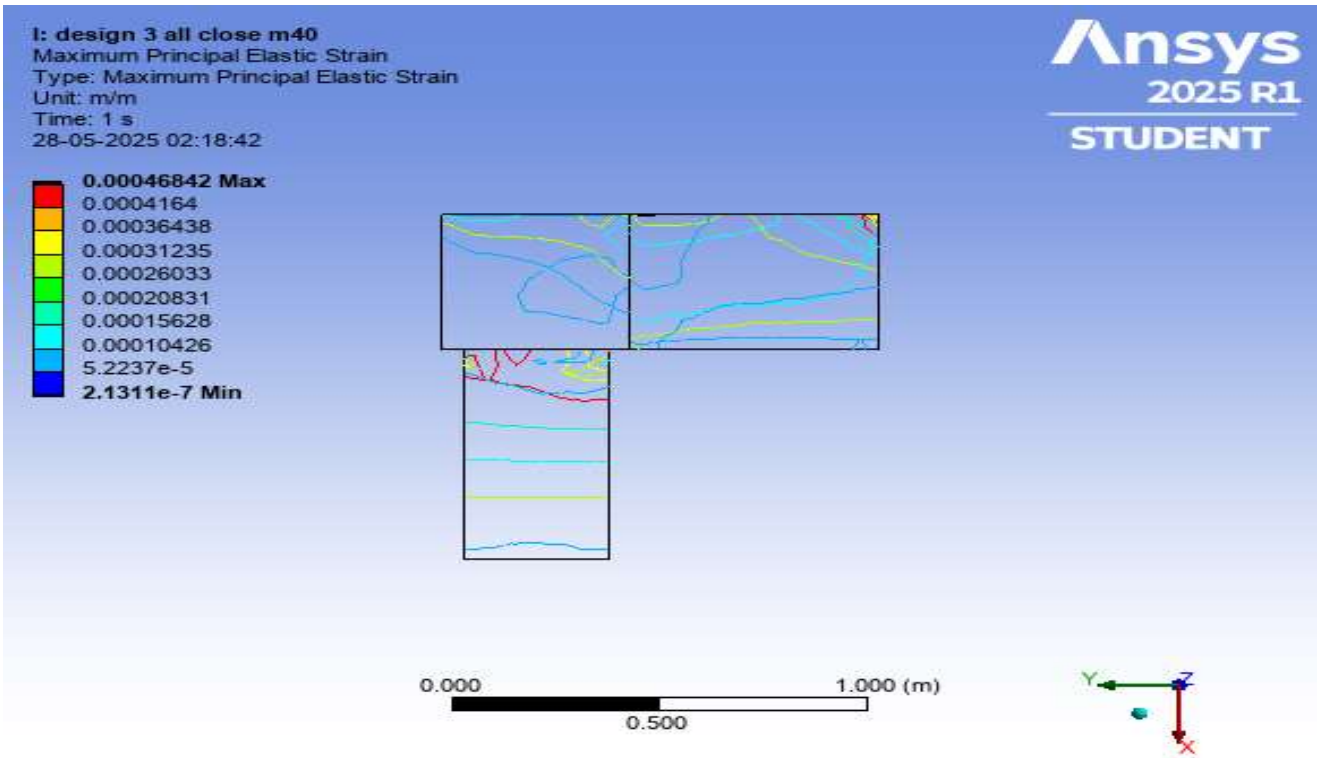

Figure 5.27: Maximum Principal elastic strain plot

S.No	Time [s]	Minimum [m/m]	Maximum [m/m]	Average [m/m]
1	0.125	2.66E-08	5.86E-05	1.06E-05
2	0.25	5.33E-08	1.17E-04	2.11E-05
3	0.375	7.99E-08	1.76E-04	3.17E-05
4	0.5	1.07E-07	2.34E-04	4.23E-05
5	0.625	1.33E-07	2.93E-04	5.29E-05
6	0.75	1.60E-07	3.51E-04	6.34E-05
7	0.875	1.86E-07	4.10E-04	7.40E-05
8	1	2.13E-07	4.68E-04	8.46E-05

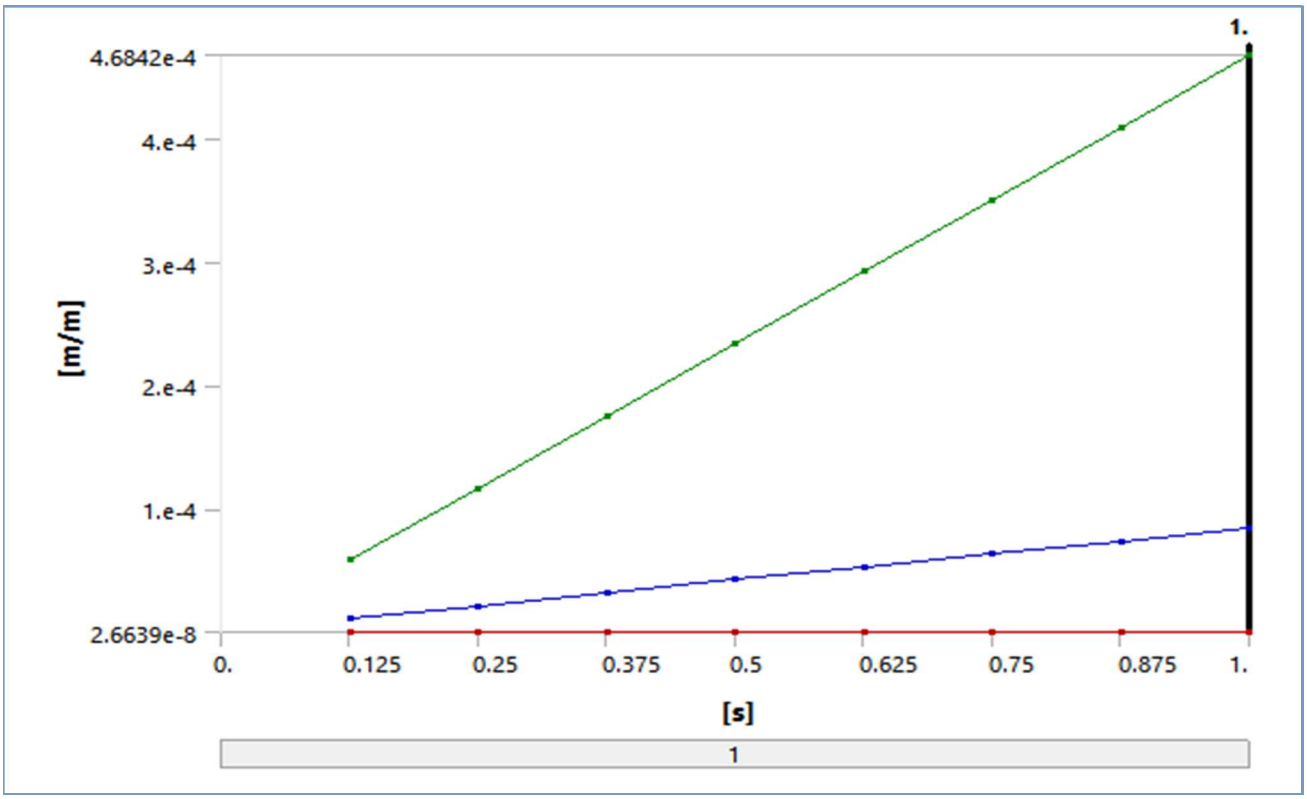

The deformation pattern shows sharp, localized angular strain variations. While M40's strength reduces the magnitude of strain, the abruptness of the transitions implies potential for cracking due to differential movements. The design must balance strength with ductility to avoid premature failure.

Table 4.1: M25 RCC material results

Design	Max Shear stress (MPa)	Max Strain energy (mJ)	Maximum Principal elastic strain (mm/mm)
D1	13.86	190.64	0.000569
D2	17.84	421.16	0.000511
D3	43.4	479.66	0.000853

Table 4.2: FRC material results

Design	Max Shear stress (MPa)	Max Strain energy (mJ)	Maximum Principal elastic strain (mm/mm)
D1	11.8	153.18	0.000428
D2	28.24	482.58	0.000685
D3	36.14	385.7	0.000615

Table 4.3: M40 material results

Design	Max Shear stress (MPa)	Max Strain energy (mJ)	Maximum Principal elastic strain (mm/mm)
D1	1.84	215.56	0.000343
D2	4.46	415.61	0.000485
D3	5.17	347.13	0.000468

Starting with the shear stress behavior, it is observed that the joints constructed with M25 concrete exhibit the highest stress values among the three material types. The D3 design in this group shows a maximum shear stress of 43.456 MPa, significantly higher than that observed in D2 and D1, which recorded values of 17.84 MPa and 13.86 MPa respectively. These values far exceed the permissible shear stress for unreinforced M25 concrete, suggesting a high likelihood of shear failure in the absence of proper reinforcement. The trend from D1 to D3 clearly indicates that the complexity of the geometry plays a significant role in amplifying the internal shear demands. The D3 configuration, with its more intricate structural features, appears particularly vulnerable under lateral forces due to the concentration of stress at the beam-column interface.

When the same joint designs are constructed using fiber-reinforced concrete, the shear stress values reduce considerably. For FRC, the maximum shear stress recorded for D3 is 36.165 MPa, followed by D2 with 28.24 MPa and D1 with 11.8 MPa. The reduction in stress values compared to M25 concrete highlights the effectiveness of fiber inclusion in redistributing internal forces and delaying crack initiation. Fibers act as bridging elements across potential crack paths, thereby improving the post-cracking behavior of the concrete and enhancing the structural integrity of the joint under high stress. Even in the D3 configuration, which is more susceptible to stress concentration due to its geometry, the reduction in peak shear stress demonstrates the role of FRC in mitigating the risk of brittle failure.

The M40 concrete group exhibits the lowest shear stress values among the three materials. In this case, the D3 design shows a peak shear stress of 5.1665 MPa, while D2 and D1 register 4.4575 MPa and 1.8316 MPa respectively. These values fall within the permissible limits for M40 concrete, indicating that the material's high compressive strength contributes to an improved resistance to shear forces. However, it is important to note that although the stress levels are lower, the lack of ductility in high-strength concrete such as M40 may result in a brittle mode of failure under dynamic or cyclic loads. Thus, while M40 is structurally capable of handling higher loads, it necessitates supplemental measures to ensure deformability under varying load conditions.

Moving to the analysis of strain energy, which represents the energy absorbed by the structure during deformation, it is evident that D2 consistently exhibits the highest energy values across all three materials. In the M25 group, D2 absorbs 421.16 mJ, followed by D3 with 479.84 mJ and D1 with 190.64 mJ. These figures suggest that D2 is more efficient in distributing and absorbing the applied energy, which is advantageous in resisting collapse during extreme loading events. However, high energy values in brittle materials like M25 may also imply a risk of concentrated stress zones, which can lead to sudden failure if the energy is not properly dissipated.

The FRC models again show a favorable performance with reduced but more evenly distributed strain energy. D2 absorbs 482.58 mJ, D3 absorbs 385.66 mJ, and D1 absorbs 153.18 mJ. These values are lower than those in the M25 group but are more evenly spread across the joint, reducing the risk of localized failure. The use of fibers aids in spreading the deformation over a wider area, making the structure more resilient to repeated loading and increasing its fatigue life. This suggests that FRC not only enhances the strength of the structure but also contributes to its energy dissipation capability, which is crucial in seismic design.

In the case of M40 concrete, the energy absorption trend remains consistent with D2 at 415.61 mJ, D3 at 347.13 mJ, and D1 at 215.56 mJ. Although the values are substantial, the high stiffness of M40 means that the energy is absorbed in a more localized manner, increasing the risk of brittle fractures if not complemented with ductile reinforcement. While M40 is capable of handling high loads, the energy absorption pattern indicates that the material's brittleness must be carefully considered in design to avoid sudden failure during seismic or impact loading.

Lastly, the shear elastic strain results provide insight into the deformability of each configuration. M25 concrete shows the highest strain values, with D3 at -0.0006381 mm/mm, D2 at -0.0005024 mm/mm, and D1 at -0.0000341 mm/mm. These values indicate significant angular deformation, especially in the D3 and D2 joints, highlighting their susceptibility to joint rotation and potential loss of serviceability under high shear. The negative strain values reflect compressive angular distortion, suggesting zones of high torsional influence in the joint core.

The D2 geometry consistently demonstrates the best balance between stress, strain, and energy absorption across all material types. FRC emerges as the most versatile and structurally efficient material, offering a reliable combination of strength, deformability, and energy dissipation. M25 concrete, while common and economical, requires extensive reinforcement to manage its limitations under shear and energy absorption. M40 concrete, though inherently strong, should be used cautiously in dynamic applications due to its limited strain tolerance. These results provide

clear guidance for selecting material and geometry combinations that optimize the structural performance of beam-column joints under lateral and seismic loads.

Table 4.4: Shear stress comparison

	M25 RCC	FRC	M40
D1	13.86	11.8	1.84
D2	17.84	28.24	4.46
D3	43.4	36.14	5.17

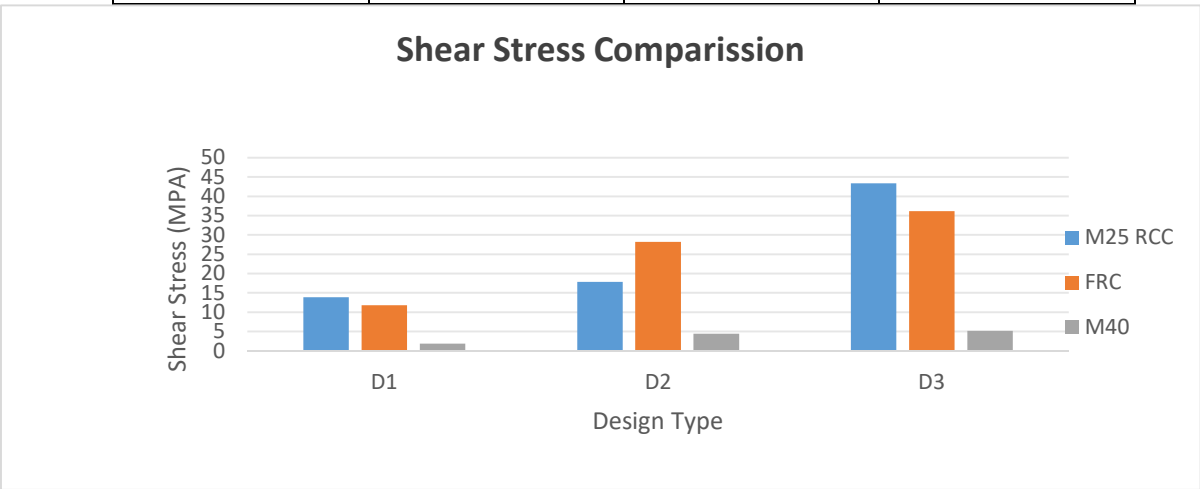

Figure 5.37: Shear stress comparison chart

Figure 4.4 illustrates the comparative behavior of three different beam-column joint designs D1, D2, and D3 under varying material configurations: M25 concrete, fiber-reinforced concrete (FRC), and M40 concrete. The parameter evaluated is the maximum shear stress (in MPa) sustained by each configuration under applied lateral load. The values reflect the intensity of tangential forces developed within the joint due to structural loading and are critical in assessing the likelihood of shear failure or cracking.

For the D1 configuration, the shear stress values are lowest across all materials, with M25 registering 13.86 MPa, FRC at 11.8 MPa, and M40 significantly lower at 1.84 MPa. This pattern suggests that the D1 geometry experiences the least internal stress concentration. However, even in this simple geometry, the shear stress in M25 concrete far exceeds its design shear capacity, indicating potential vulnerability unless reinforced. FRC shows a reduction of about 15% compared to M25, showcasing its ability to redistribute stress through fiber bridging. M40

performs the best in limiting shear stress, with its inherent high strength and stiffness keeping the value well below failure thresholds, though at the expense of ductility.

In the D2 configuration, which is more structurally complex than D1, shear stress values increase across all materials. M25 experiences a significant jump to 17.84 MPa, FRC follows at 28.24 MPa, and M40 rises to 4.4575 MPa. This indicates that the D2 geometry induces higher shear stress concentration due to more efficient force transmission across the joint. Although M25 again exceeds typical safe stress levels, FRC helps reduce the peak stress by about 16%, affirming its effectiveness in moderating internal force gradients. M40, while showing an increase from D1, still remains within safe structural limits due to its superior compressive and shear strength properties.

The D3 configuration displays the highest shear stress values among all three geometries. M25 reaches a peak of 43.456 MPa, a dangerously high value that would likely cause severe shear cracking or failure without reinforcement. FRC reduces this peak to 36.165 MPa, offering a 17% reduction, but the value still remains relatively high, emphasizing that geometry alone significantly amplifies internal forces. M40 exhibits a much lower value of 5.1665 MPa in the same configuration, reinforcing its potential in resisting shear stress buildup. However, the relative rise in stress from D2 to D3 within M40 also highlights that despite its strength, M40 joints may still face localized stress issues that require consideration.

Overall, the chart reveals a clear trend: as joint complexity increases from D1 to D3, shear stress also increases, regardless of material. However, the material choice plays a decisive role in moderating this effect. M25, being a normal-strength concrete, is insufficient on its own for D2 and D3 configurations due to excessive stress development. FRC consistently lowers the stress values due to its ductile nature and crack-bridging capabilities, making it more suitable for complex and dynamically loaded joints. M40, although the best in limiting stress magnitudes, lacks ductility and may not perform well under cyclic or seismic loading unless supplemented with additional confinement or detailing.

While FRC offers a balanced solution with moderate stress and high ductility, M40 is most suitable for static, high-load scenarios, and M25 requires reinforcement to be viable in complex geometries. The D2 geometry appears to offer a favorable balance between stress concentration and structural performance, especially when paired with FRC.

Table 4.5: Max strain energy comparison

	M25 RCC	FRC	M40
D1	190.64	153.18	215.56
D2	421.16	482.58	415.61
D3	479.66	385.7	347.13

Strain energy represents the internal energy absorbed by the structure as it deforms under loading, providing a direct indication of its ability to withstand and dissipate stresses without failure. A higher strain energy value generally implies greater deformation capacity, which is particularly valuable in structures exposed to dynamic or cyclic loading conditions such as earthquakes.

In the D1 configuration, which has the simplest geometry among the three, the M40 concrete joint records the highest strain energy at 215.56 mJ, followed by M25 at 190.64 mJ and FRC at 153.18 mJ. This indicates that M40, due to its higher stiffness and strength, is capable of absorbing greater amounts of energy before yielding, although this energy is likely concentrated rather than dispersed. While M25 absorbs a relatively high amount of energy, it may not manage the energy efficiently due to its limited ductility, potentially resulting in cracking or sudden failure. FRC shows the lowest energy absorption in this configuration, which may seem less favorable at first glance, but actually reflects the material's ability to more uniformly distribute loads, reducing peak deformations and minimizing localized stress concentrations.

In the D2 configuration, all materials exhibit a substantial increase in absorbed strain energy compared to D1. FRC shows the value at 482.58 mJ, followed by M25 at 421.16 mJ and M40 at 415.61 mJ. The spike in energy absorption is indicative of the D2 geometry's increased capacity to engage in deformation and structural interaction under loading. However, in the case of FRC, the high energy level also signals a potential concern: the energy is not effectively dissipated and is more likely to be concentrated at critical points, heightening the risk of brittle failure. FRC, while showing slightly lower energy absorption, offers a more favorable performance profile by ensuring distributed absorption and improved crack control. M40 shows a slightly reduced capacity compared to M25 and FRC, suggesting that while it is strong, its rigidity limits its ability to undergo large-scale deformation, which is a critical trait in energy dissipation during seismic events.

The D3 configuration, which is the most complex geometrically, shows a decrease in maximum strain energy across all materials compared to D2. M25 absorbs 479.66 mJ, FRC 385.86 mJ, and M40 347.13 mJ. The reduction in energy values may be attributed to more localized stress concentrations and stiffness imbalances introduced by the complex geometry. M25 again leads in energy absorption but remains less reliable due to the likelihood of abrupt cracking under dynamic conditions. FRC continues to exhibit consistent and stable behavior with sufficient energy capacity and enhanced ductility. M40, while structurally stable, shows limitations in strain energy uptake, reaffirming its more brittle nature.

In interpreting these results, it is clear that D2 consistently offers the highest energy absorption capability, which suggests that it is structurally optimized for transferring and dissipating internal loads across the joint area. However, the effectiveness of this capacity is strongly influenced by

the material type. M25 shows the highest absolute values but lacks the ductility required to safely manage this energy, which could result in structural damage under extreme loading. FRC demonstrates a better balance between energy absorption and deformation control, making it well-suited for seismic applications. M40 performs reliably under static conditions but is not ideal for energy-intensive dynamic applications unless supplemented with ductile detailing.

The table highlights the critical interaction between geometry and material in influencing a joint's energy dissipation characteristics. The combination of D2 geometry and FRC material emerges as the most structurally resilient solution, offering significant energy absorption with enhanced durability and ductile response.

Table 4.6: Maximum Principal elastic strain comparison

	M25 RCC	FRC	M40
D1	0.000569	0.000428	0.000343
D2	0.000511	0.000685	0.000485
D3	0.000853	0.000615	0.000468

Table 4.6 presents a comparative evaluation of the maximum Principal elastic strain observed in three beam-column joint designs D1, D2, and D3 constructed using three distinct materials: M25 concrete, fiber-reinforced concrete (FRC), and M40 concrete. Principal elastic strain, expressed in mm/mm, measures the angular deformation occurring within a structural element due to shear stress. It is a critical indicator of a structure's ability to undergo elastic deformation without leading to permanent damage or failure. Higher strain values imply greater deformation capacity, which is beneficial for ductility but could also suggest susceptibility to instability if not properly controlled.

In the D1 configuration, the simplest of the three designs, M40 concrete shows the lowest principal elastic strain at approximately 0.000343 mm/mm, while FRC registers a significantly higher value of 0.000428 mm/mm, and M25 falls in between at 0.000569 mm/mm. The very low strain value in M40 suggests minimal angular distortion, but this could also indicate brittle behavior, as the material may fail suddenly without showing significant deformation. FRC, with its higher strain capacity, allows greater angular movement, reflecting its enhanced ductility and energy absorption capabilities. M25, though more deformable than M40 in this configuration, remains relatively stiff, limiting its strain response while still offering more safety margin than M40 in the elastic range.

In the D2 configuration, principal strain values increase significantly for all materials, which is expected due to the greater structural interaction and complexity inherent in this joint design. M25 reaches 0.000511 mm/mm, FRC slightly less at 0.000685 mm/mm, and M40 at 0.000485mm/mm. This suggests that D2 geometry introduces more torsional and shear effects due to load redistribution across the joint, necessitating materials with higher deformation capacity. The slightly lower strain in M25 compared to FRC indicates a more controlled deformation behavior, facilitated by the fibers that restrain crack propagation and enhance the material's ability to return to its original shape. M40, despite its stiffness, shows a modest increase in strain capacity in this configuration, reflecting its better accommodation of geometric complexity through strength rather than flexibility.

The D3 configuration, which is the most geometrically complex and stress-intensive, results in the highest shear elastic strains across all materials. M25 records a peak value of 0.000853mm/mm, followed by FRC at 0.000615mm/mm, and M40 at 0.000468 mm/mm. The sharp increase in strain for M25 indicates a high level of angular distortion, which can significantly compromise structural performance, especially under repeated or cyclic loads. FRC, while also showing increased strain, maintains a more balanced behavior, confirming its ability to accommodate deformation without sudden cracking. M40, as expected, shows the least strain among the three, suggesting high stiffness and resistance to angular deformation, but this also confirms its reduced ductility and potential for brittle failure under dynamic conditions.

In interpreting these results, it becomes evident that material properties have a significant influence on the deformation characteristics of beam-column joints under shear loading. M25 concrete, while offering basic performance, lacks the ductility needed to safely accommodate higher shear strains, especially in more complex geometries like D3. FRC consistently demonstrates improved deformation capacity, allowing for larger elastic movements while maintaining structural integrity. This behavior is essential for applications requiring resilience under seismic or cyclic loading. M40, with its lower strain values, excels in stiffness and strength but may need additional ductile reinforcement or confinement to prevent brittle failure in high-strain scenarios.

Overall, the data suggests that FRC offers the best compromise between flexibility and stability, making it suitable for a wide range of structural applications. M25 should be used with caution, particularly in geometries prone to high strain, unless additional reinforcement is provided. M40 is best suited for high-strength requirements but must be paired with design strategies that compensate for its limited strain tolerance. The D2 configuration again stands out as structurally balanced, handling strain effectively across all materials while maintaining stability, which underscores its suitability for design optimization.

Chapter 6

Conclusion and Future Scope

6.1 Conclusion

1. The shear stress results indicate a clear trend of increasing stress with joint complexity from D1 to D3, regardless of the material used. This underscores the critical influence of joint geometry on stress concentration.

2. M25 concrete consistently recorded the highest shear stress and strain energy values across all configurations, suggesting that while it can absorb large amounts of energy, it lacks the ductility required to safely dissipate this energy, making it vulnerable to brittle failure.

3. FRC showed a notable reduction in shear stress across all joint types compared to M25, with reductions of approximately 17%, indicating its effectiveness in moderating stress concentration through fiber bridging and enhanced load distribution.

4. In terms of strain energy, the D2 configuration consistently outperformed D1 and D3, regardless of material. This implies that D2 offers an optimal balance between structural complexity and energy absorption, making it well-suited for dynamic loading scenarios.

5. M40 concrete, despite showing the lowest shear elastic strain, exhibited the least energy absorption and deformation capacity. This behavior reflects its high stiffness but also highlights its limited ductility, which may lead to brittle failure under seismic or repeated loading.

6. Shear elastic strain values were highest in the D3 configurations for all materials, confirming that this joint geometry experiences the most angular distortion and requires careful reinforcement to maintain stability.

7. FRC provided a balanced performance across all criteria—moderate stress levels, sufficient strain energy absorption, and controlled shear deformation—making it the most resilient and versatile material among the three for complex and cyclic loading conditions.

8. M25 should be applied with caution in geometries like D2 and D3, where stress and strain demands are high. Without additional reinforcement or ductile detailing, its performance under lateral or seismic loading is inadequate.

9. The performance of M40 concrete is more suited to static high-load applications, where strength is prioritized over flexibility. However, it must be complemented with ductile design measures if used in seismic zones to counter its brittle nature.

10. The combined analysis of stress, strain energy, and elastic strain confirms that the D2 configuration paired with FRC offers the most structurally efficient and durable solution for beam-column joints subjected to lateral and dynamic loads.

11. FRC reduces shear stress consistently across all joint types by approximately 16–17% when compared to M25 concrete, confirming its effectiveness in mitigating stress concentration through fiber reinforcement and enhanced load redistribution.

12. M40 concrete demonstrates the most substantial reduction in shear stress, ranging from 83.28% to 88.11% across D2 and D3 configurations. This underscores its superior material strength and stiffness, which help it withstand shear loads with minimal internal stress development.

13. In the D3 configuration, which is the most structurally complex, the shear stress reduction achieved by M40 (88.11%) is the highest among all cases, indicating that M40 is especially effective in handling high shear demands in complex joint geometries**,** provided brittleness is accounted for.

14. Although FRC does not match M40 in terms of absolute stress reduction, its consistent performance across all joint types indicates a reliable balance between strength and ductility**,** making it a more versatile and safer option for dynamically loaded or seismic environments.

15. The small variation in FRC's percentage reduction (between 16.07% and 16.77%) suggests that FRC's shear stress mitigating capacity is less affected by changes in joint geometry, contributing to predictable and stable structural behavior.

16. The dramatic reduction in shear stress in M40 is largely attributed to its high modulus of elasticity and compressive strength; however, its brittle failure mode must be counteracted through ductile detailing or confinement reinforcement in seismic-prone areas.

17. M25 concrete, in all cases, exhibits the highest shear stress values**,** reinforcing the conclusion that it is the least effective of the three materials in resisting shear without reinforcement, particularly in geometrically complex joints like D2 and D3.

18. FRC consistently shows approximately 80% strain energy compared to M25 concrete across all joint designs (D1, D2, D3), indicating lower energy absorption capacity relative to M25.

19. M40 exhibits variable strain energy relative to M25, with a higher strain energy (about 111%) in design D1 but significantly lower values in D2 (67%) and D3 (72%), suggesting that its performance is design-dependent.

20. Design D1 shows the highest strain energy for M40, surpassing M25, which could imply better stiffness or energy absorption under the specific loading and configuration conditions of this design.

21. In designs D2 and D3, M40's strain energy is notably lower than M25 and FRC, indicating that the use of higher concrete grade does not always translate to increased strain energy in all joint configurations.

22. FRC, despite having lower strain energy than M25, maintains a consistent percentage across all designs, suggesting predictable behavior that may be advantageous for design considerations requiring uniform energy dissipation.

23. FRC exhibits extremely high shear elastic strain relative to M25 in design D1 (over 700%), indicating significantly greater shear deformation in this joint configuration. This could be due to the fiber reinforcement providing additional flexibility or a more ductile response under shear loading in this specific design.

24. M40 also shows increased shear elastic strain relative to M25 in D1 (about 350%), suggesting that higher-grade concrete allows more elastic deformation under shear in this configuration, possibly because of altered stiffness and stress distribution at the joint.

25. For designs D2 and D3, both FRC and M40 show lower shear elastic strains than M25 (between 64% and 80%), indicating that in these configurations, the stiffer materials (FRC and M40) resist shear deformation better than M25 concrete.

26. The dramatic difference in D1 compared to D2 and D3 suggests that the joint design and loading significantly influence how materials respond in shear FRC and M40 may perform very differently depending on joint detailing and stress concentrations.

27. Higher shear elastic strain implies greater reversible deformation under load, which can be beneficial for ductility and energy dissipation but may also indicate potential for larger displacements. Lower shear strains may indicate stiffer but potentially more brittle behavior.

6.2 Future Scope

1. Future studies can incorporate nonlinear dynamic simulations under seismic or cyclic loading conditions to better understand the inelastic behavior and energy dissipation capacity of beam-column joints, especially for different materials such as FRC and higher-grade concrete.

2. Investigating the impact of temperature variations, moisture content, and environmental degradation on the structural performance of beam-column joints would provide a more realistic assessment of joint durability over service life.

3. A detailed parametric study varying reinforcement patterns, anchorage lengths, and stirrup configurations can be conducted to optimize joint design for improved strength and ductility, supported by advanced FEM models.

4. Further experimental investigations should be undertaken to validate and calibrate the FEM models for different joint types and materials, enhancing the accuracy and reliability of numerical simulations.

5. Incorporating soil-structure interaction (SSI) in the modeling of beam-column joints can help analyze the influence of foundation flexibility on joint behavior, especially for structures subjected to dynamic loading.

6. Research can focus on developing or refining design codes and guidelines specifically for beam-column joints using fiber reinforced concrete and high-strength concrete, bridging the gap between experimental results and practical applications.

7. Implementing multi-scale modeling techniques that link microstructural properties of concrete and fibers to the macroscopic joint behavior can provide deeper insights into failure mechanisms and performance optimization.

References

[1] Ghayeb HH, Razak HA, Sulong NR. Performance of dowel beam-to-column connections for precast concrete systems under seismic loads: a review. Constr Build Mater 2020;237:117582. https://doi.org/10.1016/j. conbuildmat.2019.117582

[2] Webber A, Orr JJ, Shepherd P, Crothers K. The effective length of columns in multistorey frames. Eng Struct 2015;102:132–43. https://doi.org/10.1016/j. engstruct.2015.07.039.

[3] Batalha N, Rodrigues H, Arˆede A, Furtado A, Sousa R, Varum H. Cyclic behaviour of precast beam-to-column connections with low seismic detailing. Earthq Eng Struct Dyn 2022;51(5):1096–114. https://doi.org/10.1002/eqe.3606.

[4] Kremmyda GD, Fahjan YM, Psycharis IN, Tsoukantas SG. Numerical investigation of the resistance of precast RC pinned beam-to-column connections under shear loading. Earthq Eng Struct Dyn 2017;46(9):1511–29. https://doi.org/10.1002/ eqe.2868.

[5] Cimmino M, Magliulo G, Manfredi G. Seismic collapse assessment of new European single-story RC precast buildings with weak connections. Bull Earthq Eng 2020;18 (15):6661–86. https://doi.org/10.1007/s10518-020-00952-7.

[6] Magliulo G, Cimmino M, Ercolino M, Manfredi G. Cyclic shear tests on RC precast beam-to-column connections retrofitted with a three-hinged steel device. Bull Earthq Eng 2017;15(9):3797–817. https://doi.org/10.1007/s10518-017-0114-x.

[7] Tafsirojjaman T, Fawzia S, Thambiratnam D, Zhao XL. FRP strengthened SHS beam-column connection under monotonic and large-deformation cyclic loading. Thin-Walled Struct 2021;161:107518. https://doi.org/10.1016/j. tws.2021.107518.

[8] Tafsirojj

[10] H. Behnam, J.S. Kuang, R.Y.C. Huang, Exterior RC wide baman T, Fawzia S, Thambiratnam DP. Structural behaviour of CFRP strengthened beam-column connections under monotonic and cyclic loading. Structures 2021;33:2689–99. https://doi.org/10.1016/j.istruc.2021.06.028.

[9] H.A. Waqas, M. Sahil, M.M. Khan, A.W. Anwar, M.U. Shah, M. Usman, Optimizing reinforcement strategies for robust beam-column joints in seismic-resistant structures, Arabian J. Sci. Eng. (2024), https://doi.org/10.1007/s13369-023- 08591-1.

eam-column connections: effect of beam width ratio on seismic behaviour, Eng. Struct. 147 (2017) 27–44, https://doi.org/10.1016/J.ENGSTRUCT.2017.05.044.

[11] S. Alavi-Dehkordi, D. Mostofinejad, P. Alaee, Effects of high-strength reinforcing bars and concrete on seismic behavior of RC beam-column joints, Eng. Struct. 183 (2019) 702–719, https://doi.org/10.1016/J.ENGSTRUCT.2019.01.019.

[12] H.A. Waqas, M. Sahil, M.M. Khan, M. Hasnain, Predictive model for load-carrying capacity of reinforced concrete beam–column joints using gene expression programming, in: Proceedings of the ASEC 2023, MDPI, Basel Switzerland, October 26 2023, p. 67.

[13] A. Zabihi, H.H. Tsang, E.F. Gad, J.L. Wilson, Seismic retrofit of exterior RC beam column joint using diagonal haunch, Eng. Struct. 174 (2018) 753–767, https://doi. org/10.1016/J.ENGSTRUCT.2018.07.100.

[14] M.I. Khan, M.A. Al-Osta, S. Ahmad, M.K. Rahman, Seismic behavior of beam column joints strengthened with ultra-high performance fiber reinforced concrete, Compos. Struct. 200 (2018) 103–119, https://doi.org/10.1016/j. compstruct.2018.05.080.

[15] R. Sharma, P.P. Bansal, Behavior of RC exterior beam column joint retrofitted using UHP-HFRC, Construct. Build. Mater. 195 (2019) 376–389, https://doi.org/ 10.1016/j.conbuildmat.2018.11.052.

[16] A.-D.G. Tsonos, Performance enhancement of R/C building columns and beam–column joints through shotcrete jacketing, Eng. Struct. 32 (2010) 726–740, https://doi.org/10.1016/j.engstruct.2009.12.001.

[17] G.L. Wang, J.G. Dai, Y.L. Bai, Seismic retrofit of exterior RC beam-column joints with bonded CFRP reinforcement: an experimental study, Compos. Struct. 224 (2019) 111018, https://doi.org/10.1016/J.COMPSTRUCT.2019.111018.

[18] E. Ilia, D. Mostofinejad, Seismic retrofit of reinforced concrete strong beam–weak column joints using EBROG method combined with CFRP anchorage system, Eng. Struct. 194 (2019) 300–319, https://doi.org/10.1016/J. ENGSTRUCT.2019.05.070.

[19] C.T. Dang, N.H. Dinh, Experimental study on structural performance of RC exterior beam-column joints retrofitted by steel jacketing and haunch element under cyclic loading simulating earthquake excitation, Adv. Civ. Eng. 2017 (2017), https://doi. org/10.1155/2017/9263460.

[20] A.S. Jape, S.B. Gayake, P.D. Dhake, Structural Behavior of Beam Column Joint Retrofitted Using Carbon Fiber Reinforced Polymer, vol. 8, 2021.

[21] C. del Vecchio, M. di Ludovico, A. Balsamo, A. Prota, G. Manfredi, M. Dolce, Experimental investigation of exterior RC beam-column joints retrofitted with FRP systems, J. Compos. Construct. 18 (2014) 04014002, https://doi.org/10.1061/ (ASCE)CC.1943-5614.0000459.

[22] C. del Vecchio, M. di Ludovico, A. Prota, G. Manfredi, Analytical model and design approach for FRP strengthening of non-conforming RC corner beam–column joints, Eng. Struct. 87 (2015) 8–20, https://doi.org/10.1016/J. ENGSTRUCT.2015.01.013

[23] C. del Vecchio, M. di Ludovico, A. Prota, G. Manfredi, Modelling beam-column joints and FRP strengthening in the seismic performance assessment of RC existing frames, Compos. Struct. 142 (2016) 107–116, https://doi.org/10.1016/J. COMPSTRUCT.2016.01.077.

[24] G. Genesio. Seismic Assessment of RC Exterior Beam- Column Joints and Retrofit with Haunches Using Post-Installed Anchors, University of Stuttgart, Dissertation, 2012. https://doi.org/10.18419/opus-472.

[25] Z. wei Cai, X. Liu, L. Li, Lu zhi, Z. dao, Y. Chen, Seismic performance of RC beamcolumn-slab joints strengthened with steel haunch system, J. Build. Eng. 44 (2021), https://doi.org/10.1016/j.jobe.2021.103250.

[26] R. Realfonzo, A. Napoli, J.G.R. Pinilla, Cyclic behavior of RC beam-column joints strengthened with FRP systems, Construct. Build. Mater. 54 (2014) 282–297, https://doi.org/10.1016/j.conbuildmat.2013.12.043.

[27] H. Wang, F. Barbagallo, P. Pan, Test of precast pre-stressed beam-to-column joint with damage-free reinforced concrete slab, Eng. Struct. 210 (2020) 110368, https://doi.org/10.1016/j.engstruct.2020.110368.

[28] B. Wang, S. Zhu, Y.L. Xu, H. Jiang, Seismic retrofitting of non-seismically designed RC beam-column joints using buckling-restrained haunches: design and analysis, J. Earthq. Eng. 22 (2018) 1188–1208, https://doi.org/10.1080/ 13632469.2016.1277441.

[29] Marta Kosior-Kazberuka, Piotr Berkowskib, “Fracture Mechanics Parameters of Fine Grained Concrete with Polypropylene Fibres” World Multidisciplinary Civil Engineering-Architecture-Urban Planning Symposium 2016, WMCAUS 2016

[30] N. Buratti, C. Mazzotti, C., M. Savoia, Post-cracking behaviour of steel and macro-synthetic fibre-reinforced concretes, Construction and Building Materials 25 (2011) 2713-2722.

[31] Omar Algassem, Robert L. Vollum, “Behaviour and design of monotonically loaded reinforced concrete external beam-column joints” Structures 52 (2023) 946–970

[32] Dimov, D., Amit, I., Gorrie, O., Barnes, M. D., Withers, F., Russo, S., & Craciun, M. F. (2018). Ultrahigh Performance Nano engineered Graphene-Concrete Composites for Multifunctional Applications. Advanced Functional Materials, 28(23), 1705183.

[33] Al-Mahmoud, F., Shaikh, F. U. A., & Maalej, M. (2020). Graphene oxide-impregnated carbon fibers and their impact on the mechanical and durability properties of cementitious composites. Materials & Design, 188, 108412.

[34] Shaikh, F. U. A., & Loo, Y. H. (2018). The mechanical properties and durability of carbon and graphene oxide nanoparticle-reinforced cementious.